Industria Textilă

ISSN 1222–5347

1/2015

Revistă **cotată ISI** şi inclusă în **Master Journal List** a Institutului pentru Ştiinţa Informării din Philadelphia – S.U.A., începând cu vol. 58, nr. 1/2007/

ISI rated *magazine, included in the* ***ISI Master Journal List*** *of the Institute of Science Information, Philadelphia, USA, starting with vol. 58, no. 1/2007*

Editată în 6 nr./an, indexată şi recenzată în:
Edited in 6 issues per year, indexed and abstracted in:
Science Citation Index Expanded (SciSearch®), Materials Science Citation Index®, Journal Citation Reports/Science Edition, World Textile Abstracts, Chemical Abstracts, VINITI, Scopus, Toga FIZ technik ProQuest Central

Recunoscută în România, în domeniul Ştiinţelor inginereşti, de către **Consiliul Naţional al Cercetării Ştiinţifice din Învăţământul Superior** (C.N.C.S.I.S.), în **grupa A** /
Aknowledged in Romania, in the engineering sciences domain, by the ***National Council of the Scientific Research from the Higher Education*** *(CNCSIS), in* ***group A***

Contents

EDITORIAL STAFF

Editor-in-chief: Marius Iordănescu
Graphic designer: Florin Prisecaru
e-mail: marius.iordanescu@certex.ro

Journal edited in colaboration with **Editura AGIR**, 118 Calea Victoriei, sector 1, Bucharest, tel./fax: 021-316.89.92; 021-316.89.93;
e-mail: editura@agir.ro, www.edituraagir.ro

Yarn selection for weaving process to determine the parameters in OE rotor spinning machine by using TOPSIS methodology

S. MUGE YUKSELOGLU A. YESIM YAYLA KUBRA YILDIZ

REZUMAT – ABSTRACT

Selectarea firelor pentru procesul de ţesere cu scopul de a determina parametrii maşinii de filare cu rotor OE utilizând metoda TOPSIS

Selectarea parametrilor optimi ai maşinii de filare cu rotor OE pentru producerea firelor utilizată în procesul de ţesere este o problemă legată de deciziile multicriteriale. Pentru selectarea parametrilor optimi ai maşinii de filare, sunt necesare fire alternative produse pe maşina de filare cu rotor OE, îmbinând diferiţi parametri. Scopul acestei lucrări este de a propune metoda TOPSIS în selectarea parametrilor optimi ai maşinii de filare cu rotor OE pentru producerea firelor utilizate în procesul de ţesere. Prin urmare, în acest studiu sunt utilizaţi trei parametri ai maşinii: suprafaţa rotorului, profilul cilindrului destrămător şi tipul de lagăr. Pentru fiecare tip parametru, au fost alese variante diferite, ale suprafeţei rotorului: placat cu bronz sau diamant, profilul cilindrului destrămător OB 20 şi B174 şi tipurile de lagăr CK, CK4 şi CK8. Utilizând fiecare parametru selectat, firul filat pe maşina de filare cu rotor Ne 30 este produs pentru a fi utilizat pe maşina de ţesut. În final, vor fi obţinute 12 tipuri diferite de fire pentru selecţia firelor. Alternativele posibile sunt clasificate pe baza parametrilor de calitate ai firelor utilizând metoda TOPSIS, iar cea mai bună alternativă pentru creşterea eficienţei maşinii de ţesut este selectată. Conform clasificării finale, condiţiile de filare în care mostra este filată folosind suprafaţa rotorului placat cu diamant, un profil al cilindrului destrămător OB 20 şi un tip de lagăr CK prezintă cel mai mare coeficient de apropiere faţă de soluţia ideală, cu un scor de 0,981.

Cuvinte-cheie: *ţesere, fir filat cu rotor OE, metoda TOPSIS, imperfecţiune, tenacitate*

Yarn selection for weaving process to determine the parameters in OE rotor spinning machine by using TOPSIS methodology

Selection of the optimum OE rotor spinning machine parameters for yarn production which is used in weaving process is a multi-criteria decision-making problem. For the selection of the optimal spinning machine parameters, alternative yarns produced in OE rotor spinning machine with each different parameters combined are needed. The aim of this paper is to propose TOPSIS to select the optimum OE rotor spinning machine parameters for yarn production which is used in weaving process. Therefore, in this study there are three machine parameters which are rotor surface, beater-wire profile and navel type. For each parameter different types are chosen like bronze and diamond rotor surface, OB 20 and B174 beater-wire profiles and finally CK, CK4 and CK8 navel types. By using each of the parameters Ne 30 rotor spun yarn is manufactured for the use in a weaving machine. Ultimately, 12 different yarn alternatives will be obtained for the yarn selection. Possible alternatives are ranked on the basis of the yarn quality parameters by the TOPSIS methodology and the best alternative for increasing weaving machine efficiency is selected. According to the final ranking, the spinning condition in which the sample is spun by using a diamond rotor surface, an OB 20 beater-wire profile and a CK navel type has the highest closeness coefficient to the ideal solution with the 0.981 score.

Keywords*: weaving, OE rotor-spun yarn, TOPSIS methodology, imperfection, tenacity*

INTRODUCTION

OE rotor spinning technology is not really a new concept, as it has been in commercial applications for over four decades. Hence, a survey of the literature will reveal that there have been great deals of researches done on rotor speed, yarn structures, roller drafting systems, mechanical properties [1–3]. It is also well known that OE rotor spinning technology is especially used for the coarser yarns and with this method the production of the yarn depends not only on raw material characteristics but also on conditions of machine parts i.e. rotor surface, beater-wire profile, navel and so on, have a significant effect on OE rotor-spun yarn characteristics. On the other hand, woven fabrics are one of preferred subsequent products for OE rotor-spun yarns, which are produced by one of the most popular methods of yarn production in textiles. From 1990s some researchers stated the relationship between cotton fibre parameters i.e. maturity, fineness and micronaire, staple length and their effects on OE rotor-spun yarn structure and its properties [4–5]. Studies [6–7] show that the relationship between the above mentioned variables and yarn characteristics is profound and complex. As a consequence, selecting the suitable processing condition among variable alternatives is a difficult task and better outcomes about the desired end product properties will be achieved if the priorities of the spinner are taken into account [8].

In recent years, multi-criteria decision making (MCDM), which is a branch of operations research, is widely employed in various disciplines [9–15]. And it solves

the problems while a finite number of decision criteria and alternatives are present. According to some researchers [16], TOPSIS (Technique for Order Preference by Similarity Ideal Solution), AHP (Analytic Hierarchy Process), TOPSIS and ELECTRE are three popular MCDM techniques in spinning problem. On the other hand, there is finite study using TOPSIS in the textile literature. In one of these studies [17], TOPSIS methodology was adopted in order to select the appropriate doffing tube components and its adjustment for Ne 30 rotor-spun yarn, which is intended to be used for weft-knitted fabrics. It was concluded that TOPSIS and statistical analysis results are in harmony with each other and the possible alternatives are ranked on the basis of the yarn quality parameters. Later, another work [18] revealed that, an extended version of TOPSIS approach used exact values (interval data) on obtaining appropriate doffing tube components and its adjustment for OE-rotor spun yarn, which is also intended to be used in weft knitting machine. This study shows that using spiral nozzle and doffing tube without a torque stop and a closer setting between nozzle and rotor has the best performance on the knit ability of the yarn. Another study [19] indicated a suitable navel for denim fabrics which was selected by combining two popular MCDM methods namely TOPSIS and AHP; in this study relative importance of the yarn quality parameters is evaluated by using AHP method. The final ranking of navels is derived in accordance with relative closeness value determined by TOPSIS methodology.
Incidentally, it can be said that TOPSIS is new in the field of textile. Therefore, the current study makes a contribution to the weaving process with an attempt to use TOPSIS methodology in accomplishing acceptable solution in order to choose the appropriate yarn selection which enables to determine the parameters in OE rotor spinning machine. By doing this, OE rotor–spun yarns can be selected according to the best quality parameters to use in weaving process and to compare their final rankings.

EXPERIMENTAL WORK

Materials and Method

In this study, 100% cotton fibres with a 25 mm mean fibre length, 4.0 micronaire and 79.06 maturities (%) were used. The detailed properties of the cotton fibre are given in table 1.
A 192 head of commercial scale Schalfhorst Autocoro was used to spin the OE-rotor spun yarns for the use of weaving. Conditions for spinning were 20 ± 2 °C, 65% ± 2 RH. According to the spinning specifications of the machine used in the study, a total of twelve different OE-rotor spun yarns were produced with the same yarn linear density (20 tex) from a second draw frame passage sliver with a linear density of 5.76 ktex. Table 2 presents the OE-rotor machine specifications.
All the yarns were acclimatized at the standard atmosphere (20 ± 2 °C, 65% ± 2 RH) conditions for 48 hours and later the load-elongation characteristics

Table 1

COTTON FIBRE PROPERTIES	
Fibre properties	**Values**
Micronaire	4.00
Maturity (%)	79.06
50% span length (mm)	15.37
2.5 % span length (mm)	30.04
Uniformity (%)	51.20
Tenacity (cN/tex)	22.04
Elongation (%)	7.00
Trash (%)	3.01

Table 2

OE-ROTOR MACHINE SPECIFICATIONS			
Parameters	**Values**		
Raw material	100% cotton		
Sliver linear density (ktex)	5.76		
Draft	75		
Yarn linear density (tex)	20		
Twist factor (α_m)	146		
Beater-wire profile	OB 20 saw-tooth with 22.44 teeth/cm	B174 saw-tooth with 20.52 teeth/cm	
Beater speed (rpm)	7700		
Rotor speed (rpm)	70500		
Rotor cross-section	T type		
Rotor surface	Boron plated	Diamond plated	
Navel	CK steel, smooth	CK-4 steel, 4 notches	CK-8 steel, 8 notches
Rotor diameter (mm)	38		

of the yarns were determined with the Uster Tensorapid 3. A test specimen of 500 mm was elongated at an extension rate of 1000 mm·min^{-1}. The unevenness and imperfections of five yarn samples for each group were measured with Uster Tester 3 with a test speed of 400 m·min^{-1} for a period of 2.5 min. The hairiness of the yarns was also determined with Uster Tester 3. Hairiness (H) is a non-dimensional quantity and can be defined as the total protruding fibre lengths (cm) which projects from the yarn body and measured by the hairiness measurement unit where approximately 1 cm yarn lengths are considered. Table 3 presents the OE rotor-spun yarn alternatives and their parameters and table 4 shows all the test results of the OE rotor-spun yarns used in this study.

MCDM AND TOPSIS METHODOLOGY

Decision-Making problem is the process of finding the best option from all of the feasible alternatives. In

almost all such problems there are so many criteria and the process of evaluating the efficiency of alternatives is a complicated problem. That is, for many such problems, the decision makers put Multiple Criteria Decision Making (MCDM) techniques into account [20–21]. Multiple Criteria Decision Analysis (MCDA) or (MCDM) is a sub-discipline and full-grown branch of operations research that is concerned with designing mathematical and computational tools to support the subjective evaluation of a finite number of decision alternatives under a finite number of performance criteria by a single decision maker or by a group [22], [23]. There are many MCDM approaches which differ in how they combine and utilize data. MCDM approaches can be classified based on the major components of MCDM analysis. Three different classifications can be made as Multi Objective Decision Making (MODM) versus Multi Attribute Decision Making (MADM); individual versus group decision maker problems; and decisions under uncertainty [24], [21]. The TOPSIS methodology is a linear weighting technique first developed by Hwang and Yoon (1981) and is one of the known classical MADM methods [21]. In this study, the selection of the optimum OE rotor spinning machine parameters for yarn production which is used in weaving process is handled as a MCDM problem. This difficult and sensitive problem has many quantitative attributes and complexity. Those kinds of attributes make the evaluation process hard. Hierarchical structure is a good approach to describe a complicated system. Among several MCDM methods, TOPSIS is adopted for problem solving. Three are the most relevant characteristics of TOPSIS which have leaded us to suggest its use in the problem. First, differing from AHP, a kind of commonly used MCDM method or simple weighted sum methods, TOPSIS ranks different alternatives measuring their relative distances to ideal positive and negative solutions, providing then a meaningful performance measurement for each candidate. Second, in TOPSIS, weights and ratings can be directly assigned by decision makers. This feature is extremely useful in case of shallow and wide decisional hierarchies, since it avoids the need for cumbersome pair wise comparisons and makes the practical application of the methodology very straightforward. Third, the TOPSIS approach has been proven to be robust in dealing with MCDM problems. Moreover, the method is intuitive, easy to understand and to implement [25].

A CASE STUDY

In this section, first a hierarchical decision model which consists of seven main criteria for yarn evaluation and selection for weaving process to determine the parameters in OE rotor spinning machine is constructed. It is known that some of the most important physical characteristics of a yarn can give a good indication of the appearance of a finished fabric which is made of rotor-spun yarn. Afterward**s**, a hierarchical TOPSIS methodology is applied to solve the complex selection problem with crisp data.

Construction of the Hierarchical Decision Model

The relevant alternatives (OE rotor-spun yarn) and evaluation criteria are obtained from the task group. The group is organized for solving the problem by management. Two textile engineers from R&D department (full time involvement), R&D manager (part time involvement) and two academicians (part time involvement) from University are involved in the group. One of the academicians is an expert on spinning techniques and the other one is an expert on MCDM techniques. Among the techniques of group decision making (GDM), brainstorming technique is used by the group to determine the common decision. Based on the group decision hierarchical decision model is constructed as in figure 1.

The group decides three main parameters of OE rotor-spun yarn which are rotor surface, beater-wire profile and navel type and seven sub-parameters which are bronze and diamond for rotor surface, OB 20 and B 174 for beater-wire profile and CK, CK-4, CK-8 for navel type. Twelve alternatives are gained based on seven sub parameters combination. OE rotor-spun yarn production details in experimental

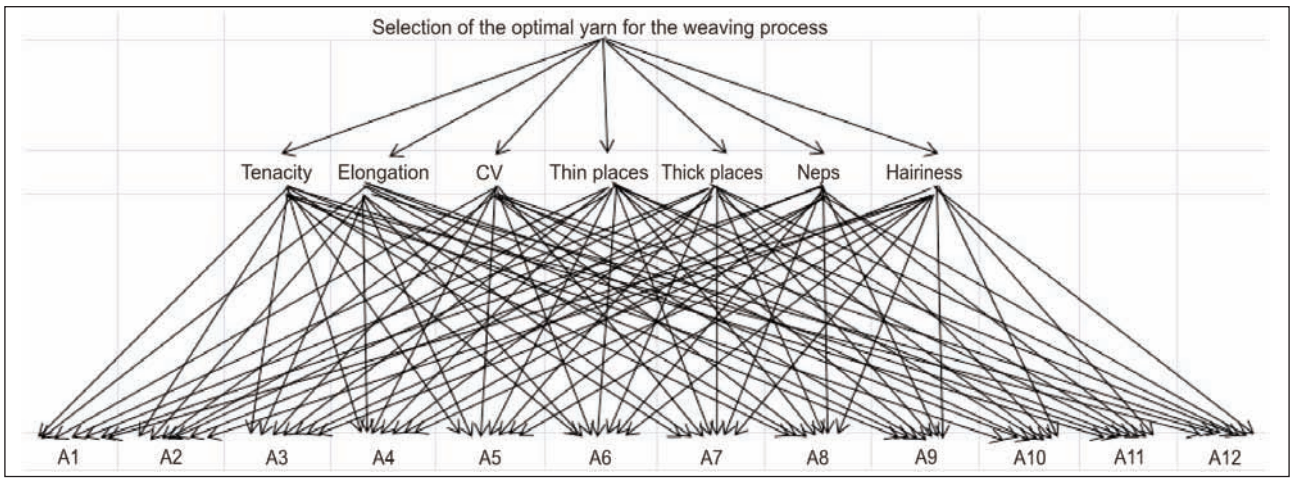

Fig. 1. Hierarchical decision model

work which is involved in the model and their parameters are as seen in table 3. The quantitative data set of alternatives for the OE rotor-spun yarns is obtained by test and measurement as shown in table 4.

Performing of the TOPSIS Methodology

In this section TOPSIS method is proposed for the problem introduced above of a textile company. The algorithm of the suggested method [22] is performed as follows:

Step 1: Construct the normalized decision matrix

In this study, table 2 is used as decision matrix for performing the TOPSIS methodology. Afterwards the table is normalized by using eq.1. The normalized decision matrix is given in table 5.

$$r_{ij} = x_{ij} / \sqrt{(\sum x_{ij}^2)} \quad \text{for } i = 1,\ldots,m;\ j = 1,\ldots,n; \quad (1)$$

Table 3

EXPERIMENTAL DESIGN OF THE OE ROTOR-SPUN YARNS AND THEIR PARAMETERS

Alternative	Rotor surface	Beater-wire profile	Navel type
A1	Bronze	OB 20	CK
A2	Diamond	OB 20	CK
A3	Bronze	B 174	CK
A4	Diamond	B 174	CK
A5	Bronze	OB 20	CK-4
A6	Diamond	OB 20	CK-4
A7	Bronze	B 174	CK-4
A8	Diamond	B 174	CK-4
A9	Bronze	OB 20	CK-8
A10	Diamond	OB 20	CK-8
A11	Bronze	B 174	CK-8
A12	Diamond	B 174	CK-8

Table 4

QUANTITATIVE DATA SET FOR ALTERNATIVES OF OE ROTOR-SPUN YARNS

Alternative	Tenacity (cN/tex) X1(+)	Elongation (%) X2(+)	CV (%) X3(–)	Thin places (–50%) X4(–)	Thick places (+50%) X5(–)	Neps (+280%) X6(–)	Hairiness (H) X7(–)
A1	11.62	6.08	12.81	0.8	20.8	2.1	5.5
A2	12.66	6.9	11.46	0	5.28	0.55	4.78
A3	11.51	6.04	12.8	1	18.05	1.5	5.54
A4	12.99	6.22	11.1	0	4.23	1	4.8
A5	11.27	5.6	13.2	0	34.04	3.3	8.25
A6	12.71	5.95	11.75	0.25	6.76	1.05	5.4
A7	11.72	5.5	13.26	0.25	38.03	6.05	7.9
A8	13.14	6.16	11.57	0	3.5	1.06	5.25
A9	10.70	5.01	14.08	1.5	101.1	15.56	9.46
A10	12.50	5.55	12.15	0.5	15	1.01	6.15
A11	11.28	5.13	13.62	1.75	62.3	11.3	9.3
A12	12.74	5.64	11.93	0	9.51	2.28	6.14
Best value	13.14	6.90	11.1	0	3.5	0.55	4.78

Table 5

THE NORMALIZED DECISION MATRIX

Alternative	Tenacity (cN/tex) X1(+)	Elongation (%) X2(+)	CV (%) X3(–)	Thin places (–50%) X4(–)	Thick places (+50%) X5(–)	Neps (+280%) X6(–)	Hairiness (H) X7(–)
A1	0.277	0.301	0.296	0.296	0.156	0.101	0.235
A2	0.302	0.341	0.264	0.000	0.039	0.026	0.205
A3	0.275	0.299	0.295	0.369	0.135	0.072	0.237
A4	0.310	0.308	0.256	0.000	0.032	0.048	0.206
A5	0.269	0.277	0.305	0.000	0.255	0.158	0.353
A6	0.303	0.294	0.271	0.092	0.051	0.050	0.231
A7	0.280	0.272	0.306	0.092	0.284	0.291	0.338
A8	0.314	0.305	0.267	0.000	0.026	0.051	0.225
A9	0.255	0.248	0.325	0.554	0.756	0.747	0.405
A10	0.298	0.275	0.280	0.185	0.112	0.048	0.263
A11	0.269	0.254	0.314	0.646	0.466	0.543	0.398
A12	0.304	0.279	0.275	0.000	0.071	0.109	0.263

where x_{ij} and r_{ij} are original and normalized score of decision matrix, respectively.

Step 2: Construct the weighted normalized decision matrix

In weaving, tenacity and yarn elongation are very important yarn properties, therefore it must be noted that the loss of elongation during sizing varies to 1.5% for a cotton OE rotor-spun yarn, even with ideal sizing machine settings [26], [27], [28]. In this context, table 6 is determined by the task group. Then, by using eq.2, the weighted normalized decision matrix is formed as in table 7.

$$V_{ij} = w_i r_{ij} \quad (2)$$

where w_i is the weight for j criterion.

Table 6

MATRIX OF IMPORTANCE OF THE CRITERIA (FROM 1 TO 7) AND VECTOR OF THE CORRESPONDING WEIGHT OF EACH CRITERION

Criteria	Relative importance	Weight of each criterion
Tenacity	4	0.174
Elongation	4	0.174
CV	4	0.174
Thin places	3	0.130
Thick places	3	0.130
Neps	3	0.130
Hairiness	2	0.087

Table 7

THE WEIGHTED NORMALIZED DECISION MATRIX

Alternative	Tenacity (cN/tex) X1(+)	Elongation (%) X2(+)	CV (%) X3(–)	Thin places (–50%) X4(–)	Thick places (+50%) X5(–)	Neps (+280%) X6(–)	Hairiness (H) X7(–)
A1	0.048	0.052	0.051	0.039	0.020	0.013	0.020
A2	0.053	0.059	0.046	0.000	0.005	0.003	0.018
A3	0.048	0.052	0.051	0.048	0.018	0.009	0.021
A4	0.054	0.054	0.045	0.000	0.004	0.006	0.018
A5	0.047	0.048	0.053	0.000	0.033	0.021	0.031
A6	0.053	0.051	0.047	0.012	0.007	0.007	0.020
A7	0.049	0.047	0.053	0.012	0.037	0.038	0.029
A8	0.055	0.053	0.046	0.000	0.003	0.007	0.020
A9	0.044	0.043	0.057	0.072	0.099	0.097	0.035
A10	0.052	0.048	0.049	0.024	0.015	0.006	0.023
A11	0.047	0.044	0.055	0.084	0.061	0.071	0.035
A12	0.053	0.049	0.048	0.000	0.009	0.014	0.023

Table 8

THE POSITIVE AND NEGATIVE IDEAL SOLUTIONS

A^+	0.055	0.059	0.045	0.000	0.003	0.003	0.018
A^-	0.044	0.043	0.057	0.084	0.099	0.097	0.035

Step 3: Determine the positive ideal and negative ideal solutions

For each selection criterion, the positive ideal and negative ideal solutions are calculated by using eq.3. and eq.4. The calculation results are given in table 8.

Positive ideal solution

$$A^+ = \{v_1^+, \ldots, v_n^+\},$$

$$\text{where } v_1^+ = \{\max(v_{ij}) \text{ if } j \in J; \min(v_{ij}) \text{ if } j \in J'\} \quad (3)$$

Negative ideal solution

$$A^- = \{v_1^-, \ldots, v_n^-\},$$

$$\text{where } v_1^- = \{\min(v_{ij}) \text{ if } j \in J; \max(v_{ij}) \text{ if } j \in J'\} \quad (4)$$

Step 4: Calculate the separation measures for each alternative

The distance from positive ideal solution is calculated by using eq. (5):

$$S_i^+ = [\sum(v_i^+ - v_{ij})^2]^{1/2} \quad i = 1, \ldots, m \quad (5)$$

Similarly, the distance from the negative ideal solution is calculated by using eq.(6):

$$S_i^- = [\sum(v_i^- - v_{ij})^2]^{1/2} \quad i = 1, \ldots, m \quad (6)$$

The calculation results are given in table 9.

Table 9

DISTANCE OF EACH ALTERNATIVE FROM THE POSITIVE AND NEGATIVE IDEAL SOLUTION					
Alternative	**Distance from positive ideal (S_i^+)**	**Distance from negative ideal (S_i^-)**	**Alternative**	**Distance from positive ideal (S_i^+)**	**Distance from negative ideal (S_i^-)**
A1	0.094	0.186	**A7**	0.053	0.112
A2	0.003	0.159	**A8**	0.008	0.158
A3	0.052	0.126	**A9**	0.155	0.012
A4	0.007	0.158	**A10**	0.030	0.139
A5	0.040	0.132	**A11**	0.125	0.046
A6	0.016	0.150	**A12**	0.018	0.149

Table 10

RELATIVE CLOSENESS COEFFICIENT OF EACH ALTERNATIVE TO THE IDEAL SOLUTION			
Alternative	**Relative closeness coefficient (C_i)**	**Alternative**	**Relative closeness coefficient (C_i)**
A1	0.664	**A7**	0.678
A2	0.981	**A8**	0.954
A3	0.708	**A9**	0.072
A4	0.960	**A10**	0.822
A5	0.767	**A11**	0.271
A6	0.905	**A12**	0.895

Table 11

FROM THE BEST ALTERNATIVE TO THE WORST
A1 → A4 → A8 → A6 → A12 → A10 → A5 → A3 → A7 → A1 → A11 → A9

Step 5: Calculate the relative closeness to the ideal solution C_i

$$C_i = S_i^- / (S_i^+ + S_i^-) \qquad 0 < C_i < 1 \qquad (7)$$

Select the alternative with C_i closest to 1.

Relative closeness coefficient of each alternative to the ideal solution is calculated by using eq.(7) and given in table 10.

Table 11 includes sorting alternatives from the best to the worst, formed based on table 10. According to table 11, the best alternative is A2.

More detailed description of TOPSIS methodology can be found in several articles [21], [29], [25], [30].

RESULTS

The experimental variables, namely rotor surface, beater-wire profile and navel type were found to have significant impact on the 100 % cotton OE rotor-spun yarn selection for the weaving process. In figure 2 the final decision according to the TOPSIS solution is depicted. As shown in figure 2, A2 is the best rotor-spun yarn which has the highest relative closeness

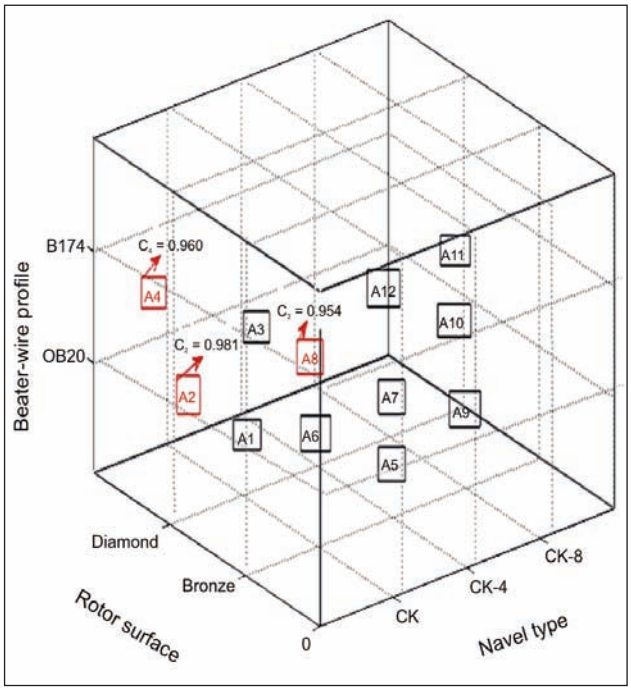

Fig. 2. Final decision according to the TOPSIS solution

coefficient to the ideal solution with the C_2 = 0.981 score. A4 (with the C_4 = 0.960 score) and A8 (with the C_8 = 0.954 score) are preferable alternatives which have closest scores to A2 respectively.

As a result, OB 20 with a 38 mm diamond plated rotor surface and CK navel can be suggested for this kind of application according to final decision based on the TOPSIS solution. Therefore, the selection of these specified optimal spinning machine parameters is recommended for Ne 30 OE rotor-spun yarns to use in weaving process.

According to the evaluations made using USTER Statistics, it can be also concluded that A2 sample, which is produced with nozzle type CK, beater-wire profile OB20 and diamond plated rotor surface, does have a significant effect on elongation, CV (%), thin places, neps and hairiness whereas in tenacity and thick places there is a moderate effect. It can be concluded that best elongation (6.9%) with moderately lower CV (11.46%) was obtained, on the specified spinning machine parameters given above where is especially important for the performance which is reflected in the USP^{TM} levels. These two values of combination will easily lead to the weaver's decision to use this yarn especially for warp in the weaving process. In this particular study and according to the USTER Statistics 2013, the highest elongation (6.9%) is expected to behave about the 25% in statistics which have considerably very low risk of breaking [26] in terms of performance in weaving with a reasonable good tenacity (12.66 cN/tex). Moreover, A2 sample has shown the best neps (0.55) and hairiness (4.78) values which leads to a superior fabric surface, which can be illustrated on weaving process.

Acknowledgements

The authors would like to express their appreciation for R&D Manager Samir SADIKOGLU and Textile Engineer Sabiha AKCAY for their support.

BIBLIOGRAPHY

[1] Plonsker H.R., Backer S. *The Dynamics of Roller Drafting, Part I: Drafting Force Measurement*, In: Textile Research Journal, 1967, vol. 37, pp. 673-687

[2] Das A., Ishtiaque M., Niyogi R. *Optimization of Fiber Friction, Top Arm Pressure and Roller Setting at Various Drafting Stages*, In: Textile Research Journal, 2006, *vol.* 76, no.12, pp. 913-921

[3] Ishtiaque M., Mukhopadhyay A., Kumar A. *Impact of High-speed Draw Frame and Its Preparatory on Fiber Orientation Parameters at Sliver*, In: Journal of the Textile Institute, 2007, vol. 98, no 6, pp. 501-512

[4] Hill D.J., Busby K., Yukseloglu S.M. *The Development Of A Colorimetric Method For The Study Of Structural Differences Between Cotton Yarns Spun By The Ring And Rotor Techniques*, In: Textile Science 91 International Conference, vol. 1, Liberec, Czechoslovakia, 16-18 September 1991

[5] Yukseloglu S.M., Busby K., Hill D.J. *The Application of Factorial Experiment Design To A Study Of Yarn Regularity And Imperfections*, In: Narrow Fabrics Group Conference, The Textile Institute, Derby, UK. 11 June 1994

[6] Koc, E., Demiryurek, O., *Predicting the tensile strength of polyester/viscose blended open-end rotor spun yarns using the artificial neural network and statistical models*, In: Industria Textila, 2010, vol. 62, no. 2, pp. 81-87

[7] Ishtiaque S.M., Mukhopadhyay A., Kumar A. *Impact of High-Speed Draw Frame and Its Preparatory on Packing and Related Characteristics of Ring Spun Yarn Properties*, In: Journal of the Textile Institute, 2009, vol. 100, no. 8, pp. 657-667

[8] Kaplan, S., Araz C., Goktepe O. *A Multi-Criteria Decision Aid Approach on Novel Selection Problem for Rotor Spinning*, In: Textile Research Journal, 2006, vol. 76, no. 12, pp. 896-904

[9] San Cristóbal J.R. *Multi-criteria Decision making in the Selection of a Renewable Energy Project in Spain: The VIKOR Method*. In: Renewable Energy, 2011, vol. 3, pp. 498-502

[10] Ertuğrul İ.,Karakaşoğlu N. *Comparison Of Fuzzy AHP And Fuzzy TOPSIS Methods For Facility Location Selection,* In: Int J Adv Manuf Technol, 2008, vol. 39, pp. 783–795

[11] Yayla A. Y., Yildiz A., Yildiz K. *Generalized Choquet Integral Algorithm for Subcontractor Selection in the Textile Industry - A Case Study for Turkey*, In: Fibers & textiles in Eastern Europe, 2013, vol. 21, no. 6, pp. 16-21

[12] El Mikawi M., Mosallam A.S. *A Methodology for Evaluation of The Use Of Advanced Composites In Structural Civil Engineering Applications,* In: Composites: 1996, Dart B 27 B 203-215

[13] İç Y.T. *Development of a credit limit allocation model for banks using an integrated Fuzzy TOPSIS and linear programming*, In: Expert Systems with Applications, April 2012, vol. 39, no. 5, pp. 5309-5316

[14] Büyüközkan G., Çifçi G.A. *Combined Fuzzy AHP and Fuzzy TOPSIS Based Strategic Analysis of Electronic Service Quality in Healthcare Industry,* In: Expert Systems with Applications, Issue 3, 15 February 2012, vol. 39, pp. 2341-2354

[15] Torlak G., Sevkli M., Sanal M., Zaim S. *Analyzing Business Competition by Using Fuzzy TOPSIS Method: An Example of Turkish Domestic Airline Industry*, In: Expert Systems with Applications, April 2011, vol. 38, no 4, pp. 3396-3406

[16] Fallahpour, A. R., Moghassem A. R. *Evaluating Applicability of VIKOR Method of Multi-Criteria Decision Making for Parameters Selection Problem in Rotor Spinning,* In: Fıbers And Polymers, Jul 2012, vol.13, no 6, pp. 802-808

[17] Hasani, H., Semnani, D., Tabatabaei, S., *Determining the optimum spinning conditions to produce the rotor yarns from cotton wastes,* In: Industria Textila, 2010, vol. 86, no. 6, pp. 259-264

[18] Moghassem A., Fallahpour A. *Selecting Doffing Tube Components for Rotor-Spun Yarn for Weft Knitted Fabrics Using Multi-criteria Decision-making Approach with Interval Data*, In: Journal Of Engineered Fibers And Fabrics, 2011, vol. 6, no. 3, pp. 44-53

[19] Majumdar A., Kaplan S., Goktepe O. *Navel selection for rotor spinning denim fabrics using a multi-criteria decision-making process*, In: Journal of the Textile Institute, 2010, vol. 101, no. 4, pp. 304-309

[20] Chen C.T. *Extensions Of The Topsis for Group Decision-Making Under Fuzzy Environment*, In: Fuzzy Sets& Systems, 2000, vol. 114, issue 1, pp. 1-9

[21] Zaerpour N., Rabbani M., Gharehgozli A.H., Tavakkoli-Moghaddam R.*A. Comprehensive Decision Making Structure For Partitioning Of Make-To-Order, Make-To-Stock And Hybrid Products*, In: Soft Computing, 2009, vol. 13, pp. 1035-1054

[22] Behzadian M., Otaghsara S. K., Yazdani M., Ignatius J.*A State-Of The-Art Survey of TOPSIS Applications,* In: Expert Systems with Applications*, 2012, vol.* 39, pp. 13051-13069

[23] Lootsma F.A. *Multi-Criteria Decision Analysis Via Ratio And Difference Judgment*, Kluwer Academic Publishers, 1999

[24] Malczewski J.*GIS and Multi-Criteria Decision Analysis*, John Wiley & Sons Inc. New York, 1999

[25] Bottani E., Rizzi A. *A Fuzzy TOPSIS Methodology to Support Outsourcing of Logistics Services*, In: Supply Chain Management: An International Journal, 2006, vol. 11, no. 4, pp. 294-308

[26] Uster Statistics Application Handbook, 2013, Uster Technologies AG, Switzeland

[27] Buharalı G., Ömeroğlu S. *Open-End Rotor İplik Özelliklerine Etki Eden Faktörler, Uludag University* Journal of The Faculty of Engineering and Architecture, 2013, vol. 18, no. 2

[28] Taher Halimi M., Ben Hassen M., Azzouza B., Sakli F. *Effect Of Cotton Waste And Spinning Parameters On Rotor Yarn Quality,* In: Journal of The Textile Institute, 2013, vol. 98, no. 5, pp. 437-442

[29] Majumdar A., Kaplan S., Goktepe O. *Navel selection for rotor spinning denim fabrics using a multi-criteria decision-making process*, In: The Journal of the Textile Industry, April 2010, vol. 101, no.4, pp. 294-308

[30] Lin M.C., Wang C.C., Chen M.S., Chang C.A. *Using AHP and TOPSIS Approaches In Customer-Driven Product Design Process*, In: Computers in industry, 2008, vol. 59, pp. 17-31

Authors:

S. MUGE YUKSELOGLU[1]
A. YESIM YAYLA[2]
KUBRA YILDIZ[3]

Marmara University
[1] Faculty of Technology, Department of Textile Engineering
[2] Faculty of Technology, Department of Mechanical Engineering
[3] Institute of Pure and Applied Sciences

Goztepe-34722
Istanbul-TURKEY
e-mail: myukseloglu@marmara.edu.tr, yayla@marmara.edu.tr, kubra_yldz89@hotmail.com

Corresponding author:

S. MUGE YUKSELOGLU
myukseloglu@marmara.edu.tr

The influence of nozzle pressure and yarn count on vortex spun yarn properties produced by MVS machine

GİZEM KARAKAN
SEMA PALAMUTÇU

RAMAZAN ERDEM
GABİL ABDULLA

REZUMAT – ABSTRACT

Influența presiunii duzelor și a finețiifirelor asupra proprietăților firelor filate Vortex produse cu ajutorul mașinii MVS

Pe lângă alte tehnologii de filare tradiționale și moderne, firul filat Vortex reprezintă una dintre cele mai înfloritoare tehnologii de filare. Fiind o tehnologie nouă, aceasta este încă în faza de îmbunătățire tehnologică intensivă și a lucrărilor academice. Ca o contribuție suplimentară la studiile despre firele filate Vortex, această lucrare abordează proprietățile firelor filate Vortex din bumbac 100%. În cadrul studiului experimental, au fost produse trei tipuri de fire cu diferite finețiți (Ne 20, Ne 30 și Ne 40), cu trei niveluri diferite de presiune a duzelor (4 kgf/cm^2, 4.5 kgf/cm^2, 5 kgf/cm^2). Probele de fire produse sunt apoi evaluate, luând în considerare caracteristicile lor de aspect, pilozitate, uniformitate, imperfecțiuni și rezistență la rupere. Se constată că rezultatele obținute sunt în conformitate cu lucrările experimentale anterioare.

Cuvinte-cheie: filare vortex Murata, bumbac, proprietățile firelor

The influence of nozzle pressure and yarn count on vortex spun yarn properties produced by MVS machine

Vortex spun yarn is one of the flourishing spinning technology among other traditional and non traditional spinning technologies. As one of the new technology, it is still on the phase of intensive technological improvement and academic works. As one additional contribution to the vortex spun yarn studies this paper involves with the 100% cotton vortex spun yarn properties. In the content of the experimental study three different number of yarns (Ne 20, Ne 30 and Ne 40) produced with three different levels of (4 kgf/cm^2, 4.5 kgf/cm^2 , 5 kgf/cm^2) nozzle pressure. The manufactured yarn samples are then evaluated considering their visual aspect, hairiness, evenness, imperfections, and tensile properties. Obtained results are found attributable to the previous experimental works.

Keywords: Murata vortex spinning, cotton, yarn properties.

In general, three main spinning methods are used for cotton yarn production in industrial scale; ring spinning, open-end spinning and air-jet spinning. In the case of ring spinning, the twist is inserted into yarn by a circulating traveler, and winding action is realized by a rotating spindle. Open-end spinning method has different working principle that an opening roller and an air stream separates the fiber bundles into individual ones first, and then the fibers are collected again in the form of continuous yarn strand. In air jet spinning, there are two nozzle systems generate swirling air currents in opposite directions to form the yarn. Compared with the other two techniques, air-jet spinning achieves greatest yarn production speeds [1].

In Murata vortex spinning, compressed air is transferred into the twisting chamber through the jet orifices, thereby; the high-speed whirled air current is created. This generates the negative pressure effect at the inlet of the nozzle block. The drafted fibers are drawn into the spiral fiber passage under the negative pressure; subsequently the preceding parts of those fibers are drawn into the vortex spun yarn trail along the guide needle. When the trailing ends of the drafted fibers are departed from the front roller nip point and have passed through the spiral fiber passage, the trailing portions of those fibers are inverted at the inlet of the hollow spindle and form the open-end trailing fibers because of the whirling force of the high-speed air stream. The high-speed whirled air current enables the open-end trailing fibers rotate around the core fibers, and finally the fiber bundles are twisted into the vortex spun yarn [2]. Vortex yarn has different yarn structure comparing the conventional yarn structures. Vortex spun yarn consists in two-segmented structure which includes core and wrapper fibers which covers the core part of the fiber grouping the yarn body [3].

It is known that vortex yarn and fabrics produced using vortex yarn possess several unique properties including low hairiness, outstanding pilling and abrasion resistance, high moisture absorption and diffusion properties, fast drying characteristics, high color fastness and better durability that maintains functionality over a long time [5].

Previous studies proved that the structure and performance of vortex spun yarns were influenced by the effects of nozzle angle, nozzle pressure, spindle

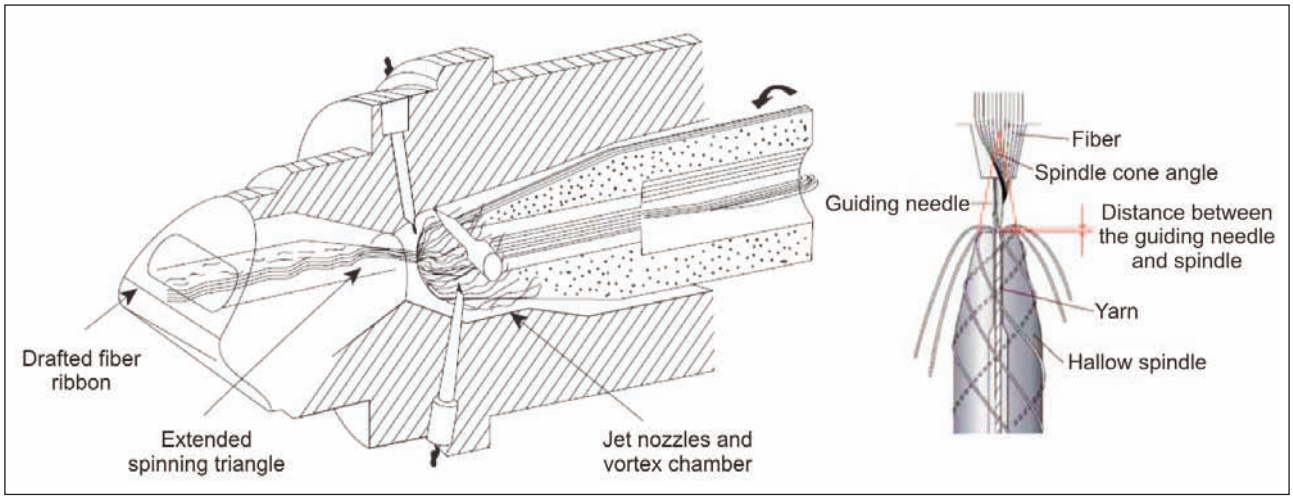

Fig. 1. Shematic diagram of the nozzle block of vortex spinning machine [4]

diameter, yarn delivery speed, yarn linear density, fiber composition and the distance between the front roller and the spindle. Nozzle pressure was defined as one of the most effective parameters. The theoretical and practical works, based on the impacts of nozzle pressure on vortex spun yarns, presented that the nozzle pressure directly influences the fiber configuration and consequently the yarn structure [6–8]. Tyagi et. al. reported that the changes in nozzle pressure influenced the tightness of wrapping fibers along the yarn strand, as well as the amount of wrapping and the proportion of unwrapped sections [8]. Moreover, it was stated that the alterations in nozzle pressure change the number of core-fibers that affect the flexural rigidity and tensile properties of the vortex spun yarns. Some authors strongly claimed that yarn evenness and imperfections are also significantly affected by the nozzle pressure [9,10]. Yarn count is also another dominant factor on the structural properties of vortex spun yarn. Yarn evenness, the number of imperfections and tensile properties are greatly influenced by the yarn count as well [9–12].

Machine producers claimed that the range of yarn count spinnable on vortex system is between Ne 15 – Ne 60 [13]. Ortlek and Ulku explored the influences of nozzle pressure and delivery speed on 100% carded cotton vortex spun yarns of Ne 20/1, Ne 30/1 and Ne 40/1. They produced vortex spun yarns on MVS 851, and from the slivers that were drafted in various ratios [14]. According to their findings, nozzle pressure and yarn count were highly influent factors for the vortex yarn properties. Decreases in the nozzle pressure resulted in improved evenness and imperfection; on the other hand, increases in the nozzle pressure resulted in highly improved hairiness and tensile properties of MVS yarns because of the better wrapping. In the case of yarn count, it was concluded that better yarn properties regarding evenness, imperfection values, hairiness and tensile properties were obtained for coarser yarns.

Our experimental studies were performed on MVS 861, and the drafting ratios and delivery speed of slivers fed to the machine were 90/26, 130/40, 173/54, and 330 m/min, respectively. Yarn numbers were ranged between Ne 20 and Ne 40 for carded cotton (100%) yarns. The optimum ones were chosen for the measurements. The main purpose of this research is to examine the effects of two important parameters, nozzle pressure and yarn count, on the properties of Vortex spun yarns, including structure, tensile strength, elongation, evenness and hairiness.

EXPERİMENTAL PART

Materials

In order to analyze the influence of nozzle pressure and yarn count on the properties of vortex yarns, 9 different types of cotton carded sample yarns were produced on the MVS 861 spinning machine. Processing cotton (100%) fibers on the systems based on jet spinning principle is still a major matter. For this reason, the proper selection of cotton fibers for the vortex spinning is vital. The properties of used cotton fibers for the experimental studies are illustrated in table 1.

Table 1

PROPERTIES OF COTTON FIBER USED IN VORTEX SPINNING PROCESS

Fiber	Fineness (micronaire)	Elongation (%)	Length (mm)	Strength (g/tex)
Cotton	4.3	5.4	30.14	33.2

Yarn preparation

In the first place, cotton fibers were opened and carded, then, they were subjected to drawing process. For the sliver preparation, three passages of drawing were applied by utilizing Rieter SB-D15 type draw machines. Good fiber alignment and sliver evenness are prime parameters in order to gain satisfactory production results, hence special care was required

for the preparation of slivers. After three passages of drawing, the slivers with a linear density of approximately Ne 0,20 were transferred to vortex spinning machine. Delivery speed of the slivers was remained the same. The list of yarn samples and corresponding test conditions are presented in table 2.

Two process parameters, which were considered to influence the properties and structure of vortex yarns, were chosen for the investigation. These were: nozzle pressure and yarn count. Therefore, three different nozzle pressures (4.0 kgf/cm^2, 4.5 kgf/cm^2, 5.0 kgf/cm^2) were determined for vortex spinning and three different yarn counts Ne 20, Ne 30 and Ne 40 were optimally produced with a constant delivery speed of 330 m/min (table 2). All the sample yarns were produced with the following spinning conditions; 70° nozzle discharge angle, **2**p130d L7 -9.3 type needle holder, 1.2 mm spindle inner diameter on MVS-861 vortex spinner.

Measurements of yarn properties

For the observation of yarn structures, a stereo microscope (Olympus SZ61) with a software analysis system (BABSOFT) was used to investigate side visual assessment of the yarn structures. Fiber arrangements were carefully observed by using this set-up. Uster Tester 4 was utilized to explore the evenness and hairiness properties of the sample yarns. Vortex yarn samples were compared in terms of structures, yarn evenness, imperfections, hairiness, tenacity, elongation and work-to break values (B-work) by using measurement data of Uster Tensojet 4. Ten bobbins were chosen for the efficient assessment of each yarn sample and ten different yarn pieces were taken from each bobbin. All the measurements were conducted under standard test conditions, 65 ± 2% relative humidity and 20 ± 2°C. Test results were analyzed for significance in differences using two way repeated measures analysis of variance (ANOVA) and Tukey HSD tests at the 0.05 level in the SPSS statistical package.

RESULTS AND DISCUSSIONS

Yarn structure

Optical images of nine different vortex yarn samples spun in various counts and nozzle pressures are shown in figure 2. Tyagi et. al. [8] used fiber tracing technique to analyze the structural properties of spun yarns and they classified the structure of vortex spun yarns into three main categories as core fibers, wrapper fibers and wild fibers. Core fibers were defined as straight or inclined fibers that constitute the most part of the yarn. Wrapper fibers are wrapped around the core fibers along the yarn central axis. Wild fibers protrude from the yarn strand in various directions and sometimes they were observed in loop formation. Our visual analysis presented that all sample yarns had these three fiber types in different amounts.

Table 2

NOMINAL YARNS AND PROCESS PARAMETERS				
Samples No.	**Yarn Count**	**Nozzle pressure (kgf/cm²)**	**Delivery Speed (m/min)**	**Total Draft/Main Draft**
1	20	4	330	90/26
2	20	4.5	330	90/26
3	20	5	330	90/26
4	30	4	330	130/40
5	30	4.5	330	130/40
6	30	5	330	130/40
7	40	4	330	173/54
8	40	4.5	330	173/54
9	40	5	330	173/54

As can be clearly seen from the images that as the yarns get finer, the amount of wrapper fibers increases. This situation was also previously reported by Erdumlu et. al. [15]. During the vortex spinning process fiber bundle are drawn into the hollow spindle where yarn formation occurs. Trailing ends of some fibers are separated from fiber bundle, because of the swirling air current, and form the wrapper fibers as well as wild fibers. When more fibers in the fiber bundle fed into the vortex system, higher inter-fiber cohesion takes place which retards the separation of trailing ends of the fibers, and less wrapper and wild fibers form in coarse counts. On the other hand, in finer counts fewer fibers are located on the yarn strand means that fibers exposed more to the swirling force of air current. Consequently, greater amount of wrapper fibers form along the yarn axis. The influence of nozzle pressure can also be seen clearly from the images. Amount of wrapper fibers increases as the nozzle pressure gets greater. Zou et.al. analyzed the flow field characteristics inside the nozzle block. They mentioned that increasing nozzle pressure generates an increase in the velocity of the air flow at the exit of the jet orifice as well as an increase in axial, radial and tangential velocities inside the nozzle block that enhance the number of open trail end fibers and therefore wrapper fibers [16]. It is also visually validated in the frame of our experimental work that yarn samples which are spun with high nozzle pressure have intense number of wrapper fiber in the yarn body.

Yarn hairiness

Comparing with other spinning techniques, one of the most spectacular characteristics of vortex spun is claimed as the low hairiness [12]. Basal and Oxenham also specifically stated that the vortex spun yarns possess lower hairiness than air jet spun yarns [17]. The reason for low hairiness was attributed to the uniformly distributed layer of wrapper fibers [18]. Hairiness properties of vortex spun yarns were measured with the help of hairiness module attached on

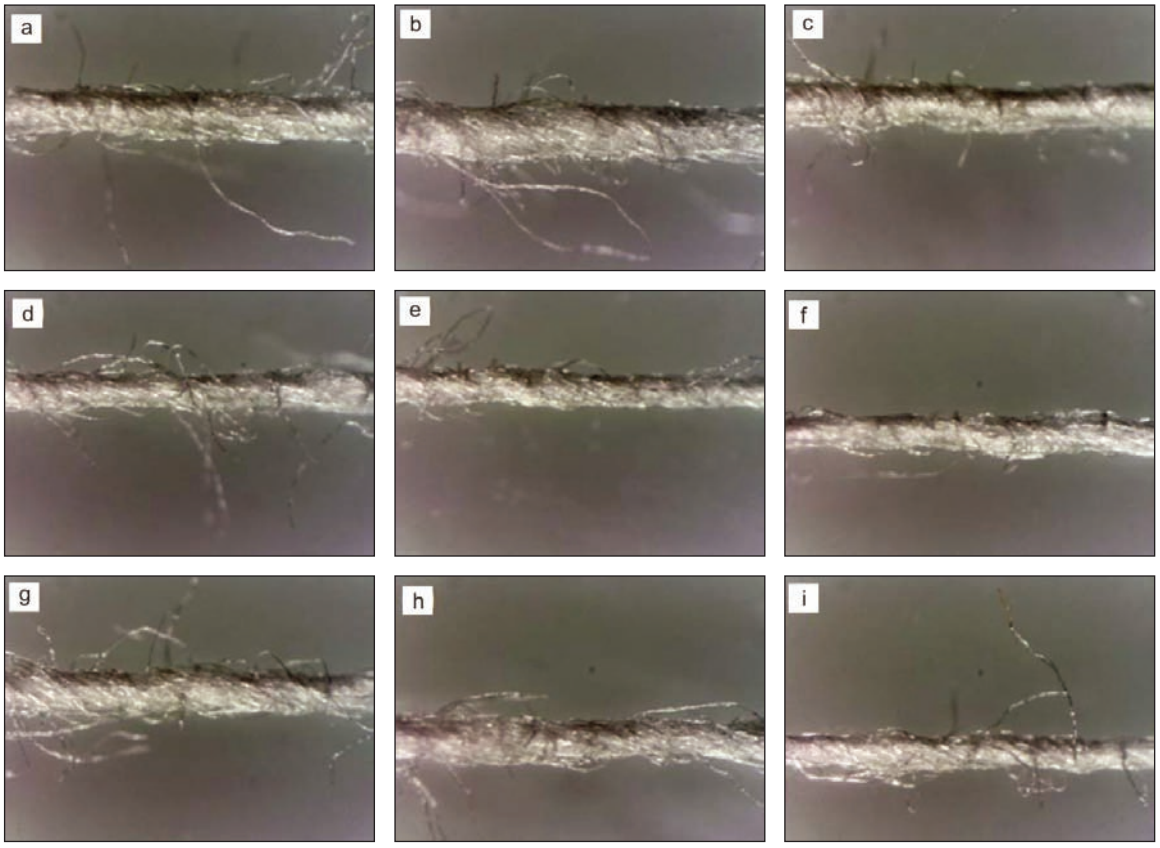

Fig. 2. Yarn samples spun in different counts and nozzle pressures; (a) Ne 20, 4 kgf/cm^2; (b) Ne 20, 4.5 kgf/cm^2; (c) Ne 20, 5 kgf/cm^2; (d) Ne 30, 4 kgf/cm^2; (e) Ne 30, 4.5 kgf/cm^2; (f) Ne 30, 5 kgf/cm^2; (g) Ne 40, 4 kgf/cm^2; (h) Ne 40, 4.5 kgf/cm^2; (i) Ne 40, 5 kgf/cm^2

Uster Tester 4 laboratory equipment. Test results are exhibited in table 3. "H" Index value stands for the total number of hairy ends on 1 cm length of yarn surface. During the experiments, 400 meters of yarn from each bobbin was tested. According to Tukey HSD test results and ANNOVA data, it was found that nozzle pressure and yarn count are important parameters that affect yarn hairiness.

The Tukey HSD test results from table 3 revealed that yarn hairiness decrease with increased nozzle pressure. The decreased hairiness at higher nozzle pressures was attributed to the fact that the whirling force of the nozzle air stream which increases with the nozzle pressure, therefore, the amount of wrapping fiber and the uniformity of wrapping are enhanced [14]. Table 3 results also indicate that as the vortex spun yarns get finer, lower hairiness values are obtained. This may be explained by the fiber packing density of vortex spun yarns [19]. Coarser yarns have higher fiber packing density that extends the probability of increasing amount of hairy ends on the yarn surface.

Table 3

EFFECTS OF NOZZLE PRESSURE AND YARN COUNT ON MVS YARN HAİRİNESS PROPERTİES, TUKEY HSD TEST RESULTS	
H (USTER INDEX)	
Nozzle Pressure	
4 kgf/cm^2	13.9737 ^{b}
4.5 kgf/cm^2	14.0890^a
5 kgf/cm^2	14.1077^a
Yarn Count	
Ne 20	12.3373^c
Ne 30	14.3260^b
Ne 40	15.5070^a

Note: a,b,c indicates the groups of data that are not different from each other at 0.95 significancy level.

Yarn evenness and imperfection properties

We compared the vortex yarn samples on the basis of yarn evenness and imperfections including thin places, thick places and neps. Table 4 presents the evenness and imperfection test results of vortex spun yarns samples produced with various nozzle pressures and yarn counts. ANOVA analysis and Tukey HSD test results proved that both air pressure and yarn count were significant factors for yarn evenness and imperfection properties.

It was noticed that as the yarn gets finer, it becomes more uneven and the amount of thin places, thick places and neps increases markedly. This was explained by the deterioration of fiber arrangement within the yarn. The decline in number of fibers in the yarn cross section makes the uniform arrangement of

Table 4

EFFECTS OF NOZZLE PRESSURE AND YARN COUNT ON MVS YARN EVENNESS AND İMPERFECTİON PROPERTİES, TUKEY HSD TEST RESULTS				
	CVm (%)	**Thin Places (–50%)**	**Thick Places (+50%)**	**Neps (+200%)**
Nozzle Pressure				
4 kgf/cm^2	13.9737 ^{b}	13.9737 ^{b}	58.0000 ^{b}	95.8333 ^{b}
4.5 kgf/cm^2	14.0890 ^{a}	31.5833 $^{a\,b}$	63.4167 $^{a\,b}$	98.8333 ^{b}
5 kgf/cm^2	14.1077 ^{a}	36.4167 ^{a}	67.1667 ^{a}	111.3333 ^{a}
Yarn Count				
Ne 20	12.3373 ^{c}	.7500 ^{c}	11.7500 ^{c}	23.9167 ^{c}
Ne 30	14.3260 ^{b}	15.8333 ^{b}	55.4167 ^{b}	109.6667 ^{b}
Ne 40	15.5070 ^{a}	78.2500 ^{a}	121.4167 ^{a}	172.4167 ^{a}

Note: a,b,c indicates the groups of data that are not different from each other at 0.95 significancy level.

the fibers more difficult. This result is consistent with the findings of the previous studies [9–14].

Figure 3 shows the measurement results of yarn evenness. It was observed that yarn evenness became worse for all sample yarns as the nozzle pressure and yarn count are increased. The highest unevenness rate was obtained from the Ne 40 vortex yarn that was spun with the nozzle pressure of 5 kgf/cm^2. The best evenness result was recorded for Ne 20 vortex yarn that was spun with the nozzle pressure of 4 kgf/cm^2. Zou et.al. reported that when the nozzle pressure is too high, the high speed air flow takes the separated fibers out of the fiber bundle. This generates the more amounts of wild fibers and increases the fiber loss. At the end, the uniformity of vortex spun yarn is deteriorated [16, 20].

Figure 4 shows the impact of yarn count and nozzle pressure on the occurrence of thin places along the yarns. According to the graph, the number of thin places increased enormously on Ne 40 yarn compared with the Ne 20 and Ne 30 yarns. The greatest number of thin places was obtained from Ne 40 yarn that was spun with the nozzle pressure of 5 kgf/cm^2. The least amount of thin places was observed on Ne 20 yarn that was spun with the nozzle pressure of 4 kgf/cm^2. As it can be clearly seen from the graph that the amount of thin places increase, as the yarn becomes finer and as the nozzle pressure gets greater. This situation was explained by the increase in whirling force of air current inside the nozzle that causes more amount of fiber lost. This effect becomes more influent for finer yarns due to the low number of fibers located in the yarn cross section [8, 10].

Figure 5 presents the impact of yarn count and nozzle pressure on the occurrence of thick places along the yarns. According to the graph, it can be stated that there was not a regular trend among the test results; however, number of thick places was greater on finer yarns. The lowest amount of thick places was recorded for Ne 20 yarn that was spun with the nozzle pressure of 4.5 kgf/cm^2, on the other hand, the highest number was observed for Ne 40 yarn that was spun with the nozzle pressure of 4.5 kgf/cm^2. This irregular data distribution was also observed by Ortlek and Ulku for vortex spinning of carded cotton (100%) [14, 15]. Undesired alterations in efficiency of nozzle air pressure during the spinning process may cause such irregularities.

Figure 6 illustrates the influence of yarn count and nozzle pressure on the neps formation along the yarns. According to the graph, the number of neps

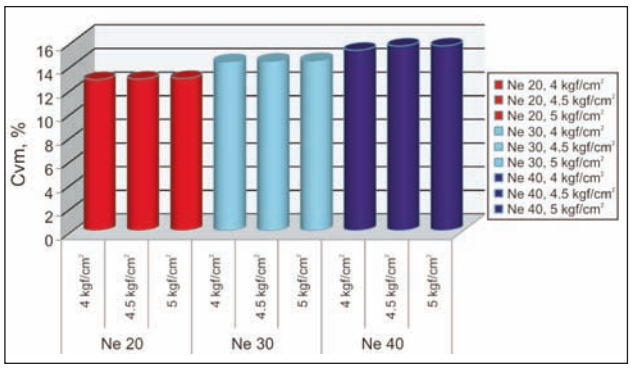

Fig. 3. The impact of nozzle pressure and yarn count on yarn evenness (CVm%, per km)

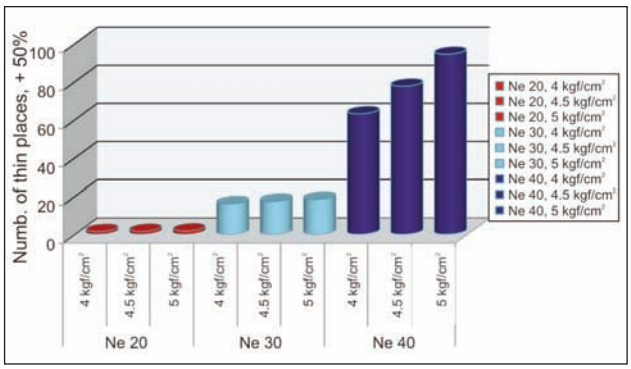

Fig. 4. The impact of yarn count and nozzle pressure on the occurrence of thin places (per km) along the yarns

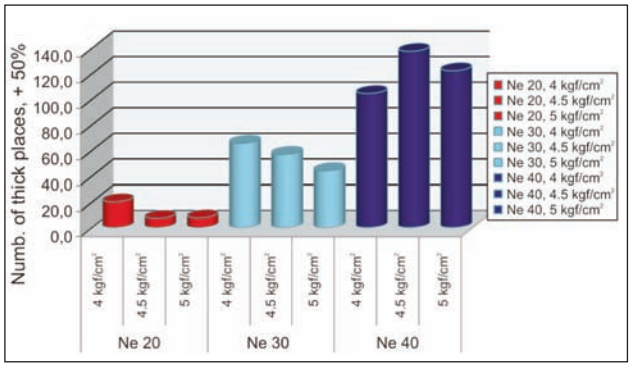

Fig. 5. The impact of yarn count and nozzle pressure on the occurrence of thick places (per km) along the yarns

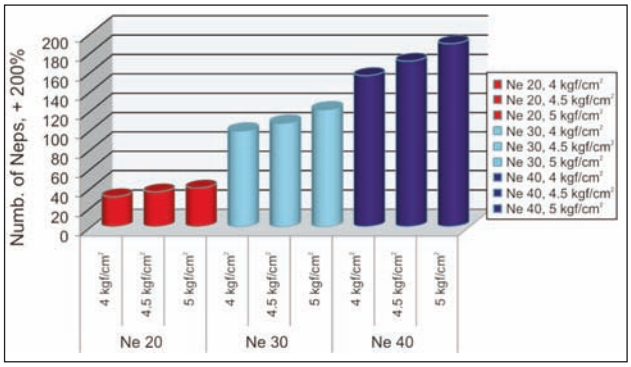

Fig. 6. The influence of yarn count and nozzle pressure on the neps formation (per km) along the yarns

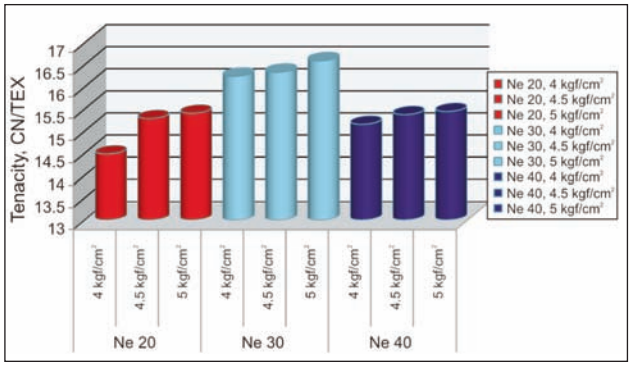

Fig. 7. The results of tenacity measurements of 100% cotton vortex spun yarns

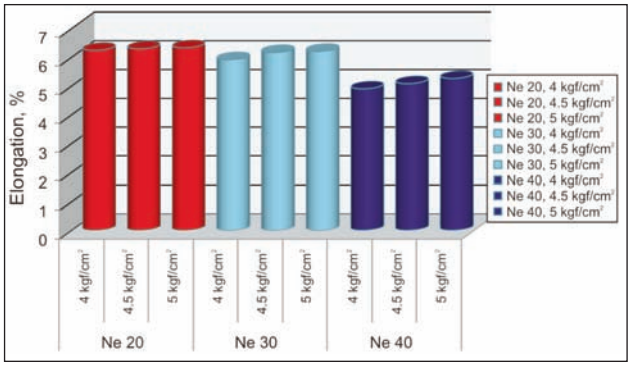

Fig. 8. The impact of nozzle pressure and yarn count on the breaking elongation of vortex spun yarns

formation increased as the nozzle pressure increased. In addition, more amounts of neps were observed on finer yarns. The highest amount was measured for Ne 40 yarn that was spun with the air pressure of 5 kgf/cm^2, whereas, the lowest amount was observed on Ne 20 yarn that was spun with the air pressure of 4 kgf/cm^2.

Tensile properties of vortex spun yarns

In terms of tenacity properties of vortex spun yarns, there are various opinions mentioned by different researchers. Tyagi et.al and Ortlek and Ulku claimed that compared with the finer yarns, coarser yarns performed better in terms of tenacity, breaking elongation and work-to break values. On the other hand, Murata Machinery Ltd. stated that the yarn tenacity increases as the yarn becomes finer [9–11]. Leitner et.al. also confirmed that coarser yarns possess higher tenacity and breaking elongation [12].

In figure 7, the results of tenacity measurements of 100% cotton vortex spun yarns are shown. It was observed that the tenacity of Ne 30 yarns achieved the greatest value with the applied nozzle pressure of 5 kgf/cm^2. On the other hand, the lowest value was obtained for Ne 20 yarns produced with the nozzle pressure of 4 kgf/cm^2. In general, increasing nozzle pressure caused a noticeable growth in tenacity. Analysis of experimental results revealed that tenacity values follow a decreasing trend as the yarn becomes too much finer or too much coarser. This could be explained by the wrapping length of the edge fibers and the ratio of wrapper and core fibers. Generally, vortex spun yarns contain 50–60 % of core fibers and the rest of them are wrapper fibers, respectively. Finer yarns have more amounts of wrapper fibers which means less amount of load bearing core fibers exist within the yarn. Consequently, tenacity and breaking elongation values decline in too much finer yarns. In too much coarser yarns, wrapping length of the edge fibers in the fiber bundle gets smaller and hence the tenacity declines [11].

The impact of nozzle pressure and yarn count on the breaking elongation of vortex spun yarns is illustrated in figure 8. Statistical analysis revealed that increase in nozzle pressure also increases the breaking elongation value for all vortex spun yarn samples. The highest value was obtained from the Ne 20 yarn that was spun under the nozzle pressure of 5 kgf/cm^2, whereas, the lowest value noted for Ne 40 yarn produced with nozzle pressure of 4 kgf/cm^2. It was also noticed that coarser yarns had greater breaking elongation values compared with finer yarns (figure 8). Alterations in breaking elongation values may be explained by the amount of wrapper fibers and wrapping length of the edge fibers on the yarn.

The effect of nozzle pressure and yarn count to the work-to break values of vortex spun yarns is illustrated in figure 9. According to the statistical analysis, it can be expressed that similar trend was observed for breaking elongation ratios and work-to break values of vortex yarn samples. As the yarn becomes coars-

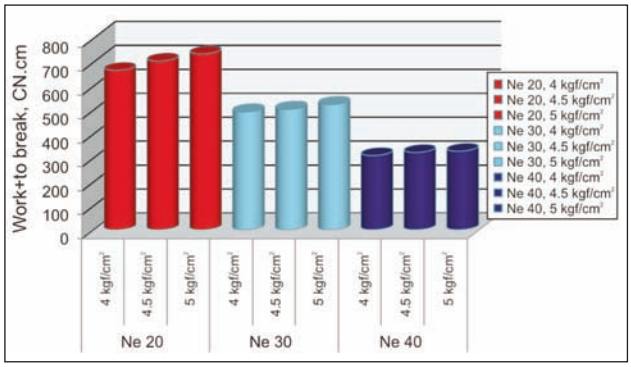

Fig. 9. The effect of nozzle pressure and yarn count to the work-to break values of vortex spun yarns

er, work-to break value rises up. Nozzle pressure also affected the work-to break values of yarns markedly. Work-to break values were triggered when the nozzle pressure was enhanced.

CONCLUSIONS

Vortex spun technology is a flourishing spinning technology among other traditional spinning technologies. Even the expansion speed of the technology settlement is going well all over the world; there are still some abstainable approaches about the vortex spun yarn production technology. This study is conducted aiming to better understand vortex spun technology, to support steady implementation of the technology among the textile world, and experimenting the influence of the nozzle pressure on the yarn properties for the cotton carded yarn production.

As result of the experimental work that has been carried out in the frame of the paper below listed conclusions can be drawn out;

1. Produced vortex spun yarn samples have three basic parts of a typical vortex yarn, core fibers, wrapper fibers and wild fibers. Experienced visual evaluation proved that amount of wrapper fibers increases with the increasing nozzle pressure. On the other hand, a decline in the amount of wrapper fibers was observed in coarser yarns.
2. Measured results and statistical analysis work prove that nozzle pressure and yarn count are important parameters that affect yarn hairiness. Yarn hairiness decrease with increased nozzle pressure as result of the fact that the whirling force of the nozzle air stream increases with the nozzle pressure, causes raised amount of uniform wrapping fiber. Finer yarn number of vortex spun yarn results lower hairiness values comparing the coarser vortex spun yarns.
3. Measured results and statistical analysis work prove that both air pressure and yarn count were significant factors for yarn evenness and imperfection properties. It was noticed that as the yarn gets finer, it becomes more uneven and the number of imperfections increases markedly.
4. Measured results show that the highest tenacity belongs to the Ne 30 yarns spun with the nozzle pressure of 5 kgf/cm^2; the lowest tenacity belongs to Ne 20 yarns spun with the nozzle pressure of 4 kgf/cm^2. In general, increasing nozzle pressure caused a noticeable growth in tenacity. Analysis of experimental results and previous literature studies revealed that tenacity values follow a decreasing trend as the yarn becomes too much finer or too much coarser. This could be explained by the rate of core and wrapper fibers of yarn body. Finer yarns have more amounts of wrapper fibers which mean less amount of load bearing core fibers resulting lower tenacity and breaking elongation.
5. Calculated work-to break values and statistical analysis work show that as the vortex spun yarn becomes coarser, work-to break value rises up. Increasing nozzle pressure also causes the higher value of the work-to break results.

ACKNOWLEDGEMENT

We would like to express our appreciation to Gülfiye Akbaş of Ayka Tekstil (Turkey) and Bülent Eren of Anteks (Turkey) for their valuable support during yarn processing and testing stages; to Assoc. Prof. Dr. Hüseyin Gazi Örtlek of Textile Engineering Department of Erciyes University (Turkey) for capturing optical images of the yarns; and to Scientific Research Projects Coordination Unit of Süleyman Demirel University (Turkey), (Project no: 1966-D-09) for the financial support.

BIBLIOGRAPHY

[1] Soe, A.K., Takahashi, M., and Nakajima, M. *Structures and properties of MVS yarns in comparison with ring yarns and open-end rotor spun yarns.* In: Textile Research Journal, 2004, vol. 74, issue 9, pp. 819-826.

[2] Zou, Z.Y., Yu, J.Y., Xue, W.L., Zhu, Y.D., Wu, J.M., Cheng, L.D. *Analysis of the fiber spatial trajectory in vortex spun yarn*. In: Textile Research Journal, vol. 79, issue 10, pp. 924-929.

[3] Altas, S.; Kadoglu, H.. *Comparison of the evenness, faults and hairiness of compact and conventional spun ring yarns*. In: Industria Textila, 2013, vol. 64, issue 3, pp. 65-69.

[4] Pei, Z., Yu, C. *Prediction of the vortex yarn tenacity from some process and nozzle parameters based on numerical simulation and artificial neural network*. In: Textile Research Journal, 2011, vol. 81, issue 17, pp. 1796-1807.

[5] Ortlek, H. G.; Kilic, G.; Bilgin, S., *Comparative study on the properties of yarns produced by modified ring spinning methods*. In: Industria Textila, 2011, vol. 62, issue 3, pp. 129-133.

[6] Basal,G. The Structure and Properties of Vortex and Compact Spun Yarns, PhD Thesis, 2003, North Carolina State University.

[7] Basal, G., Oxenham, W. *Effects Of some process parameters on the structure and properties of vortex spun yarn.* T In: Textile Research Journal, 2006, vol. 76, issue 6, pp. 492-499.

[8] Tyagi, G.K., Sharma, D., Salhotra, K.R. *Process-structure-property relationship of polyester-cotton MVS yarns: Part I-Influence of processing variables on the yarn structural parameters.* In: Indian Journal of Fiber & Textile Research, 2004, vol. 29, pp. 419-428.

[9] Tyagi, G.K., Sharma, D., Salhotra, K.R. *Process-structure-property relationship of polyester-cotton MVS yarns: Part II-Influence of processing variables on the yarn structural parameters.* In: Indian Journal of Fiber & Textile Research, 2004, vol. 29, pp. 429-435.

[10] Ortlek, H.G., Ulku S. *Effect Of some variables on properties of 100% cotton vortex spun yarn.* In: Textile Research Journal, 2005, vol. 75, issue 6, pp. 458-461.

[11] Oxenham,W. *Fasciated Yarns-A Revolutionary Development?*. In: Journal of TATM, 2001, vol. 1, issue 2, pp. 1-7.

[12] Leitner, H., Schwippl, H., Baldischwieler, O. *Air-jet spinning – yarns&fabrics compared to established spinning systems.* XIIth International Izmir Textile &Apparel Symposium, October 28-30 October 2010, Izmir, Turkey.

[13] Nazan Erdumlu, Bulent Ozipek, William Oxenham. *The structure and properties of carded cotton vortex yarns.* In: Textile Research Journal, 2012, vol. 82, issue 7, pp. 708-718.

[14] Ortlek, H. G., Ulku, S. *Effect of some variables on properties of 100% cotton vortex spun yarn.* In: Textile Research Journal, 2005, vol. 75, issue 6, pp. 458-461.

[15] Erdumlu, N. *An approach to investigate the Spinnability of fine count yarns on vortex spinning system.* İstanbul Technical University, Institute Of Science And Technology, Phd Thesis, p. 154, İstanbul (2011).

[16] Zou, Z., Liu, S., Zheng, S., Cheng, L. *Numerical computation of a flow field affected by the process parameters of murata vortex spinning*. In: Fibres and Textiles in Eastern Europe, 2010, vol.18, issue 2, pp. 35-39.

[17] Basal, G., Oxenham,W. *Vortex spun yarn vs. air-jet spun yarn*. In: Autex Research Journal, 2003, vol. 3, issue 3, pp. 96-101.

[18] Kılıc, M., Okur, A. *The properties of cotton-Tencel and cotton-Promodal blended yarns spun in different spinning systems.* In: Textile Research Journal, 2010, vol. 81, issue 2, pp. 156-172.

[19] Zheng, S., Zou, Z., Shen, W., Cheng, LD. *A Study of the fiber distribution in yarn cross section for vortex spun yarn.* In: Textile Research Journal, 2012, vol. 82, issue 15, pp. 1579–1586.

[20] Zou, Z., Cheng,L., Xue,W., Yu, J. A. *Study of the twisted strength of the whirled airflow in murata vortex spinning.* In: Textile Research Journal, 2008, vol. 78, issue 8, pp. 682-687.

Authors:

Chief of works Dr. Eng. GİZEM KARAKAN

Dr. RAMAZAN ERDEM

Textile Technology Department, Serik G-S Süral Vocational School of Higher Education,

Akdeniz University, Aspendos Yolu No 1 Belkıs, Serik, Antalya, Türkiye, 07500

e-mail: karakan_gizem@hotmail.com, ramazanerdem@akdeniz.edu.tr

Assoc. Prof. Eng. SEMA PALAMUTÇU

Textile Engineering, Engineering Faculty, Pamukkale University,

Kınıklı Kampüsü, Denizli, Türkiye, 20070.

e-mail: spalamut@pau.edu.tr

Prof. Dr. Eng. GABİL ABDULLA

Textile Engineering, Engineering Faculty, Süleyman Demirel University,

Çünür, Isparta, Türkiye, 32260.

e-mail: gabil@mmf.sdu.edu.tr

Protective properties against UV radiation of natural silk textiles

BARBARA BINKOWSKA
ANDRZEJ SAPIEJA
ROMUALDA MARSZAŁEK
TERESA HERNIK

REZUMAT – ABSTRACT

Caracteristicile de protecție ale textilelor din mătase naturală împotriva radiațiilor UV

Studiul determină caracteristicile de protecție împotriva radiațiilor UV ale diverselor țesături albe din mătase pură și efectul modificării acestor țesături cu colorantul complex metalic în raport 1:2 colorant și absorbanți UV, cu structură chimică diferită pentru a le crește caracteristicile de protecție. Evaluarea a fost realizată prin determinarea Factorului de Protecție împotriva radiațiilor ultraviolete (UPF) și prin compararea acestuia cu cerințele standardelor relevante: din Europa și Australia. S-a evidențiat că nicio țesătură din mătase albă testată nu asigură caracteristici de protecție împotriva radiațiilor UV. În cazul materialului cu cea mai mică masă per unitate de suprafață (35 g/m^2), nicio modificare efectuată nu îmbunătățește protecția UV. Pentru celelalte materiale testate care au masa per unitatea de suprafață mai mare de 51 g/m^2, modificarea are ca rezultat o protecție UV bună sau excelentă.

Cuvinte-cheie: radiații UV, caracteristici de protecție UV, textile din mătase naturală, modificare, coloranți, absorbanți UV

Protective properties against UV radiation of natural silk textiles

The study determines the protective properties against UV radiation of different white pure silk fabrics and the effect of modification of these fabrics with metal complex 1:2 dyestuff and UV absorbers, with different chemical structure, to increase their protective properties. Evaluation was performed by determining the Ultraviolet Protection Factor (UPF) and comparing it to the requirements of the relevant standards: European and Australian. It was found that none of the white silk fabric tested have protective properties against UV radiation. None of the modifications for the item with smallest surface mass (35 g/m^2) improves the UV protection. For other tested materials that have surface mass higher than 51 g/m^2 the modification results in good or excellent UV protection result.

Key-words: UV radiation, UV protective properties, natural silk textiles, modification, dyes, UV-absorbers

INTRODUCTION

The hazard linked to the effect of UV radiation from sunlight on human skin is commonly acknowledged. This radiation has strong photochemical activity which affects the immune system of the organism. When reaching the dermis it damages collagen and elastin fibres, accelerating ageing of skin, causes allergies, damages blood vessels, drying of skin and finally causes skin cancers. This danger is even higher because of the ozone depletion phenomenon. Clothes and other textile products may act as an efficient protection against sun radiation. When UV rays interact with a textile product, the photoenergy of the rays becomes partially reflected, partially absorbed and finally in some part permeates through the textile material (transmission) reaching human organism. The ratio of these three components (spectra) is different and depends on a number of physical and chemical parameters of the textile product. [1–4]

The requirements for clothing products include a wide range of features and properties and have risen over the last decades, especially in terms of hygienic and physiological properties. Increasingly more often the textile products are designed not only for comfort of users but also with the view to their health and safety. The issue of developing textile with UV protection properties is great importance in Poland and the whole world. In this area the studies on textile modification focus mainly on cellulosic or synthetic fibres but the knowledge on UV protection properties of natural silk textiles are limited. [5–9]

The evaluation of UV protection properties is conducted by determination of the so called UPF (Ultraviolet Protection Factor). The value of UPF for textiles depends on the following factors: raw material and its structure, type and intensity of dyeing and the presence of nondyeing organic substances that selectively absorb UV rays.

UPF indicates how many times the textile product weakens the effect of UV rays on the skin, i.e. how much longer the sun would have to fall directly on the skin to cause its reddening. For example, when the UPF of a given product is 30 and the reddening of the unprotected skin occurs after 1 h of exposure, in case of using such a product reddening will occur only after 30 hours. [1, 3]

EXPERIMENTAL PART

Research methodology

The basic problem to be solved was decreasing the intensity of UV radiation that passes through the silk textile and affects human skin. The silk textiles were designed to absorb high amount of the UV rays within the textiles structure.

To achieve this property, white silk textiles of various porosity (with different weave, linear mass of the yarn, density of threads, surface mass of the product, thickness, type of raw material i.e. filament or staple fibre) were subject to modification with chemical substances, which chemicals due to their structure could serve as UV absorbers. The applied substances that included synthetic organic dyes of various colour systems and functional groups were used separately and in combinations. Moreover, the substances that do not have dyeing properties, but are potentially able to absorb UV rays, were studied.
The evaluation of the UV protection properties of the modified textiles made of natural silk was performed by determining UPF i.e. Ultraviolet Protection Factor according to the PN-EN 13758-1:2007 standard by Cary 50 Solarscreen.
The rating of silk fabrics' protective properties against UV radiation was given on the basis of the determined factor of UPF by comparing its value to the requirements set out in the following standards:

- Australian / New Zealand Standard No. AS / NZS 4399:1996 "Sun protective clothing – Evaluation and classification" – according to the standard specified

UPF Range	UV protection category
15-24	Good protection
25-39	Very Good protection
Above 40	Excellent protection

- European Standard EN 13758-2:2007 "Textiles – Solar UV protective properties – Part 2: Classification and parking of apparel" – standard specifies the required value for the coefficient UPF fabric barrier against UV radiation (UPF 40 +).

MATERIALS USED

In the study the following materials with a broad spectrum of parameters describing their structure were used: white filament, natural silk fabric (Georgette, Crepe, Satin, Taffeta) and staple fiber (Bourette). Table 1 shows the basic metrological parameters.

Application research

The processes of dyeing and treatment with UV absorbers were made by E. Benz laboratory jigger.

Dyeing

The dye used in the study is metal complex 1:2 dyestuff. A mixture of surfactants with wetting and dispersing properties was used as the leveling agent for dyeing. Silk fabrics (Georgette, Crepe, Satin, Bourette) were dyed in three intensities (light, medium, dark).
As table 2 shows the dye bath ingredients which were used to obtain specific effect of dyeing.

Application works with UV absorbers

As chemical companies do not offer any UV absorbers for natural silk, the study tested products that are applied on fabrics with similar chemical structure, ie. wool, polyamide.
According to the manufacturer, UV Absorber 1 is an anionic product used for cellulose fibers and polyamide. It is a white viscous liquid. As far as the chemical structure is concerned, it is a heterocyclic compound which reacts with the hydroxyl groups of cellulose and polyamide amine. UV Absorber 2 is an anionic product used for wool fibers – a yellow – brown, transparent, viscous liquid. It belongs to sulfonated derivatives of benzotriazoles. The product can be used in exhaustion and continuous application, and can bind the application process with dyeing or apply it after the treatment.
Both products were applied on silk fabric in accordance with the technological conditions indicated by the manufacturers after some necessary modifications required due to the properties of silk. Absorbers were applied on white textiles, and not washed ones. After drying, the modified (UV absorber No. 1 or No. 2) samples were tested to determine the UPF. The results were compared with the coefficients determined for adequate unmodified samples. The comparison showed that increase of the UPF in relation to non-modified fabrics was obtained only by absorber No. 2 (exhaust method). Therefore, further work was performed only with the absorber applied by exhaust.

Table 1

BASIC METROLOGICAL PARAMETERS OF WHITE SILK FABRICS USED IN TESTS

Parameter	Filament fibre				Staple fibre
	Georgette	*Crepe*	*Satin*	*Taffeta*	*Bourette*
Surface mass [g/m^2]	35	51	87	89	148
Thickness [mm]	0.15	0.16	0.19	0.16	0.54
Number of threads of warp in the woven fabric [1/dm]	394	616	1342	728	202
Number of threads of weft in the woven fabric [1/dm]	320	396	544	302	146
Weave [-]	plain	plain	satin	plain	plain

Table 2

METAL-COMPLEX DYE COMPOSITIONS USED IN DYEING PROCESSES		
Sample No.	**Colour**	**Metal-complex dyes for dyeing**
1	pink	Red G 0.8%
2	red	Red G 3%
3	cocoa	Brown RL 1% C. I. Acid Brown 365
4	dark green	Navy Blue RL 2% C. I. Acid Blue 193 Yellow RL 1% C. I. Acid Yellow 194
5	navy blue	Navy Blue RL 2,5% C. I. Acid Blue 193 Black RL 0.6% C. I. Acid Black 194
6	vanilla	Brown RL 0.1% C. I. Acid Brown 365 Yellow RL 0.1% C. I. Acid Yellow 194
7	claret	Brown RL 1% C. I. Acid Brown 365 Red G 0.5%

For three samples of the modified fabrics water washing process was performed. The process conditions were the same as the silk washing conditions at home.

RESULTS AND ANALYSIS

The test results are shown in table 3. On the basis of the results it was observed that:

- Out of five white silk fabrics two (Taffeta and Bourette) have a UPF factor of 10, one (Satin) 5, and two others (Crepe and Georgette) 0. There are no protective properties against UV radiation according to both European and Australian standards.
- Taffeta fabric made of dark-coloured silk yarn has a UPF greater than 50. Therefore, it has excellent barrier properties against UV radiation.
- Bourette fabric dyed in medium (claret), Satin fabric dyed in light (pink) and dark (red, blue) colour have a UPF greater than 50, and thus also have excellent barrier properties against UV radiation.
- Crepe fabric dyed in dark colour (navy blue, red) has a UPF of 15, the average colour (cacao) – 5, and light colour (vanilla) – 0. According to the Australian Standard only crepe in dark colorus have protective properties against UV radiation at a good level. According to the European standard silk fabric – crepe, regardless of dyeing intensity, does not have barrier properties.
- Georgette fabric dyed both in light colour (pink) and dark (blue) has a UPF 0. In this case metal complex 1:2 dyes do not affects the protective properties against UV radiation.
- Modification of white Satin (which left colour of the fabric intact) with the UV absorber has increased the UPF values from 5 to 50 and thus gave it better barrier properties against UV radiation. The same modification has increased the white Crepe UPF values but only from 0 to 15 and gave it good barrier properties against UV radiation according to Australian standards. Modification of white Georgette with UV absorber does not result in any changes in the UPF that remained at 0.
- Modification of Satin previously dyed in light colours (pink) or dark (red, green) with UV absorber has not changed the UPF properties, which were excellent even before the process (> 50). No change of the UPF after the washing process was observed.
- Modification of Crepe dyed light (vanilla) with UV absorber, increased UPF from 0 to 15, and colour (cocoa) from 5 to 15, giving it thus good protection against UV radiation according to Australian standards. Modification of Crepe with UV absorber, previously dyed dark colours (red, blue) increased the UPF value from 15 to 20, improving the already good protective properties. Unfortunately, the process of washing of earlier modified Crepe, dyed in dark blue, made the UPF fell back to 15.

Table 3

VALUES OF BARRIER COEFFICIENT AGAINST UV RADIATION FOR NATURAL SILK FABRICS				
Type of fabric				**UPF**
Fabric	**Treatment method**			
	colour	***absorber no. 2***	***washing***	
Taffeta	white	-	-	**10**
	eggplant	-	-	**+ 50**
Bourette	white	-	-	**10**
	claret	-	-	**+ 50**
Satin	white	-	-	**5**
		+	-	**+ 50**
	pink	-	-	**+ 50**
		+	-	**+ 50**
	red	-	-	**+ 50**
		+	-	**+ 50**
		+	+	**+ 50**
	green	+	-	**+ 50**
		+	+	**+ 50**
	navy blue	-	-	**+ 50**
Crepe	white	-	-	**0**
		+	-	**15**
	vanilla	-	-	**0**
		+	-	**15**
	cocoa	-	-	**5**
		+	-	**20**
	red	-	-	**15**
		+	-	**20**
	navy blue	-	-	**15**
		+	-	**20**
		+	+	**15**
Georgette	white	-	-	**0**
		+	-	**0**
	pink	-	-	**0**
		+	-	**0**
	navy blue	-	-	**0**

- Modification of Georgette with UV absorber, previously dyed light and dark did not result in a UPF higher than 0.

CONCLUSIONS

1. None of the white, silk fabric (with different linear and surface mass of the product density of threads, thickness, weave, type of raw material ie filament or staple fiber) that were tested have protective properties against UV radiation according to both European and Australian.
2. Metal complex 1:2 dyes provide barrier properties against UV radiation (UPF 50) for silk fabrics like Taffeta, Satin, Bureta, and others with the greater surface mass of fabrics (over 87 g/m^2).
3. Crepe with a surface mass 51 g/m^2 can provide some protection from UV radiation when dyed dark. In case of white or dyed fabrics, they have to be modified and dyed light / medium color with UV absorber. Maximum UPF achieved by tested fabrics is 15–20, which in accordance with the Australian is lowest level to ensure good protection against UV radiation.
4. For Georgette as the lightest of the test fabrics, (surface mass 35 g/m^2), none of the modifications performed – dyeing, finishing with UV absorber, dyeing followed by a UV absorber treatment – resulted in an increase in the protective properties against UV radiation. UPF in each option was equal to 0.
5. The fabric modified with UV absorber used in the study is not resistant to washing in water. Therefore, to maintain the absorber-related protective properties of fabrics (Crepe) the modification must be repeated during care process.

BIBLIOGRAPHY

[1] Jędrzejewski, W. *The barrier properties of fabrics and UV radiation* In: Przegląd Włókienniczy, 2001, issue 2, p. 22

[2] Przybył, K., Bącler, M. *About textiles and ultraviolet radiation* In: Przegląd Włókienniczy – WOS, 2004, issue 8, p. 44

[3] Zielińska, J., Kuś, S., Marszałek, R. *Study on protective properties against UV radiation of flax and hemp textiles*. In: Przegląd Włókienniczy, 2001, issue 8, p. 10

[4] Lewartowska, J., Gajdzicki , B., Sójka-Ledakowicz, J., Kudzin, M. *Knitwear with optimal performance and UV barrier* In: Przegląd Włókienniczy – WOS, 2006, issue 5, p. 38

[5] Schmidt-Przewoźna, K., Zimniewska, M. *The barrier properties of flax and hemp fabrics naturally colored – UV protection.* In: Spektrum, 2006, issue 1, p. 26

[6] Michałowski, W. *The barrier properties of flax and hemp fabrics naturally colored – UV protection.* In: Przegląd Włókienniczy, 1996, issue 5, p. 27

[7] Paluszkiewicz, J., Czajkowski, W. *Reactive Dyes for Cellulose Fibers Including UV Absorbers* In: Fibers & Textiles in Eastern Europe, 2005, p. 76-80

[8] Algaba, I., M. *Correlation between the ultraviolet protection factor and the weight and thickness of undyed cellulosic woven fabrics.* In: Fibers & Textiles in Eastern Europe, 2008, p. 85-89

[9] Gabrijelčič, H. *Influence of fabrics constructional parameters and thread colour on UV radiation protection.* In: Fibres & Textiles in Eastern Europe, 2009, p. 46-54

Authors:

BARBARA BINKOWSKA
ROMUALDA MARSZAŁEK
ANDRZEJ SAPIEJA
TERESA HERNIK
Institute of Natural Fibres & Medicinal Plants
ul. Wojska Polskiego 71 b, 60-630 Poznań
Poland

Corresponding author:

ROMUALDA MARSZAŁEK
e-mail: romualda.marszalek@iwnirz.pl

A research on various comfort properties of interlock knitted fabrics

EMİNE UTKUN

REZUMAT – ABSTRACT

Studiu privind varietatea proprietăţilor de confort ale tricoturilor interloc

Tricoturile, care au avut o mare popularitate în ultimii ani, sunt printre materialele textile preferate pentru realizarea îmbrăcămintei de zi cu zi, a îmbrăcămintei sport şi a lenjeriei. În cadrul acestui studiu au fost examinate şi comparate permeabilitatea la aer, permeabilitatea la apă şi capacitatea de alungire pe direcţia rândurilor şi a şirurilor de ochiuri din structura tricotului interloc din bumbac, acesta fiind unul dintre cele mai preferate tricoturi pentru domeniile menționate. Se știe faptul că preţul firelor mai subţiri este mai ridicat decât cel al firelor mai groase. Scopul acestui studiu a fost de a prezenta textilele din bumbac cu proprietăţi optime pentru realizarea îmbrăcămintei de zi cu zi şi a celei sport şi, pe de altă parte, de a face o evaluare ţinând cont de factorul cost.

Cuvinte-cheie: tricot interloc, permeabilitate la aer, permeabilitate la apă, proprietăţi de alungire

A research on various comfort properties of interlock knitted fabrics

Knitted fabrics, which have been very popular in recent years, are amongst the preferred fabrics in casual wear, sportswear and underwear. Within the scope of this study, air permeability, water permeability and course & wale elongation amount of the texture of cotton interlock fabric, which is one of the most preferred fabric textures in casual wear and sportswear, were examined and compared. As it is known, the prices of thinner yarns are higher than thicker yarns. The purpose of this study was specifying the cotton fabrics which have the optimum properties for casual wear and sportswear, and on the other hand to make an evaluation by taking the cost factor into consideration.

Key-words: interlock knitted fabric, air permeability, water permeability, elongation properties

INTRODUCTION

When designing fabrics, the functional properties and the main structural parameters of fabrics must be fully understood [1]. Turan and Okur (2008) examined the model studies, which were developed by different researchers, in the light of literature in order to estimate the relationship between the fabric's structural parameters and the product performance, the parameters that affect the air permeability of the fabric. In the study, it was emphasized that taking the place and conditions of the product use into consideration, evaluating them considering the relationship of the structural factors and progressing with the product development stages under control would gain advantage to the manufacturers in terms of time and cost [2].

Clothing comfort is an important factor in the stage where people make their clothing selections [3]. There are many studies in literature regarding the research of the comfort properties of knitted fabrics. Uçar and Yılmaz (2004) examined the thermal properties of 1×1, 2×2 and 3×3 rib knitted fabrics [4]. Güneşoglu et. al. (2005) researched the thermal contact properties of 2-yarn fleece knitted fabrics which are widely used in outerwear [5]. Marmaralı et. al. (2007) examined the effect of the elastic yarn amount in knitted fabric structure on the thermal properties of the fabrics [6]. Oğlakcioğlu and Marmaralı (2007) researched the thermal comfort properties of single jersey, rib and interlock knitted fabrics, which were produced from cotton and polyester yarns, by using Alambeta and Permetest devices [7]. Özdil et. al. (2007) examined the thermal comfort properties of knitted fabrics with 1x1 rib structure by using yarns with different properties [8]. Çil et al. (2009) studied the comfort properties of cotton, acrylic and cotton-acrylic mix knitted fabrics, such as water vapor permeability, transfer and longitudinal wicking abilities, drying properties [9]. Hes et. al. (2009) researched the thermo-physiological and thermal contact properties of knitted fabrics with single jersey structure, which were produced from non-traditional natural fibers such as maize, soy and bamboo viscose fibers, under dry and wet conditions [10]. Mavruz and Oğulata (2009) determined the air permeability values of cotton knitted fabrics with different yarn count, knitted type and loop density, and tried to form regression equations in order to estimate the air permeability value with definite fabric parameters before the production [11]. Majumdar et. al. (2010) analyzed the thermal comfort properties of fabrics with single jersey, rib and interlock structure, which were produced from cotton, bamboo and cotton-bamboo mix yarns [12]. Ramachandran et. al. (2010) examined the thermal properties of knitted fabrics with single jersey, rib and interlock structure, which were produced from ring and compact-spun yarns [13]. Bivainyte and Mikucioniene (2011) researched the effect of the knit structure, fiber type and yarn properties in double-layered knitted fabrics on the air and water vapor permeability properties [14]. Cubric et. al.

(2012) produced single jersey knitted fabrics and analyzed the significant fabric parameters that affected the heat transfer of fabrics through a porous structure [15]. Onofrei (2012) researched slowness of drying, intrinsic fabric thermal insulation, fabric permeability and fabric wicking properties of knitted fabrics, which were contained Outlast® and Coolmax® yarns [16].

The purpose of this study was to compare the air permeability, water permeability and course & wale elongation amount of cotton interlock fabrics, which were manufactured with different yarn counts. Thus, this could allow the manufacturers to manufacture cost-efficient fabrics with optimum properties. Unless there were statistically significant differences amongst the fabrics in terms of the required properties, it was possible to prefer the cost-efficient fabric. In this way, consumers would have the opportunity to purchase the products, which have the required properties, for a better price.

EXPERIMENTAL PART

Materials

Values related to yarns of the fabrics within the scope of the study are shown in table 1.

All the fabrics were produced in circular knitting machines. Technical data of the knitting machines, in which the fabrics were produced, are given in table 2. The fabrics were subjected to the commercial finishes used in the market. Grease remover, wetting, antipilling enzyme, acetic acid, fabric protector, respectively were applied on fabrics. After the wet finishes, they were dried and sanforized. The weight, thickness and density values of the fabrics are given in table 3.

Method

All the experimental studies in this section were performed in the Textile Laboratories in the Technical Chieftaincy of Denizli Textile Laboratory of Turkish Standards Institution. All the fabric samples were conditioned by being kept under the atmosphere conditions (20 ± 2 °C temperature and % 65 ± 5 relative humidity) for at least 24 hours before the experimental studies. The analysis of the obtained data was made by using SPSS 15.0 statistical packaged software. The properties studied on the manufactured fabrics were as follows.

The weights of the fabrics were determined according to TS EN 12127 standard and the thickness values of the fabrics were determined according to TS 7128 EN ISO 5084 standard.

Air Permeability

Air permeability is the airspeed that vertically passes through a test piece, the conditions of which such as test field, pressure drop and time are specified [17].

Table 1

CHARACTERISTICS OF THE YARNS OF THE FABRICS

Yarn Code	Raw Material	Yarn Count (Nm)	Twist Coefficient (αe)	Direction of Twist
Y1	%100 Cotton	30/1, ring	3.6	Z
Y2	%100 Cotton	40/1, ring	3.6	Z
Y3	%100 Cotton	50/1, ring	3.6	Z
Y4	%100 Cotton	60/1, ring	3.6	Z

Table 2

CHARACTERISTICS OF THE KNITTED MACHINES

Fabric code	Knitted type	Brand	Model	Production year	System count	Needle count	Inch	Fineness (inch)
1	Interlock	S Sangyoung	U-1.2.8	2007	96	2568	34	24
2	Interlock	S Sangyoung	U-1.2.8	2007	96	3000	34	28
3	Interlock	S Sangyoung	U-1.2.8	2007	96	3000	34	28
4	Interlock	S Sangyoung	U-1.2.8	2007	96	3000	34	28

Table 3

CHARACTERISTICS OF THE FABRICS

Fabric code	Weight (g/m²)	Thickness (mm)	Wales per cm	Courses per cm	Loop density (loops/cm²)	Yarn code
1	265	1.086	15	16	240	Y1
2	221	0.954	16	19	304	Y2
3	193	0.911	18	18	324	Y3
4	171	0.838	19	22	418	Y4

The air permeability of the fabrics was measured according to TS 391 EN ISO 9237 – Textiles – Determination of Air Permeability on Fabrics standard. The measurements were conducted by applying 100 Pa pressure on the surface area of 20 cm^2 in Textest FX 3300 air permeability measuring device.

Water Permeability

Water permeability is the water pressure amount at the time when the water pressure, which is applied on fabric under specific conditions, is discharged from fabric [18]. The water permeability of the fabrics was measured according to TS 257 EN 20811/T1 – Textile Fabrics – Determination of Resistance to Water Penetration-Hydrostatic Pressure Test standard. The measurements were conducted by applying 60 mbar/minute rate of increase of water pressure in Textest FX 3000 Hydrostatic Head Tester measuring device.

Elongation Properties

The elongation property of fabric is the increase of length, which is expressed with the percentage of the initial length of the fabric as a result of the load applied on fabric under specific conditions [19]. The determination of elongation properties of the fabrics was performed according to TS 10985 – Textiles – Knitted Fabrics – Low Force Applied – Permanent Elongation and Determination of Stretching Properties standard. The measurements were conducted by applying a tensile load of 45 Newton in 4–6 seconds on Instron 4465 measuring device.

RESULTS AND DISCUSSION

The mean values, standard deviations and measurement units of air permeability, water permeability, wale elongation, course elongation, which were obtained from the standard measurements conducted on the fabrics, are shown in table 4.

The significance value within the study was acknowledged as (p) 0.05. If significance value (p) of a parameter was greater than 0.05 ($p > 0.05$), it was interpreted that the parameter did not make a statistically significant difference.

One Way Analysis of Variance (ANOVA) was conducted on the independent samples in order to determine if yarn counts of the fabrics showed statistically significant differences on the air permeability, water permeability, wale elongation and course elongation values.

The hypotheses of ANOVA analysis, which were conducted for each property, were as follows.

"H0": There is not any difference between the fabrics in terms of analyzed property.

"H1": There is a difference between the fabrics in terms of analyzed property.

Before the variance analysis, Levene Test was conducted and variance homogeneity was tested. It was seen that the variances were homogeneous, and in this instance, in order to define the relationship between the fabrics, Tukey HSD multiple comparison test was conducted.

Air Permeability

According to the results of Levene Test, $F = 0.877$ and significance level was $p = 0.474$; in this case, it was observed that distribution variances were homogeneous. According to the results of ANOVA, $F = 164.345$ and $p = 0.000$. Therefore, "H1" hypothesis was accepted; in other words, there was a statistically significant difference between the air permeability values of the fabrics. According to Tukey HSD multiple comparison test, which was conducted after ANOVA test, while the fabrics 1 and 2 made one group, the fabric 3 made the second group, and the fabric 4 made another group.

Water Permeability

According to the results of Levene Test, $F = 2.131$ and significance level was $p = 0.136$; in this case, it was observed that distribution variances were homogeneous. According to the results of ANOVA, $F = 46,647$ and $p = 0,000$. Therefore, "H1" hypothesis was accepted; in other words, there was a statistically significant difference between the water permeability values of the fabrics. According to Tukey HSD multiple comparison test, which was conducted

Table 4

RESULTS OF THE STANDARD MEASUREMENTS OF THE FABRICS

Fabric code	Air Permeability (l/m²/h)			Water Permeability (mbar)			Wale Elongation (%)			Course Elongation (%)		
	N	Mean	Standard deviation	N	Mean	Standard deviation	N	Mean	Standard deviation	N	Mean	Standard deviation
1	5	2898	230	5	9.5	0.4	5	40.9	2.7	5	115.3	0.5
2	5	2662	98	5	8.8	0,8	5	32.4	1,4	5	101.3	2.2
3	5	4292	147	5	11.2	0,3	5	43.6	0,5	5	151.8	4.1
4	5	4694	198	5	11.8	0,3	5	43.8	0,5	5	141.3	2.5

after ANOVA test, while the fabrics 1 and 2 made a group, the fabrics 3 and 4 made another group.

Elongation Properties of Wale

According to the results of Levene Test, F = 2.705 and significance level was p = 0,080; in this case, it was observed that distribution variances were homogeneous. According to the results of ANOVA, F = 59.163 and p = 0.000. Therefore, "H1" hypothesis was accepted; in other words, there was a statistically significant difference between the wale elongation values of the fabrics. According to Tukey HSD multiple comparison test, which was conducted after ANOVA test, while the fabrics 1 and 3 made one group, the fabric 2 made second group, and the fabrics 3 and 4 made another group.

Elongation Properties of Course

According to the results of Levene Test, F = 2.274 and significance level was p = 0.119; in this case, it was observed that the distribution variances were homogeneous. According to the results of ANOVA, F = 375.666 and p = 0,000. Therefore, "H1" hypothesis was accepted; in other words, there was a statistically significant difference between the course elongation values of the fabrics. According to Tukey HSD multiple comparison test, which was conducted after ANOVA test, each of the fabrics 1, 2, 3 and 4 made a separate group.

CONCLUSIONS

Interlock fabrics have a closer texture compared to single jersey and rib textures. The fabrics with such texture have often been used in casual wear and sportswear in recent years. Heat and moisture transfer properties as well as elongation properties of these fabrics should be good so that they can have optimum properties.

At the end of the evaluation of the measurements and analysis which were conducted on the properties examined within this study, table 5 was generated.

Table 5

EVALUATION OF THE MEASUREMENTS				
Fabric code	**Air permeability**	**Water permeability**	**Wale Elongation**	**Course Elongation**
1	3	2	2	3
2	3	2	3	4
3	2	1	1-2	1
4	1	1	1	2

Note: While the number 1, which is used in the table for evaluation, indicates that the fabric provides the highest value for the mentioned property, an increase on the number indicates that the mentioned value lowers.

As it was understood from the results, fabric 4 provided the best values in terms of the analyzed properties. However, it was observed that fabric 3 did not have statistically significant differences compared to fabric 4 in terms of water permeability and wale elongation properties, and that it followed fabric 4 in terms of air permeability, and that it provided better values than fabric 4 in terms of course elongation.

Acknowledgement

My profound thanks to the Technical Chieftaincy of Denizli Textile Laboratory of Turkish Standards Institution that helped to carry out the experimental studies, and to Denizli Kaya Textile in the presence of Kürşat ARIKAN in the production of the fabric samples.

BIBLIOGRAPHY

[1] Behera B.K., Karthikeyan B. *Artificial neural network-embedded expert system for the design of canopy fabrics.* In: Journal of Industrial Textiles, 2006, vol. 36, issue 2, pp. 111-123.

[2] Turan R.B., Okur A. *Air permeability of fabrics.* In: The Journal of Textiles and Engineers, 2008, vol.15, issue 72, pp. 16-25.

[3] Utkun E. *Comfort-related properties of woven fabrics produced from Dri-release® yarns*. In: Industria Textila, 2014, vol. 65, issue 5, pp. 241-246.

[4] Uçar N., Yılmaz T. *Thermal properties of 1x1, 2x2, 3x3 rib knit fabrics.* In: Fibers & Textiles in Eastern Europe, 2004, vol. 12, issue 3/47, pp. 34-38.

[5] Gunesoglu S., Meric B., Gunesoglu C. *Thermal contact properties of 2-yarn fleece knitted fabrics.* In: Fibres&Textiles in Eastern Europe, 2005, vol. 13, issue 2/50, pp. 46-50.

[6] Marmaralı, A., Özdil, N., Kretzschmar, S.D. *Thermal comfort properties of plain knitted fabrics with elastic yarn.* In: Journal of Textile and Apparel, 2007, vol. 17, issue 3, pp. 178-181.

[7] Oglakcioglu N., Marmarali A. *Thermal Comfort Properties of Some Knitted Structures.* In: Fibers & Textiles in Eastern Europe, 2007, vol. 15, issue 5-6/64-65, pp. 94-96.

[8] Özdil, N., Marmaralı, A., Kretzschmar, S.D. *Effect of yarn properties on thermal comfort of knitted fabrics.* In: International Journal of Thermal Sciences, 2007, vol. 46, pp. 1318-1322.

[9] Çil, M.G., Nergis, U.B., Candan, C. *An experimental study of some comfort-related properties of cotton-acrylic knitted fabrics.* In: Textile Research Journal, 2009, vol. 79, issue 10, pp. 917-923.

[10] Hes L., Oliveira N., Neves M.M. *Thermophysiological and thermal contact properties of wet knits made of non-traditional natural fibres.* Natural Fibers of Australasia – Combined (NZ and AUS) Conference of the Textile Institute, University of Otago, Dunedin, New Zealand, 15-17 April 2009.

[11] Mavruz S., Oğulata R.T. *Investigation and statistical prediction of air permeability of cotton knitted fabrics.* In: Journal of Textile and Apparel, 2009, vol. 1, pp. 29-38.

[12] Majumdar, A., Mukhopadhyay, S., Yadav, R. *Thermal properties of knitted fabrics made from cotton and regenerated bamboo cellulosic fibers.* In: International Journal of Thermal Sciences, 2010, vol. 49, pp. 2042-2048.

[13] Ramachandran T., Manonmani G., Vigneswaran C. Thermal behavior of ring- and compact-spun yarn single jersey, rib and interlock knitted fabrics. In: Indian Journal of Fiber & Textile Research, 2010, vol. 35, pp. 250-257.

[14] Bivainyte A., Mikucioniene D. *Investigation on the Air and Water Vapour Permeability of Double-Layered Weft Knitted Fabrics.* In: Fibres & Textiles in Eastern Europe, 2011, vol. 19, issue 3, pp. 69-73.

[15] Cubric I.S., Skenderi Z., Mihelic-Bogdanic A. Andrassy M. *Experimental study of thermal resistance of knitted fabrics.* In: Experimental Thermal and Fluid Science, 2012, vol. 38, pp. 223-228.

[16] Onofrei E. *Identification of the most significant factors influencing thermal comfort using principal component analysis and selection of the fabric according to the apparel end-use.* In: Industria Textila, 2012, vol. 63, issue 2, pp. 91-96.

[17] TS 391 EN ISO 9237. Textiles – Determination of Air Permeability on Fabrics Standard, 1999.

[18] TS 257 EN 20811. Textile Fabrics – Determination of Resistance to Water Penetration-Hydrostatic Pressure Test Standard, 1996.

[19] TS 10985. Textiles – Knitted Fabrics – Low Force Applied – Permanent Elongation and Determination of Stretching Properties Standard, 1993.

Author:

Asist. prof. dr. EMİNE UTKUN
Buldan Vocational Training School
Program of Fashion Design
Pamukkale University
Denizli 20400
Turkey

Corresponding author:

EMİNE UTKUN

e-mail: eutkun@pau.edu.tr

A simulation method of plain fabric texture for image analysis

RURU PAN
BO ZHU
ZHONGJIAN LI
JIHONG LIU
WEIDONG GAO

REZUMAT – ABSTRACT

Metodă de simulare a structurii țesăturilor plane pentru analiza imaginii

Pentru simularea structurii țesăturii și pentru construirea modelului caracteristic pentru analiza imaginii textilelor, acest studiu propune o metodă de simulare pe baza distribuției nivelului de gri al flotărilor din țesătură. În primul rând, distribuția nivelului de gri al flotărilor din țesătură din imaginea țesăturii simulate este ajustată prin setarea unor parametri diferiți. Ulterior sunt simulate imaginile țesăturii în condiții diferite de iluminare, iar finețea firului și desimea țesăturii sunt ajustate prin setarea parametrilor. În final, imaginile simulate ale țesăturii pot fi extrase sub formă de imagini ale structurii. Prin ajustarea adecvată a parametrilor, metoda propusă poate avea ca rezultat un model ideal al texturii structurii plane pentru analiza imaginii.

Cuvinte-cheie: structurii țesăturii plane; simularea țesăturii; flotare în țesătură; ajustarea parametrilor

A simulation method of plain fabric texture for image analysis

In order to simulate the woven fabric texture and construct the characteristic model for textile image analysis, this paper proposes a simulation method based on the gray level distribution of weave floats. Firstly, the gray level distribution of weaving floats in the simulated fabric image is adjusted by setting different parameters. Then, the fabric images in different illumination conditions are simulated and the yarn count and fabric density are adjusted through the parameters setting. Lastly, the simulated fabric images can be output as texture images. By appropriately adjusting parameters, the proposed method can obtain an ideal model of a plain fabric texture for image analysis.

Key words: plain fabric texture; fabric simulation; weaving float; parameter setting

INTRODUCTION

With the continuous development of computer technology, automatic detection with image analysis is widely used in the textile industry for various applications, such as yarn quality assessment, fabric detect detection, and fabric structure parameter inspection [1–5]. It can be found that the fundamental theories for solving these problems are the mathematical representation of fabric texture. Applying image analysis to the fabric texture simulation not only saves time and labor, but also improves the robustness of solving targeted problems.

Fabric simulation techniques can help designers rapidly, visually, and intuitively build fabric simulation images on computers according to their design intents. For an effective simulation method, the relevant image parameters should be easily adjusted [6–7]. Different simulation methods were adopted for fabric detections [8–10]. But when a small amount of fabric detection samples were used to simulate the images, the simulation algorithm could not be totally applicable to various fabrics. The existing methods still lack the generalization and robustness.

In this paper, we propose a simulation method for plain fabric textures using image analysis. In this method, the simulation images of plain fabrics are built to truly reflect the geometric structure of plain fabric and surface luster. The detection algorithm is enhanced on the basis of the fabric images. Because the simulation images can be used to represent different plain fabric textures, the applicability of the algorithm has been greatly widened. The proposed method also allows simulation images to be generated for different fabric textures by adjusting simple parameters. The first step is to set the parameter settings to adjust the gray texture distribution of weaving floats in plain fabric simulation image. The second step is to simulate plain fabric textures in different illumination conditions, and with different yarn counts and fabric densities. The last step is to output the simulation images. The flow chart of this simulation method for plain fabric textures is shown in figure 1.

INTERLACING POINTS SETTINGS

Resolution setting

Image resolution is an important indicator to evaluate the effect of fabric simulation. The higher resolution may increase the computation of image processing, and the lower resolution may make the image unclear. Taking 21s yarn as an example, its diameter is about 0.21 mm according to equation 1.

$$d = \frac{1.13}{\sqrt{N_e / 0.583 \times 0.93}} \quad (1)$$

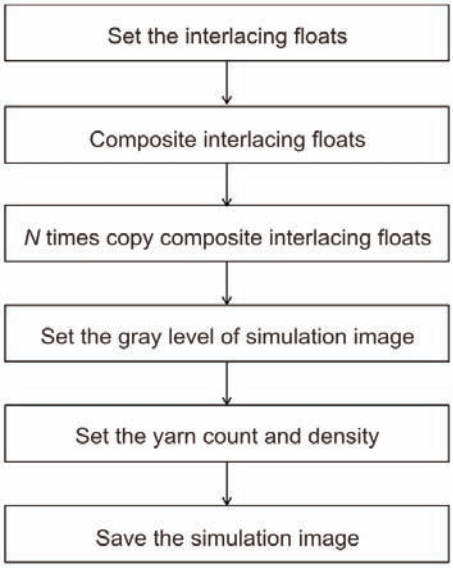

Fig. 1. Flow chart of simulation method of plain fabric texture

where d represents yarn diameter, N_e – stands for English count of cotton yarn.

To ensure the clarity of the simulated plain fabric texture, we use 1 pixel to represent millimeter in our research. The corresponding pixel number of common yarn counts is listed in table 1.

Table 1

CORRESPONDING PIXEL NUMBER OF COMMON YARN COUNTS					
Yarn count	21s (27.8tex)	50s (11.7tex)	100s (5.8tex)	150s (3.9tex)	180s (3.2tex)
Pixel number	21	13	9	7	6

Distribution of grayscale in texture setting

In a reflective fabric image, the pixels in the center of warp and weft floats should have the largest gray value and the gray value of the pixels around the center becomes lower. To obtain the stereo effect of floats, the gray value of pixels in the edge of the float is set as 0.

The height and width of warp and weft float are separately determined in the research. The default parameters are set as:

(1) the height and width of warp interlacing point are 41 and 21 pixels;

(2) the height and width of weft interlacing point are 21 and 31 pixels.

The gray value of the pixel in the center of interlacing floats is set as 220 in the default image and the gradient scale is 5. In the default image, the linear function used for obtaining the gray level distribution of the floats is

$$y = 220 - 5x \qquad (2)$$

where x represents pixel position, y – stands for the gray level of corresponding pixel.

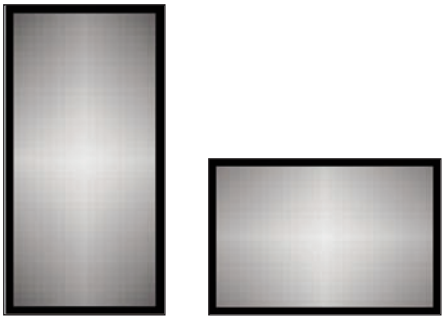

Fig. 2. Simulated image of weaving float: a – warp float; b – weft float

The simulated warp and weft float are shown in figure 2.

Composite Interlacing Floats

When simulating the composite interlacing floats, the interstices between warp and weft yarn should be confirmed. The gray level of the pixels in the interstice is set as 0 to highlight the yarn border. The equations used to calculate the height (m) and width (n) of interstice are as follows.

$$\begin{cases} m = (h_2 - h_1)/2 \\ n = (w_1 - w_2)/2 \end{cases} \qquad (3)$$

where h_1 and w_1 represent height and width warp interlacing float, h_2 and w_2 – height and width weft interlacing float. Figures 3 and 4 show the plain fabric image of interlacing floats and the N times copied composite image (the default image).

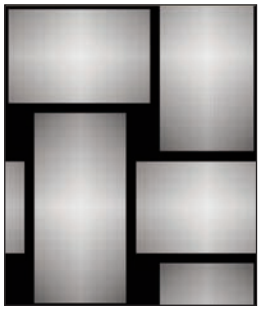

Fig. 3. Plain fabric image of warp and weft interlacing floats

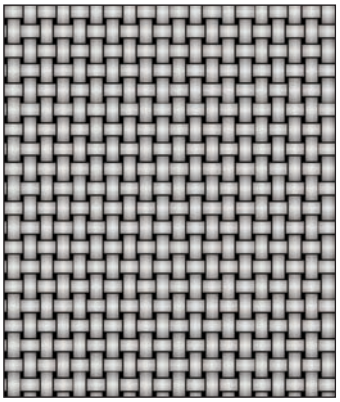

Fig. 4. N times copied composite image (the default image)

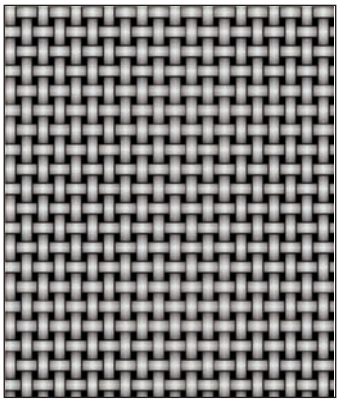

Fig. 5. Simulated plain fabric image after adjusting gray level distribution

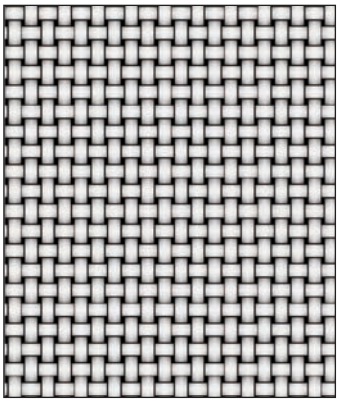

Fig. 6. Simulated plain fabric image after adjusting illumination condition

Parameters Settings

Different gray level distribution of fabric texture

Gray level distribution of fabric texture can truly reflect the structure of yarn surface and make the graphic fabric image three-dimensional. The texture of gray level distribution is represented by the difference among the pixels. By different brightness functions, we can get more simulated fabric images with different gray textures. The parameters of the gray level function can be adjusted to change the texture among the float as following quadratic function.

$$y = 230 - 0.2x^2 \quad (4)$$

The other parameters are set as the default value. The image after adjustment is shown in figure 5.

As seen in figure 5, the gray level distribution of simulated fabric texture is different from the default texture in figure 4. In figure 5, the gray level value in the center of the floats is more abrupt and the brightness change of surrounding pixels is uneven that make the whole image darksome and shaded.

Different illumination conditions

The fabric texture seems different with different illumination conditions. Similarly, the brightness of simulated image can be altered by changing the illumination parameters. In our proposed method, the illumination condition can be adjusted by changing the gray level value of the pixel in the center of interlacing float. The gray level of the pixel in the center is then set as 240 and the other parameters are not changed. The updated simulated fabric image is shown in figure 6.

In figure 6, the gray level of the pixels in the center of the floats is adjusted and the gray level of the rest pixels is reset along with this pixel except the edge pixels in interlacing floats. It can be implied that the image becomes brighter when the gray level value of the pixels in the center of the floats increases. In other words, the change of the illumination conditions can be realized by changing the gray level value of the pixel in the center of the float.

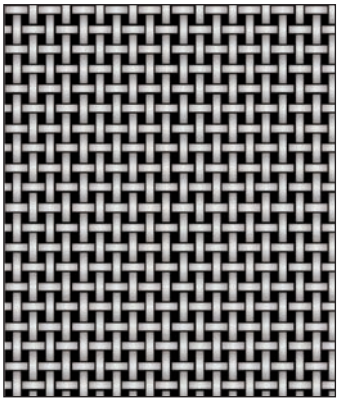

Fig. 7 Simulated plain fabric image after adjusting yarn counts

Different yarn counts

Yarn count determines the size of warp and weft interlacing floats in simulated image. The yarn count can be altered through changing the height and width of interlacing floats. Taking 100 s yarn for example, the diameter of the yarn is about 0.09 mm in theory and the corresponding pixel number in the simulated fabric image is 9. The width of warp float and the height of weft float are set as 9 and the other parameters are set as the default value. The different yarn counts of simulation images are shown in figure 7.

It is found that the yarns in figure 7 are finer than the default simulated fabric image. When the yarn counts change, the size of clearance should be calculated by equation 3. We can obtain any plain fabric simulation image of different yarn counts with the method raised in this paper.

Different fabric density

The fabric density plays a key role in the parameter setting of simulation. For instance, when the warp density is 500 thds/10 cm and weft density is 400 thds/10 cm. We set the warp yarn count 70s and weft yarn count 100s. The other parameters are same as default image. Firstly, the pixel number in the warp and weft yarn can be found in table 1. After calculation of yarn linear density, the height of warp interlacing point is 41 pixels and the width of weft interlacing

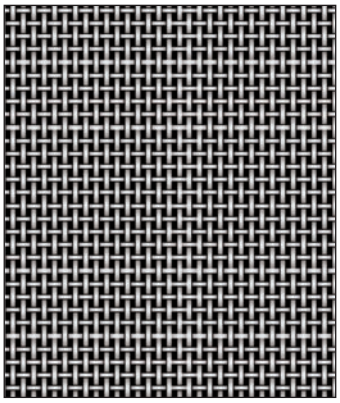

Fig. 8. Simulated plain fabric image after adjusting the fabric density

point is 29 pixels. The size of interlacing float is then confirmed. Then, the pixel number in the interstices between the yarns can also be determined through equation 3. The updated simulated fabric image is shown in figure 8.

In this case, the yarns in figure 8 are finer than the default simulated fabric image and the areas of the interstices between the yarns become larger. Thus, if the fabric density and yarn count are confirmed, the simulated image can be updated through the calculation of the size of warp and weft interlacing floats and the interstices between the yarns.

CONCLUSIONS

This paper proposes a simulation method for textile image analysis of plain fabric texture. With the proposed method, we can obtain a wide variety of fabric images with ideal image textures. By appropriately adjusting parameters, the proposed method can generate an ideal model for plain fabric texture simulation, and can output the fabric texture image for future image analysis. With the simulated fabric images, the robustness of the fabric detection algorithms can be improved to meet the demand for textile production. Although the paper only investigated the plain fabric texture simulation, it laid a solid ground for simulating twill and satin fabric textures, which has been planned in further research.

Acknowledgment

The authors are grateful for the National Natural Science Foundation of China (No.61202310), the Natural Science Foundation of Jiangsu Province (BK2011156) and the Open Project Program of Key Laboratory of Eco-Textiles (Jiangnan University), Ministry of Education, China (NO. KLET 1110), Research Fund for the Doctoral Program of Higher Education of China (20120093130001).

BIBLIOGRAPHY

[1] Shuangwu Zhu, Chongyang Hao. *Fabric defect detection approach based on texture periodicity analysis.* In: Computer Engineering and Applications, 2012, 48(21), pp. 163-166

[2] Ruru Pan, Weidong Gao, Xinxin Qian, Xiaoting Zhang. *Defect detection of printed fabrics using normalized cross correlation.* In: Journal of Textile Research, 2010, 31(12), pp. 134-138

[3] Ruru Pan, Weidong Gao, Xingye Zhang. *Fabric defect detection based on dynamic clustering arithmetic.* In: Journal of Textile Research, 2008, 29(10), pp. 122-126

[4] K.L. Mark, P. Peng. *An automated inspection system for textile fabrics based on Gabor filters.* In: Robotics and Computer-Integrated Manufacturing, 2008, 24(3), pp. 359-369

[5] Bugao Xu. *Identifying fabric structure with fast Fourier transform techniques*. In: Textile Research Journal, 1996, 66(8), pp. 496-506

[6] Xiaoping Zhang, Junze Wang. *Simulation model of 2-Step three-dimensional braided fabrics*. In: Journal of Textile Research, 2011, 32(10), pp.148-152

[7] Hui Chen, Yi Shen. *The reviewed about fabric simulation technology*. In: Silk, 2005, 8, pp. 42-45

[8] Hao Zhu, Dan Li. *An imitation method to woven fabric appearance.* In: Wool Textile Journal, 2005(7), pp. 55- 57

[9] F. Abdiwi, P. Harrison, I. Koyama, W.R. Yu, A.C. Long, N. Corriea, Z. Guo. *Characterizing and modelling variability of tow orientation in engineering fabrics and textile composites*. In: Composites Science and Technology, 2012, 72(9), pp. 1034-1041

[10] Narges Heidari, Reza Azmi, Boshra Pishgoo. *Fabric textile defect detection, by selection a suitable subset of wavelet coefficients, through genetic algorithm*. In: International Journal of Image Processing, 2011, 5(1), pp. 701-710

Authors:

RURU PAN
BO ZHU
ZHONGJIAN LI
JIHONG LIU
WEIDONG GAO
School of Textile and Clothing, Jiangnan University, Wuxi, China
e-mail: prrsw@163.com, 254678654@qq.com, 825948026@qq.com, liujihongtex@hotmail.com, gaowd3@163.com

Mechanical and drape properties of the shirt fabrics applied wrinkle resistance finishing

ARİF TANER ÖZGÜNEY NILGÜN ÖZDIL GAMZE SÜPÜREN MENGÜÇ

REZUMAT – ABSTRACT

Caracteristicile mecanice și de drapare ale finisajului cu rezistență la șifonare aplicat pe țesăturile pentru confecționarea cămășilor

Șifonarea este un efect nedorit al țesăturilor utilizate la confecționarea cămășilor, care are loc în timpul utilizării. Există diverse materiale de finisare si metode de tratament pentru a da țesăturilor proprietatea de anti-șifonare. În acest studiu, a fost realizat un experiment pentru a evalua efectul de finisaj cu rezistență la șifonare asupra caracteristicilor de revenire din șifonare, rezistență la rupere, pilling și drapaj ale țesăturilor utilizate la confecționarea cămășilor produse din țesături 100% bumbac. În acest scop, au fost produse țesături cu legătură pânză sau satin din fire de bumbac Ne 50/1 și ulterior, a fost aplicat un finisaj anti-șifonare. După aceea țesăturilor tratate le-au fost testate proprietățile fizice. O analiză statistică folosind probele independente "t-test" cu nivelul de semnificație α = 0.05 a fost efectuată pentru a determina dacă există o diferență statistică semnificativă între rezultatele testului. În concluzie, finisajul anti-cutare pare a avea un efect de creștere a unghiului de revenire din șifonare și asupra tendinței de pilling, și de scădere a unghiului de drapare, a rezistenței la rupere și la șfâșiere a țesăturilor.

Cuvinte-cheie: revenire din șifonare, unghi de revenire din șifonare, revenire din cutare, țesături din bumbac, caracteristici de rezistență la rupere, unghi de drapare

Mechanical and drape properties of the shirt fabrics applied wrinkle resistance finishing

Wrinkle is an undesirable effect for the shirt fabrics, which occurs during usage. There are various finishing materials and treatment methods to give fabrics crease resistance property. In this study, we conducted an experiment to evaluate effect of wrinkle resistance finish on wrinkle recovery, tensile, pilling and drape properties of shirt fabrics produced from 100% cotton fabrics. For this purpose, fabrics in plain and sateen constructions were woven using by Ne 50/1 cotton yarns and later, wrinkle resistance finishing was applied. Afterwards, the treated fabrics were tested for their physical properties. A statistical analysis using independent samples t-test with the significance level of α = 0.05 has been performed to determine if a statistically significant difference exists among test results. In conclusion, crease resistance finishing seems to have an increasing effect on wrinkle recovery angle (WRA) and pilling tendency, whereas it leads to a decrease in drape angle (drapeability), breaking and tearing resistance of the fabrics.

Key words: wrinkle recovery, wrinkle recovery angle, crease recovery, cotton shirt fabrics, tensile properties, drape angle

Cotton has a great economic importance and a widespread usage as a raw material for textile industry, since it can be spun into yarns easily [1]. Cotton's strength, good abrasion resistance, absorbency, quick drying, no static problems and capacity to washing and dying also make it adaptable to a considerable variety of textile products [1–2]. Cotton is most commonly used for shirt fabrics as well because of its texture, durability, softness and nice feelings against the skin.

However, there are several disadvantages associated with cotton fiber or fabric such as poor elasticity and resiliency which creates wrinkles and do not recover from wrinkling readily [1–2]. Although wrinkles could be sometimes a desirable effect for smartness of clothes, it is generally an undesirable appearance occurring during wear [3]. Fiber, yarn and fabric characteristics, and finishing processes effect the formation of wrinkles. Factors that influence wrinkle development include fiber type, bending performance of fiber, fiber diameter, yarn twist, weft-warp density, fabric construction, and fabric thickness.

The crease recovery is one of the fundamental properties of fabrics which affect product performance. Crease recovery refers to the ability of the fabric to return to its original shape after removing the folding deformations. The recovery of the fabric from creasing depends on the elastic recovery of the fibers, in particular whether the stored elastic energy is sufficient to overcome the friction that resists the movement of the yarns and fibers [4].

The ability of fabrics to recover from wrinkles is an important factor for the quality of fabrics. For this reason, the interest of buyers in wrinkle-resistant apparels has diverted the producers' attention to use easy-care finishes [5].

Wrinkle (or crease) resistance is imparted to cellulosic fibers by restricting the slippage of molecular chains through crosslinking [6]. Formulation of the finish is significant to yield the desirable balance of physical properties. If excessive crosslinking is

achieved, the strength and abrasion resistance may be too low for adequate wear life of the garment. On the other hand, if too little crosslinking is obtained, there may be inadequate shrinkage control, smoothness, crease retention, and undesirable surface appearance [7].

Wrinkle recovery performance of untreated cotton fabric is poor because creases can be stabilized by intermolecular hydrogen bonds that easily break and reform in a creased configuration within the fiber during wetting/drying of the fabric [8]. Therefore, cotton fabrics could be treated with chemicals to reduce wrinkling and this applied crease resistant finish to cotton fabrics improves comfort, ease of maintenance, dimensional stability and pilling performance [3].

There are some researches both on used chemicals and on treatment processes to make cotton fabric wrinkle resistant. In a study of Wang *et al.* chitosan and epoxy-silicone finishing agents were used for wrinkle-resistant treatment of cotton fabrics. According to the results, it was declared that, mixed finish by two agents provides higher wrinkle-resistance than single finish, due to their synergistic effect [9].

Kan *et al.* studied the structural properties of cotton fabrics after various treatments. In order to investigate surface morphology of the fibers, scanning electron microscopy was used. 1,2,3,4-butanetetracarboxylic acid (BTCA), with catalyst sodium hypophosphite (SHP) was used for wrinkle-resistant treatment. According to the SEM analysis, it was concluded that, surface roughness of the BTCA-treated fabric samples was found higher than that of the untreated fabric with the appearance of slightly wrinkled surfaces. The surface of the treated fibers had a higher deposition of crosslinking agent, leading to an increment of wrinkle recovery property of these treated fabrics [2].

In a work conducted by Hassan in 2009, dimethyloldihydroxy ethylene urea resin was used to impart crease recovery properties to cotton fabrics. Two different techniques were used for the finishing of cotton fabrics with DMDHEU; thermalcuring at 160 °C for 3 min and gamma irradiation at different doses. The color properties, crease recovery, mechanical properties, thermal properties and surface morphology after treatments were studied. It was found that the finishing of cotton fabrics with gamma irradiation affords better crease recovery values at low doses without affecting the color intensity and the physical properties than the finishing by thermal curing. However, the finishing with higher doses of gamma radiation affects the mechanical properties of cotton fabrics. On the other hand, it was found that the thermal properties were improved with increasing dose [10].

Hussain *et al.,* aimed to predict the crease recovery performance and tear strength of cotton fabric using modified N-methyloldihydroxyethylene urea, polyethylene softener, catalyst, curing time and curing temperature as the predictor variables. A quarter factorial design was constructed and regression models were built to predict crease recovery angle and tear strength of the treated fabric. The crease recovery and tear strength properties of cotton fabric were modelled through a validated regression model. The model has a strong prediction capability indicated by a high, positive correlation between the predicted and observed CRA and tear strength values [11].

Abou Nassif investigated the effects of weft density and weave structures on the physical and mechanical properties of fabrics, which are micro-polyester woven fabrics with plain, twill and satin weave structures in five different weft densities. The findings of this study revealed that increasing weft density leads to an increase in fabric breaking load, stiffness and crease recovery. Satin weaves have higher air permeability, whereas twill weaves have higher crease recovery. Weft density was found to have a profound effect on crease angle. An increasing trend was detected assuring that as the weft density increases the crease angle increases. Crease angle of micro-polyester fabrics increased by 11%, 21% and 7% for plain, satin and twill weaves with the increase in weft density from 61 to 80 picks/inch. It was also shown that twill fabrics exhibited higher crease recovery followed by plain and satin weaves respectively [12].

In the study of Omeroglu *et al.,* full and hollow fibers having round and trilobal cross-sectional shapes were produced in equal manufacturing conditions and bending, drapability and crease recovery behaviors of the woven fabrics produced from these fibers were investigated. The fabrics produced from full fibers had higher crease recovery angles than those produced from hollow fibers. Considering that the construction properties of the fabrics were kept constant, it was concluded that the differences among the properties of the fabrics which were produced from full and hollow fibers (for both round and trilobal-crosssectional shapes) basically emerged from the very high differences between moments of inertia of full and hollow cross sections. The best results were obtained with round and trilobal full fibers at fabrics in which drapability and crease recovery are desired [4].

Can *et al.,* investigated the performance of 100 % cotton plain fabrics after crease resistant finish in 2009. It was concluded that, the wrinkle recovery angle increases approximately 50% after the crease resistant finishing. Namely, the treatment improves wrinkle resistant characteristic, besides decreasing breaking strength, tearing strength and pilling [3].

The properties of TiO_2 or nano-TiO_2, acting as a co-catalyst in a BTCA wrinkle resistant finishing system were investigated by Lam *et al.* in 2010. After the treatment, the changes in surface morphology and molecular structure of cotton specimens together with the wrinkle-resistant, UV protection, yellowing, tensile and tearing properties of the treated specimens were researched. The addition of BTCA could

enhance significantly the wrinkle-resistance of cotton fabrics, especially in the presence of SHP and TiO_2/nano-TiO_2 which acted as a catalyst and co-catalyst respectively. It was obvious that the addition of TiO_2/nano-TiO_2 could slightly increase the fabric whiteness and tearing strength of the test specimens, while the effect on tensile strength was not found significant [13].

In this study it was aimed to find the effect of the wrinkle finishing treatment on the mechanical properties of the shirt fabrics and unlike the literatures the drape properties of the fabrics were investigated.

MATERIALS AND METHODS

In this study 100% cotton yarns in Ne 50/1 yarn count and in α_e = 4 twist coefficient were used. They were woven, both in warp and weft yarns, in plain weave and sateen fabric constructions which are mostly used for shirt fabrics, in the same weft densities. The properties of the fabrics were summarized in table 1.

Table 1

PROPERTIES OF THE FABRICS USED IN STUDY

Yarn count (Ne)	Twist (α_e)	Construction	Warp density	Weft density
50/1	4	plain	56	31
50/1	4	sateen	56	31

The fabrics were exposed to the standard pretreatment processes including the burning, desizing, rinsing, bleaching, mercerizing and drying. Later, crease resistance finishing process was applied to the fabrics. The recipe containing 60 g/L dimethylol dihydroxy ethylene urea (DMDHEU – Cross linking type of resins) resin, 40 g/L dimethylol urea (DMU – Resin free of formaldehyde) resin, 60 g/L polyethylene, 30 g/L polyuretan and 10 g/L Mgcl2 catalyst was padded onto the fabrics with a pickup of 80–85 % in a fulard. Then the fabrics were dried at 110 °C in eight section stenter (monforts ram). Fabrics were cured at 135 °C for 4 min. using hotflue machine. In addition, the cured fabrics were washed at 50 °C and 40 m/min speed using open-width washing machine (babcock).

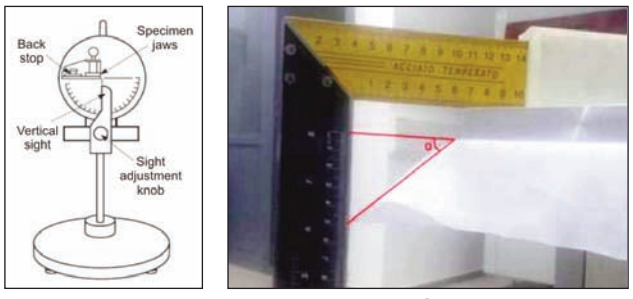

a b

Fig. 1. Wrinkle Recovery Angle Tester (a), Drape Angle Tester (b)

After the treatment, the fabrics were conditioned under standard atmosphere conditions (20 °C ± 2 °C temperature, 65% ± 4% RH) and crease recovery angles were measured by using "The Crease Recovery Tester" according to EN 22313 test method (figure 1-a). Crease recovery angle defined as the angle formed between the two limbs of a strip of fabric previously folded under defined conditions, at a specified time after removal of the creasing load. In the measurement, 20 rectangular test specimens 40 × 15 mm, ten with their long dimension parallel to the warp direction of the fabric and ten with their long dimension parallel to the filling direction are folded by means of a suitable device and maintained in this state for 5 minutes under a 10N load. Then creasing load is removed, the specimen allowed to recover for 5 minutes and the crease recovery angle then measured [14]. Higher crease recovery angle means better crease recovery of the fabric.

Tensile properties of the fabrics were measured by using Zwick Z010 Tensile Strength Tester. Breaking strength was conducted according to EN ISO 13934-1 strip method and tearing strength was measured according to EN ISO 13937-2. Pilling resistance was tested by using Martindale instrument according to EN ISO 12945-2 standard. The results were evaluated by pilling grades from 1 to 5, which 1 means excessive pilling and 5 means no pilling.

Drape properties of the fabrics were tested by "Sharp Corner" instrument, which was developed by Hes. It is based on the bending of a fabric across a horizontal plate with a 90 degree sharp corner. As an indicator of the fabric drapeability, it provides the sinus of the angle between the fabric edge and horizontal plane. The fabric becomes harder as the drape angle gets smaller (figure 1-b). [15].

RESULTS AND DISCUSSION

The results of measured parameters were statistically evaluated, whether the effects of crease recovery treatment and fabric construction parameters on fabric properties significant or not, independent samples t-test with the significance level of α = 0.05 has been performed. The calculated p values were given in table 2.

The effect of the crease resistance finishing on Wrinkle Recovery Angle (WRA) test results was given in figure 2.

According to the results and statistical evaluation outputs given in table 2, it can be said that, sateen fabrics have higher wrinkle recovery angle in all cases and the difference between the results are statistically significant. The ease of movement of yarns in the fabric structure affects the crease behavior of fabrics [4]. For this reason, yarns in the sateen structure can overcome the creases better than the plain weave structure.

In addition to this, it was also observed that wrinkle recovery treatment has also an increasing effect on

Table 2

STATISTICAL ANALYSIS OF THE TEST RESULTS (INDEPENDENT SAMPLES T-TEST)								
Physical property	**Effect of treatment**				**Effect of construction**			
	Fabric construction	**Direction**	**Compared parameters (treatment)**	**Sig. (p)**	**Treatment status**	**Direction**	**Compared parameters (fabric construction)**	**Sig. (p)**
WRA (degree)	Plain Fabric	Weft	Before Treatment	0.004*	Before Treatment	Weft	Plain	0.000
			After Treatment				Sateen	
		Warp	Before Treatment	0.045*		Warp	Plain	0.000
			After Treatment				Sateen	
	Sateen Fabric	Weft	Before Treatment	0.399	After Treatment	Weft	Plain	0.000
			After Treatment				Sateen	
		Warp	Before Treatment	0.005*		Warp	Plain	0.042*
			After Treatment				Sateen	
Breaking Strength	Plain Fabric	Weft	Before Treatment	0.001*	Before Treatment	Weft	Plain	0.179
			After Treatment				Sateen	
		Warp	Before Treatment	0.000*		Warp	Plain	0.001*
			After Treatment				Sateen	
	Sateen Fabric	Weft	Before Treatment	0.000*	After Treatment	Weft	Plain	0.500
			After Treatment				Sateen	
		Warp	Before Treatment	0.786		Warp	Plain	0.001*
			After Treatment				Sateen	
Tearing strength	Plain Fabric	Weft	Before Treatment	0.000*	Before Treatment	Weft	Plain	0.000*
			After Treatment				Sateen	
		Warp	Before Treatment	0.000*		Warp	Plain	0.000*
			After Treatment				Sateen	
	Sateen Fabric	Weft	Before Treatment	0.000*	After Treatment	Weft	Plain	0.000*
			After Treatment				Sateen	
		Warp	Before Treatment	0.000*		Warp	Plain	0.000*
			After Treatment				Sateen	
Pilling	Plain Fabric	-	Before Treatment	0.004*	Before Treatment	-	Plain	0.003*
			After Treatment				Sateen	
		-	Before Treatment	0.398	After Treatment	-	Plain	0.000*
			After Treatment				Sateen	
Draping angle	Sateen Fabric	-	Before Treatment	0.004*	Before Treatment	-	Plain	0.687
			After Treatment				Sateen	
		-	Before Treatment	0.121	After Treatment	-	Plain	0.204
			After Treatment				Sateen	

* Statistically significant according to $\alpha = 0.05$

Wrinkle Recovery Angle. That means crease resistance treated fabrics wrinkle lower as expected.

The effect of the crease resistance finishing on drape angle results was depicted in figure 3.

Crease resistance treatment appears to have a significant effect on drape properties of plain fabrics. After treatment, plain fabric becomes stiffer and drapes less. This result is found parallel to the explanations given by *Behery* (2005). It is due to the treatment agent that creates cross-linking in the fiber structure. Cross-linking stiffens the fiber so the fabric

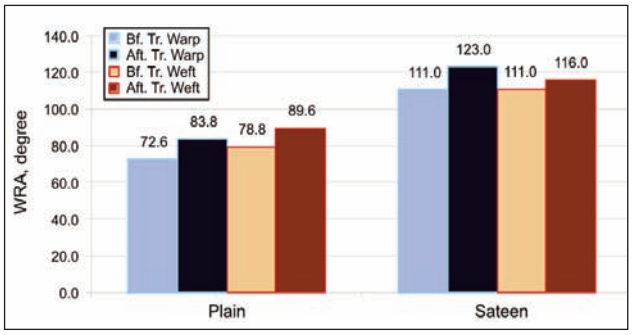

Fig. 2. Effect of crease resistance finishing on wrinkle recovery angle (WRA) results for the fabrics produced in different construction

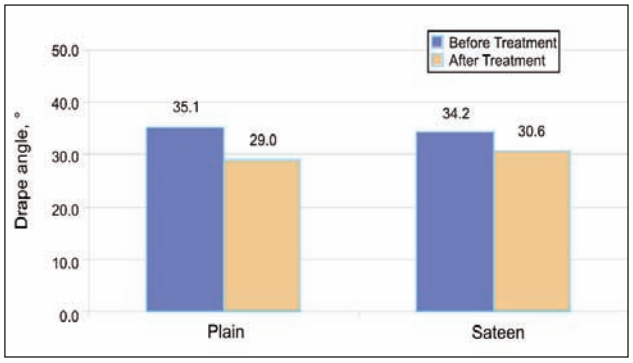

Fig. 3. Effect of the crease resistance finishing on drape angle of the fabrics

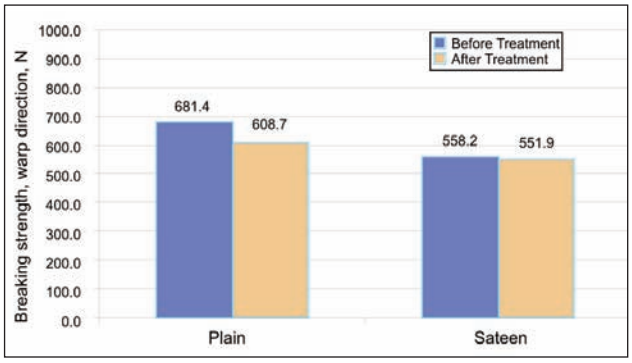

Fig. 4. Effect of crease resistance finishing on breaking strength (warp direction) of the fabrics

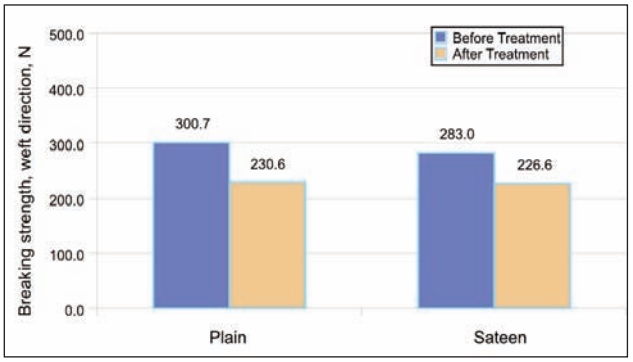

Fig. 5. Effect of crease resistance finishing on breaking strength (weft direction) of the fabrics

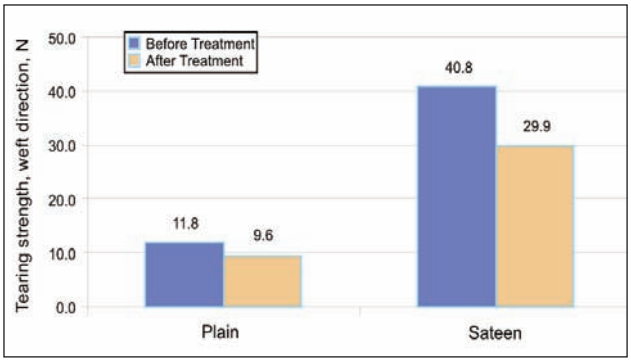

Fig. 6. Effect of crease resistance finishing on tearing strength (weft direction) of the fabrics

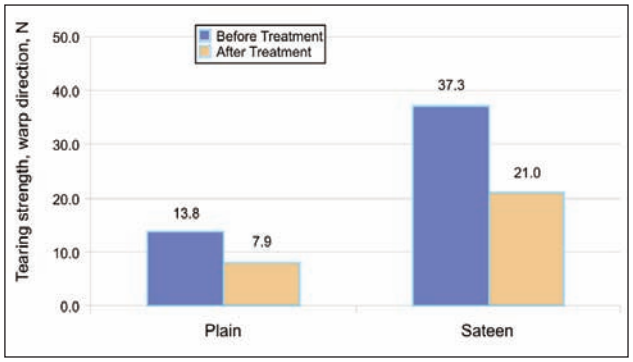

Fig. 7. Effect of crease resistance finishing on tearing strength (warp direction) of the fabrics

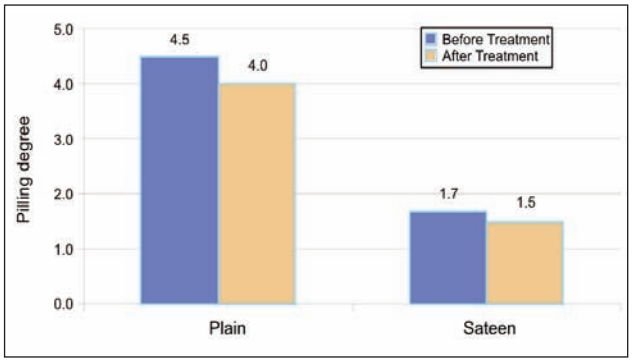

Fig. 8. Effect of the crease resistance finishing on pilling degree of the fabrics

becomes less limp. On the other hand, although there is a decrease in the mean drape angle values for sateen fabric, the difference was not found statistically significant [16].

The effect of the crease resistance finishing on tensile strength properties of the fabrics were given in figure 4–7 respectively. According to the results, breaking strength on warp direction of plain weave fabric is higher than the sateen fabric, due to the more intersection points in unit fabric pattern. Besides, wrinkle recovery treatment generally leads to decrease in the breaking strength of the fabrics.

During the treatment the crosslinks between the fibers break and does not generate new crosslinks. They limit the movements of the macromolecule chains and therefore, the macromolecule chains cannot get closer to each other and they cannot resist to the applied forces. For this reason, new generated crosslinks cause decreases the tensile properties of the fibers and consequently the fabrics.

It can be seen from the figures 6 and 7, sateen fabric is more resistant to tearing than plain weave fabric. In the case of sateen fabrics, due to the fabric construction, yarns can group together by lateral movement during tearing, thus improving the tearing resistance while more than one yarn have to be broken at a time. The ability to group is a function of the looseness of the yarns in the fabric. Sateen construction allows yarns to group better and for this reason giving better tearing resistance than a plain weave.

After the crease resistance finishing, tearing strength of the fabrics decreases in both direction and the difference between the values were found statistically significant.

The effect of the crease resistance finishing on pilling properties of the fabrics was given in figure 8. Pilling degrees of the sateen fabrics were found lower than the plain weave fabrics, which indicated the higher pilling tendency of sateen fabrics. It is due to the long yarn floats on the surface of the sateen fabric structure.

As the effect of crease resistance finishing analyzed, it was observed that, crease resistance finishing has a negative effect on pilling property of plain fabrics and it increases pilling tendency. However, there is not an apparent decrease in the case of sateen fabric and the difference between the results was not found statistically significant.

After crease recovery treatment some of the fiber elements loose their slippage and they can easily break as a force applied, whereas the partly movable fiber elements can settle parallel to the fiber axis. Treated fibers have lower elasticity and crispy structure that they can easily move out to the fabric surface as a result of abrasion. Therefore pilling tendency of the treated fabrics is higher.

CONCLUSIONS

Cotton is mostly used for shirt fabrics but due to the structural properties of fibers cotton fabric has natural tendency to wrinkle. In order to avoid and improve this property, several methods were developed in the case of wrinkle resistance finishing.

100% cotton yarns (Ne 50/1, α_e = 4) were used in the experiment. They were woven in plain weave and sateen constructions in the same tightness values. After the pretreatment processes, crease resistance finishing process was applied to determine the effect of finishing on mechanical and drapeability properties. According to the results of treated and untreated samples, following conclusions were pointed out.

- In the case of sateen fabrics, they have comparatively higher wrinkle recovery angle because of the ease movement of the yarns that can overcome the wrinkles in sateen structure. This structure also allows slippage and ability to group of the yarns during tearing that causes higher tearing resistance. On the other hand lower intersection points than plain fabrics leads to decrease in breaking strength and lower pilling degrees (higher pilling tendency) of the sateen fabrics.
- Crease resistant treated fabrics wrinkle less than untreated fabrics as expected. However, the treatment makes the fabric stiffer and causes a decrease in drape angle values for both sateen and plain type of the fabrics. Moreover, due to the breakage of crosslinks in the fiber structure, breaking and tearing resistance of the fabrics decrease. The fibers which are in the fabrics applied crease resistant finishing have lower elasticity that causes increase in the pilling tendency of the fabrics. Especially this increase was more apparently seen in plain fabrics.

ACKNOWLEDGEMENT

The authors give their special thanks to “Cotton Incorporated” for their financial support and Bossa T.A.Ş. for application of finishing process in this study.

BIBLIOGRAPHY

[1] Dalbasi, E. S., Coban, S.; Bahtiyari, M.I., *An optimization study on crosslinking of linen and cotton fabrics* In: Industria Textila, 2013, Vol. 64, no. 5, pp. 235-240

[2] Kan, C.W., Lam, Y.L., Yuen, C.W.M., *Microscopic study of cotton fiber subjected to different functional treatments.* In: Current Microscopy Contributions to Advances in Science and Technology, 2012, FORMATEX, Microscopy Series No. 5, Vol. 2, pp. 1130-1136

[3] Can, Y., Akaydin, M., Turhan, Y., Ay, E., *Effect of wrinkle resistance finish on cotton fabric properties*. In: Indian Journal of Fibre & Textile Research, 2009, Vol. 3, pp. 183-186

[4] Omeroglu, S., Karaca, E., Becerir, B., *Comparison of bending, drapability and crease recovery behaviors of woven fabrics produced from polyester fibers having different cross-sectional shapes*. In: Textile Research Journal, 2010. Vol. 80(12), pp. 1180–1190

[5] Saleemuddin, M., Ali, S.T., Pervez, M.K., Mughal, M.J., Rasheed, M., *Optimization of easy-care finishing of cotton/polyester blend fabric*. In: Journal of the Chemical Society of Pakistan, 2013, Vol. 35, No.3, pp. 560-564

[6] Lu, M., *Crease resistant finishing of cotton fabric with a complex of fibroin and citric acid*. In: Fibres & Textiles in Eastern Europe, 2010. Vol. 18, No. 3 (80) pp. 86-88

[7] *Wrinkle-Resistant Finishing Of Cotton Fabrics And Garments,* Cotton Incorporated – Technical Bulletin TRI 3013, 2000.

[8] Hauser,P., Smith, B., Hashem, M., *Fabric stabilizaton by ionic crosslinking* (C04-NS01) NTC Project: C04-NS01, *National Textile Center Research Briefs*: June 2007

[9] Wang, H., Huang, C., Liu, N., *Wrinkle-resistant property of cotton fabric treated by chitosan and epoxy-silicon micro-emulsion.* In: Advanced Materials Research, 2011, Vol. 331, pp. 382-385

[10] Hassan, M.S., *Crease recovery properties of cotton fabrics modified by urea resins under the effect of gamma irradiation*. In: Radiation Physics and Chemistry, 2009, 78, pp. 333–337

[11] Hussain, T., Ali, S., Qaiser, F., *Predicting the crease recovery performance and tear strength of cotton fabric treated with modified n-methyloldihydroxyethylene urea and polyethylene softener*. In: Coloration Technology, 2010. 126(5): 256–260

[12] AbouNassif, G.A., (2012), *Effect of weave structure and weft density on the physical and mechanical properties of micro polyester woven fabrics*. In: Life Science Journal; 2012, 9(3), pp. 1326-1331

[13] Lam, L.Y., Kan, C.W., Yuen, C.W.M., *Wrinkle-resistant finishing of cotton fabric with btca – the effect of co-catalyst*. In: Textile Research Journal, 2011, 81(5), pp. 482-493

[14] BS EN 22313:1992, ISO 2313:1972, Textile fabrics – Determination of the recovery from creasing of a horizontally folded specimen by measuring the angle of recovery

[15] Hes L., *Marketing aspects of clothing comfort evaluation*, X. International İzmir Textile and Apparel Symposium, İzmir, Turkey, 2004

[16] Behery, H.M., *Effect of Mechanical and Physical Properties on Fabric Hand*, 2005, Woodhead Publishing Limited in Association With The Textile Institute

Authors:

ARİF TANER ÖZGÜNEY
Ege University Textile Engineering Department,
Bornova-İzmir/Turkey
e-mail: arif.taner.ozguney@ege.edu.tr

NİLGÜN ÖZDİL
Ege University Textile Engineering Department,
Bornova-İzmir/Turkey
e-mail: nilgun.ozdil@ege.edu.tr

GAMZE SÜPÜREN MENGÜÇ
Ege University Emel Akın Vocational Training School
Bornova-İzmir/Turkey
e-mail: gamzesupuren@gmail.com

Identifying the points that represent potential defects in embroidery machines using infrared thermography

MARIUS ȘUTEU
LILIANA INDRIE
SABINA GHERGHEL
ADRIAN TIMOFTE

REZUMAT – ABSTRACT

Folosirea termografiei în vederea identificării defectelor la mașina de brodat HAPPY

Scopul prezentei lucrări este identificarea rapidă și precisă a punctelor ce reprezintă defecte potențiale la maşinile de brodat, prin folosirea termografiei în infraroșu. Măsurătorile de termografie au fost efectuate cu ajutorul camerei de termoviziune FLIR T335, pe mașina de brodat HAPPY, cu scopul de a se urmări modul de transmitere a temperaturii de la ac și ață la materialul pe care se execută broderia. Datorită frecărilor dintre ac și materialul pe care a fost realizată broderia precum și dintre ață și ac, în operația de brodare apare și se dezvoltă o energie termică, care este destul de mare la un regim de lucru ridicat. În mare parte această cantitate de energie termică este cumulată în acul cu care se realizează broderia. În urma măsurătorilor efectuate s-a observat că această temperatură acumulată duce la o degradare mai mare a ației de brodat și a materialului pe care se realizează broderia decât a acului, deoarece atat materialul cât şi aţa de brodat preiau o mare parte din acastă temperatură. Cu cât căldura acumulată în ață atinge un nivel mai ridicat, cu atât riscul degradărilor termice este mai mare (la ațele din fibre sintetice apare topirea lor). Topirea ației duce la ruperea ei și implicit la oprirea procesului de brodare.

Cuvinte-cheie: măsurări de termografie, cameră de termoviziune FLIR T335, degradări termice, ac, aţă, material brodat.

Identifying the points that represent potential defects in embroidery machines using infrared thermography

The purpose of this paper is to quickly and accurately identify the points that represent potential defects in embroidery machines, by using infrared thermography. The thermographic measurements were performed using the FLIR T335 thermal imager was used, on the HAPPY embroidery machine, in order to observe the heat transfer from needle and thread to the fabric being embroidered. Due to friction between the needle and the fabric on which the embroidery is done, as well as friction between needle and thread, the embroidering operation produces heat, which is quite high during an intense operating mode. For the most part, this heat is amassed in the embroidery needle. Measurements showed that this gathered heat leads to increased wear in the embroidery thread and the fabric being embroidered, because both thread and fabric absorb a significant amount of the heat. The higher the level of heat gathered in the thread, the higher the risk of thermal damage (synthetic fibers melt). The thread melting leads to thread breaking and implicitly, to halting the embroidering process.

Key-words: thermographic measurements, FLIR T335 thermal imager, thermal damage, needle, thread, embroidered fabric.

Infrared thermal imaging is a new nondestructive technique for measuring thermal fields by recording infrared radiations and observing the heat destribution across the tested surfaces. It is a nondestructive, non-contact method useful for detecting flaws in industrial systems during their operation, without halting the technological process.

Thermography – the non-contact, nondestructive method – is used for [1]:

- detecting defects during the operation of mechanical systems,
- determining the temperature of rolling and sliding bearings in dynamic rotating machinery,
- measuring the temperature of electric motors and the devices they interact with,
- determining the temperature for various manufacturing technological processes,
- studying thermal expansion in dynamic machinery and its influence on vibrations etc.

The advantages of thermography over other methods:

- it is nonpolluting;
- the thermal image is geometrically consistent with the observed object;
- systems are tested in a very economic way, without stopping the technoligical process (it does not require sampling);
- the ThermoVision system provides an image which allows a quick and pecise identification of overheated points which represent potential defects. It is also possible to make basic assessments regarding heat loss;
- moving objects or objects located in innaccesible places can also be scanned;
- defects can be discovered early, their risk level can be assessed and repairs can be planned, therefore obtaining a decrease in machine break down rates and increased safety in their operation;
- defects can be detected and corrected in early stages, thus avoiding damage;

- can be integrated with complex storage, recording, and automated data processing equipment;
- by using infrared thermography for the maintenance of machines in the textile industry, defects can be detected and corrected long before damage occurs; thus sewing and embroidering machine downtime is reduced, by eliminating unplanned shutdowns and by optimizing scheduled maintenance and repairs. The immediate effects of this are reduced costs (electricity savings, savings on repairs of fixed assets), shorter scheduled checks and inspections. Also, the uptime of the machines is increased and work safety conditions are improved.

MODELING METHOD

The thermographic measurements were performed at S.C. CONFIDEX S.R.L Oradea. The machine used for the measurements is a HAPPY professional embroidery machine.

The FLIR-T Series ThermoVision camera is a portable thermographic camera, light and simple to use. This series was designed specially for reading temperatures in the field of predictive maintenance.

Fig. 1. FLIR T335 Infrared Camera [2]

Figure 1 shows the ThermoVision FLIR T335 camera, which is the second T-Series camera.

The purpose of the thermographic measurements performed on the HAPPY embroidery machine was to observe the process through which heat is transmitted from the needle and thread to the fabric being embroidered.

Knowing the sewing needle's temperature is important for the sewing process when textile materials which are sensitive to heat are involved. [3–4]

During the sewing process, the mechanical energy needed for the needle to pierce through the fabric is transformed in the equivalent amount of thermal energy and this causes the needle to build up heat. If the fabric is made of thermoplastic fibers then it may melt or the sewing thread may melt and break. Therefore, this heat can result both in loss of needle temper and in some sewing faults resulting in a decrease in production. [4]

Figure 2 shows the infrared and visible sprectrum image of the HAPPY embroidery machine.

The tests were performed with a 0.7 mm Schmetz sewing needle. Three embroidery patterns were created, and the fabric chosen for embroidering was synthetic leather.

For the first embroidery pattern, measurements were done at an optimal operating level of 700 sinking/min. This optimal operating level was analized by the authors via the vibration measurement technique (both for embroidery machines and sewing machines) and was described in two previous works [5–6].

In this regard, to diagnose the causes of halts in sewing and embroidery machines, vibration levels were measured in each measuring point, by installing a vibration sensor on the three directions of the Cartesian coordiante system: axial (X), horizontal (Y), vertical (Z). Vibration data was collected from the sewing and embroidery machines in the following domains: velocity, displacement and acceleration. On the Z direction of measurement (the direction on

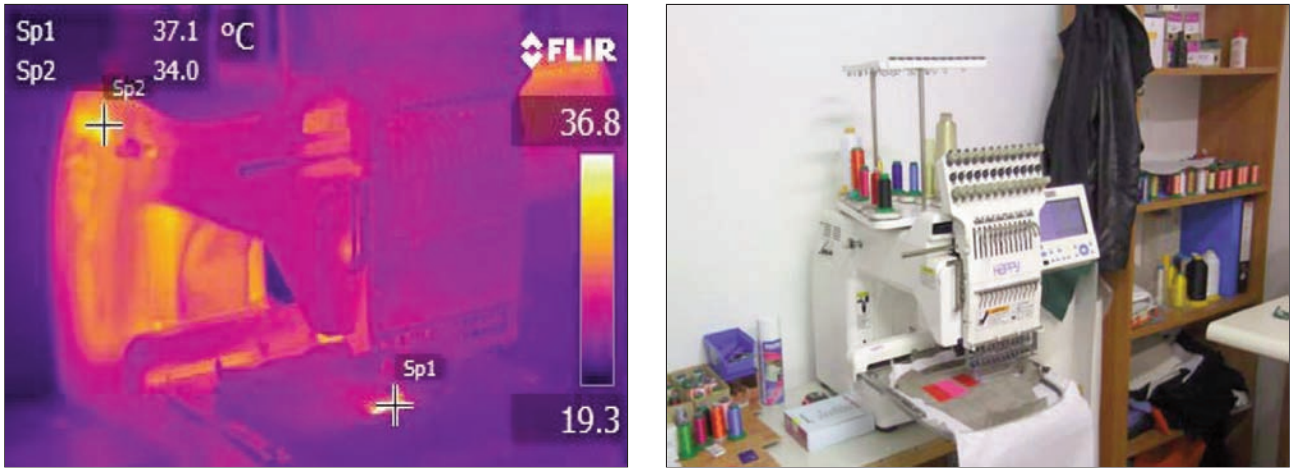

Fig. 2. The infrared spectrum and visible spectrum image of a HAPPY embroidery machine

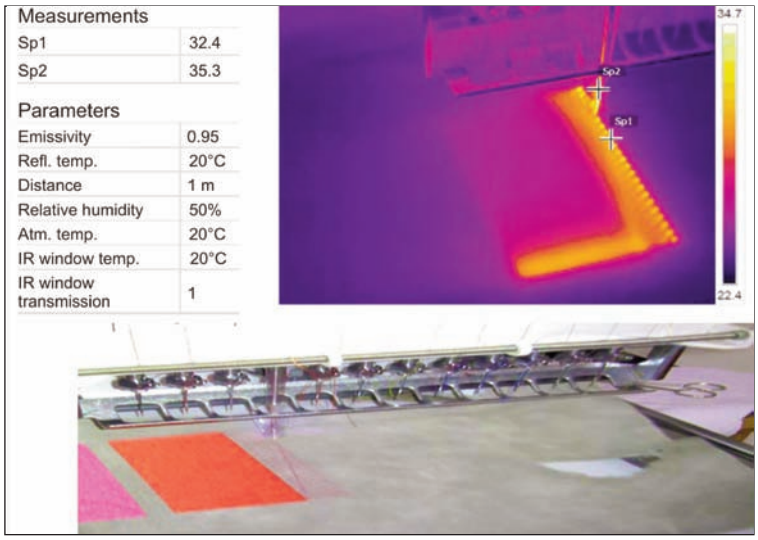

Fig. 3. The image of the machine for the first embroidery pattern, in IR spectrum and visible spectrum

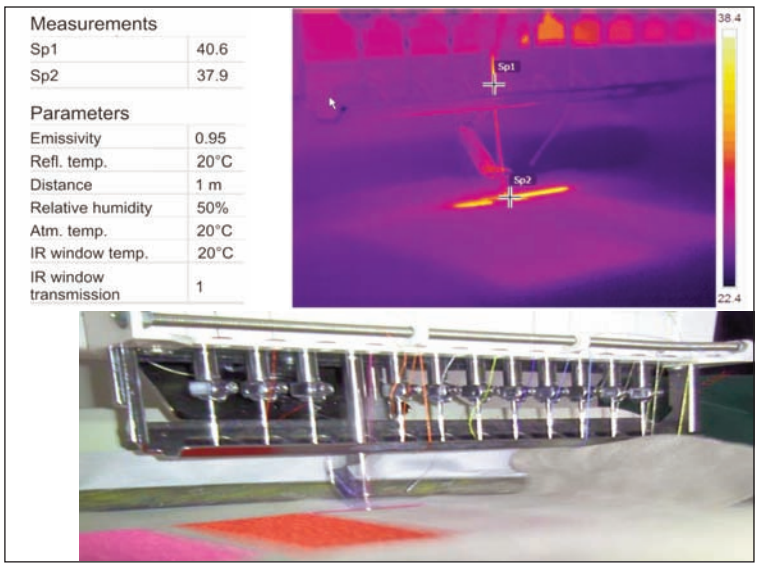

Fig. 4. The image of the machine for the second embroidery pattern, in IR spectrum and visible spectrum

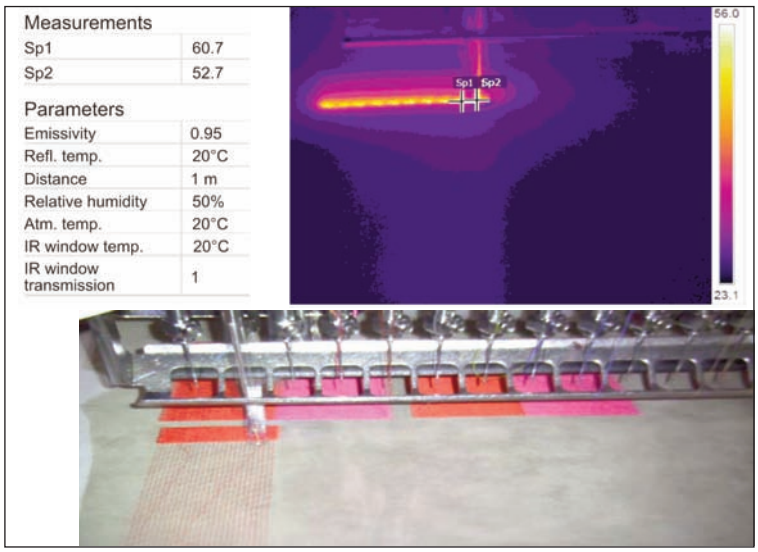

Fig. 5. The image of the machine for the third embroidery pattern, in IR spectrum and visible spectrum

which the sensor was installed), with the fabric advancing on the x direction, it was established that the optimal operating level of the HAPPY embroidery machine is at 700 sinking/min. [5–7].

RESULTS AND DISCUSSIONS

Figure 3 indicates that the first graphic cursor Sp1 is positioned on the fabric being embroidered and shows a temperature of 32.4°C, and the other graphic cursor Sp2 is placed on the needle and shows a temperature of 35.3°C. The distance from which the measurements are taken is 1 m away form the machine, the room temperature is at 20°C, and the relative humidity is 50%. Due to friction between the embroidery needle and the fabric being embroidered, and friction between the needle and the thread, the embroidery operation creates heat, which is quite high for increased operating levels. Most of the heat is gathered in the needle used for embroidery.

It was determined that the accumulated heat leads to increased damage to the thread and embroidered fabric, because both the fabric and the thread absorb a large part of that heat.

After the second pattern is embroidered, both the needle and the fabric for the embroidery show a significant raise in temperature. Thus the first graphic cursor placed on the needle shows a temperature of 40.6°C, and the second graphic cursor Sp2 positioned on the fabric indicates a temperature of 37.9°C, as shown in figure 4.

For the third embroidery pattern, both the needle and the fabric being embroidered reach significant temperatures (figure 5), the graphic cursor Sp1 positioned on the fabric showing now a total temperature of 60.7°C, and the graphic cursor Sp2 placed on the needle indicating a temperature of 52.7°C.

CONCLUSIONS

The research conducted on the HAPPY embroidery machine showed that the temperature of the needle rises as the machine sewing speed and the thread fragility increase. It was determined that the heat does not cause damage to the needle as it passes through the fabric,

but rather this damage occurs in the fabric being embroidered.

The higher the heat levels in the thread, the greater the risk for thermal damage (synthetic fiber threads melt). Thread melting leads to thread breaking and implicitly, to a halt in the sewing process.

The fabric's thermal conductivity and its thickness have a big influence on the level of accumulated heat. The longer the time needed for completing an embroidery pattern, the more relevant the needle temperature becomes.

BIBLIOGRAPHY

[1] Dima, I., C., Nedelcu, M., V., *Managementul producţiei industriale*, Editura Economică, Bucureşti, 2003.

[2] Mazari, A., Havelka, A., Zhu, G., *Sewing needle temperature of an Industrial lockstitch machine*. In: Industria Textila, 2014, vol. 65, issue 6, pp. 335-339.

[3] Oana, I.P., Oana, D., Doble, L., *Analysis of the heating needle machine, in sewing process at high speeds*. In: Annals of the University of Oradea, Fascicle of Textiles-Leatherwork, Oradea, vol. XIV, nr. 2, 2013 pp. 71-75

[4] Yukseloglu S. M., Çitoğlu F., Çetinkaya, B., *A study on the needle heating in polyester blend upholstery fabrics*. In: Industria Textila, 2013, vol. 64, nr. 5, pp. 246-253

[5] Şuteu, M., Indrie, L., Ganea, M., *Determination of optimum performance regime for SunStar buttonhole machine by vibrations measuring technique. Processing the data measured with Data Explorer Software*. In: Annals of the University of Oradea, Fascicle of Textiles-Leatherwork, Oradea, vol. XIII, nr. 1, 2012, pp. 146-157.

[6] Şuteu, M., Baidoc, M., Indrie, L., Ganea, M., *Determining the optimal operating mode for the embroidery machine by using the vibration measurement technique*. In: Industria Textila, 2014, vol. 65, nr. 1, pp. 17-21

[7] Şuteu, M., Doctorate thesis – *„Researches concerning the provision of technological processes reliability in the textile industry”*, University of Oradea, Octombrie 2013

Authors:

Chief of works dr. eng. MARIUS ȘUTEU
Associate prof. dr. eng. LILIANA INDRIE
Associate prof. dr. eng. SABINA GHERGHEL

University of Oradea
Faculty of Power Engineering and Industrial Management
Str. B. Şt. Delavrancea, no. 4, 410058, Oradea, Romania
e-mail: msuteu@uoradea.ro; lindrie@uoradea.ro; sgherghel@uoradea.ro

Associate prof. dr. eng. ADRIAN TIMOFTE
University of Oradea
Faculty of Environmental Protection
26 Gen. Magheru St., 410058 Oradea, Romania
e-mail: adi_timofte@yahoo.com

A study on DLC-coated industrial lockstitch sewing needle

ADNAN MAZARI
ANTONIN HAVELKA
JAKUB WIENER
ZBIGNIEW ROŻEK

REZUMAT – ABSTRACT

Studiu privind acele de cusut ale mașinilor de cusut industriale acoperite cu carbon tip diamant (DLC)

Acoperirile cu carbon tip diamant (DLC) sunt foarte cunoscute pentru proprietățile acestora împotriva uzurii, pentru coeficientul de frecare redusă și duritatea ridicată. În acest studiu, acele de cusut sunt acoperite cu un strat DLC și apoi sunt investigate în vederea performanței la coasere. Rezultatele acestui studiu arată că temperatura acului este mai scăzută cu aproximativ 9% la o viteză de coasere de 4000 r/min, iar tenacitatea firului cusut este cu aproximativ 6% mai mare în comparație cu a acelor neacoperite.

Cuvinte-cheie: ac de cusut, temperatura acului, fir de cusut, mașină de cusut

A study on DLC-coated industrial lockstitch sewing needle

Diamond like carbon (DLC) coatings are well-known for the properties like protection against wear, low friction of coefficient and high hardness. In this research sewing needles are coated with DLC layer and then investigated for sewing performance. The results of the research shows that the needle temperature is decreased by nearly 9% at 4000 r/min of sewing and the breaking tenacity of stitched thread is nearly 6% higher as compared to the non-coated needles.

Key-words: Sewing needle, needle temperature, sewing thread, lockstitch

In the sewing process, the sewing thread undergoes friction between fabric, guides, tension devices on machine, bobbin thread and the sewing needle. The performance of sewing thread in apparel industry has become extremely important. Every day, thousands of products ranging from shirts to automotive airbags are sewn. Hence, even small improvements may result in significant corporate benefits. Heavy industrial sewing, such as that used in the manufacture of automobile seat cushions, backs and airbags, requires not only high production but also high sewing quality (i.e. good appearance and long-lasting stitches) [1].

Needle heat-up is a major problem on the sewing floor [2]. In recent years, in order to increase production, high-speed sewing has been extensively used. Currently, sewing speeds range from 1000 to 4000 r/min. In heavy industrial sewing, typical sewing speeds range from 700 to 2000 r/min. Depending on the sewing conditions, the maximum needle temperatures range from 100°C to 300°C [1]. This high temperature weakens the thread, since thread tensile strength is a function of temperature, resulting in decreased production [12–13]. In addition, the final stitched thread has 30–40% less strength than the parent thread [3, 11, 14]. As a result of improved understanding of the causes of sewing damage, many technical developments, such as improved needle design [4], fabric finishes [5, 6], thread lubrication and needle coolers [7, 8, 15], have taken place over the years.

DLC (diamond like coatings) possesses a small friction coefficient and high wear resistance. Therefore they have been used to improve the service characteristics of various metal parts [9]. In this research we coated the needles with DLC to examine the sewing performance which includes needle temperature and tensile properties of stitched sewing thread.

EXPERIMENTAL PART

In this research, needles (100 Nm) are coated with DLC layer by radio frequency plasma assisted chemical vapour deposition/magnetron sputtering (RF/PACVD/MS) method. The coated needles are further compared with the non-coated needles in terms of needle temperature during sewing, surface roughness and sewing performance.

DLC coating of sewing needles

During the last 20 years DLC coatings became a very attractive material in many industrial applications. In our research we coated the needles (Grozbeckert, 100 Nm, R type) using RF/PAVCD/MS method. The system consists of a cylindrical chamber 290 mm in diameter and 190 mm high, with water cooled bottom electrode connected through an impedance matching network to the radio frequency of 13.56 MHz power generator. The magnetron equipped with 50 mm Ti-cathode is mounted in the chamber top cover. The parameters and steps of sample preparation are as below.

Sample cleaning: The specimens (needles) were ultrasonically cleaned in methanol for 20 min before deposition. The base pressure of the reaction chamber is kept less than 10^{-3} Pa.

Etching: The samples mounted on R.F electrode are etched in argon plasma for 10 min at self-bias voltage of –500 V, pressure of 4 Pa and Argon gas flow rate of 10 sccm.

Deposition of Ti coating: Firstly the Ti layer is deposited by DC magnetron sputtering for 5 min with pressure of 1.2 Pa, self-bias voltage of –300 V, flow rate of Ar. was 10 sccm and power on Ti sputtered target was 1025 W

Deposition of DLC coating: The DLC layer synthesis is conducted by RF/PACVD process for 20 min with methane gas at a constant flow rate of 20 sccm, pressure of 20 Pa and self-bias voltage of –600 V.

Figure 1 shows the needle after DLC coating. The needle colour changes to greyish-black due to DLC-layer.

Needle temperature measurement

Thermal camera is used to record the needle temperature during high speed sewing. The emissivity of the needle was calculated by ASTM standard E 1933 – 99a and found to be 0.71 for a DLC-coated needle at 37 °C. Lockstitch machine (Brother Company, DD7100-905) is run at high speed of 3000 and 4000 r/min and needle temperature is measured with thermal camera (FLIR X6450), whereas the needle temperature of non-coated needles is measured by inserted thermocouple method, as its difficult to find the emissivity of shinny chromium needle. From previous research of author [10, 16] it's suggested to use inserted thermocouple method. In this method a thin wire thermocouple is inserted inside the needle grove and the needle temperature is received wirelessly to computer during the sewing process as shown in figure 2. In this research, polyester-polyester (PET-PET) corespun thread with two different count are used for the experiment. The properties of sewing thread are shows in table 1. The properties of denim fabric used for the sewing process are shown in table 2. Ambient temperature and humidity are kept constant at 26 °C and 65% respectively.

Fig. 1. Needle after DLC coating

Fig. 2. Placement of thermocouple inside the needle groove

Tensile properties measurement

The breaking tenacity and elongation values of the sewing thread are measured using INSTRON Tensile strength tester according to standard ISO 2256. Tensile properties of all sewing threads are tested before sewing and after sewing process, the sewing thread is carefully removed from the seam by cutting the bobbin thread. Each thread is measured 10 times each for all speeds of sewing respectively. This experiment is necessary to compare the effect of normal and DLC-coated needle on the sewing threads after sewing process.

RESULTS AND DISCUSSION

Comparison of sewing needle temperature

The industrial lock stitch machine is run at speed of 3000 and 4000 r/min for 15 seconds and needle

Table 1

SEWING THREAD USED FOR THE EXPERIMENTS					
Thread type	**Company name/ product name**	**Fineness [tex]**	**Twist (t/m)**	**Twist direction (ply/single)**	**Coefficient of friction μ**
Polyester–polyester core spun	AMANN/Saba C-80	40(20*2)	660	Z/S	0.20
Polyester–polyester core spun	AMANN/Saba C-50	60(30*2)	640	Z/S	0.23

Table 2

FABRIC USED FOR THE EXPERIMENTS					
Fabric type	**Weave**	**Weight**	**Ends/cm**	**Picks/cm**	**Fabric thickness**
100% cotton Denim	2/1 Twill	257 g/m^2	25	20	0.035 cm

temperature of DLC-coated needles is measured using thermal camera and inserted thermocouple method for the non-coated needles. It was observed that the needle temperature is 12°C higher for normal needles as compared to coated needles 40 tex thread 8C higher for 60 tex thread; this effect is insignificant (calculated at 95% confidence interval). The low surface roughness and friction properties of DLC-coated needles causes a decrease in the frictional heat between needle and the fabric but it's impossible to determine the surface properties of inside part of needle's eye, which is the major contact for the thread to the needle. The diamond polish is the final step of DLC coated needles for better smooth surface, but in case of the needle it's impossible to polish the inside of needle eye due to complex and small shape.

Comparison of Tensile properties for DLC-coated and normal needles

Tensile properties of all sewing threads are tested before sewing and after sewing process. Sewing process is performed for 15 seconds and sewing thread is carefully removed from the seam by cutting the bobbin thread. Each thread is measured 10 times each for all thread types respectively. This experiment is necessary to compare normal and DLC-coated needle for the effect of needle temperature and friction on tensile properties of sewing thread. It is visible in figures 3–4 that there is a minor increase in tensile properties of sewing thread with DLC-coated needles as compared to normal needles. This is due to low friction properties of sewing needle coated with DLC which reduces the frictional heat.

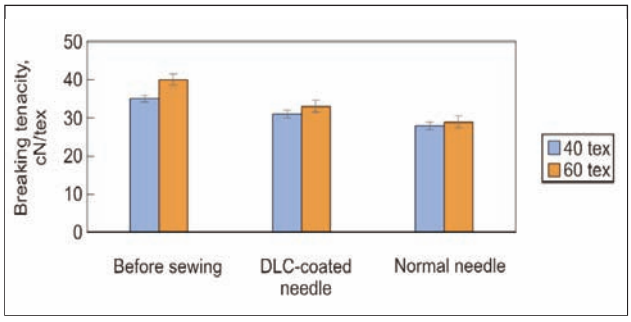

Fig. 3. Comparison of breaking tenacity of sewing threads

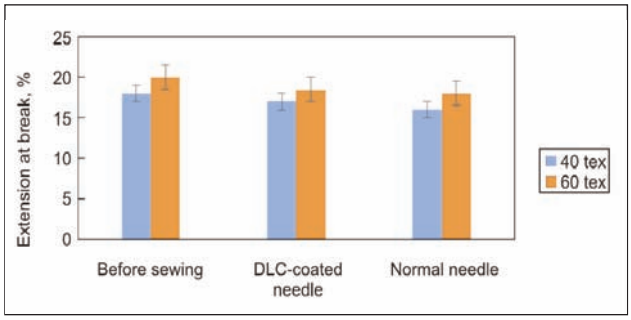

Fig. 4. Comparison of breaking extension of sewing threads

Surface properties of needle

The DLC thickness was measured using SEM (Scanning Electron Microscopy) and found to be 960 nm, whereas the Ti-gradient layer was found to be nearly 150 nm. The results (table 3) obtained from the AFM (Atomic Force Microscopy) shows that DLC-coated needles exhibit less average roughness parameters as compared to normal needles.

Figures 5–8 show the surface topography of normal needle and DLC-coated needle surface by AFM. DLC-coated needles shows better roughness property as compared to normal needles by AFM measurement. The heat is generated in needle due to friction

Table 3

ROUGHNESS PROPERTIES OF NEEDLES (100*100 μM)

	Normal needle	DLC-coated needle
Average roughness R_a	689.6 nm	657.7 nm
RMS roughness R_q	802.6 nm	763.2 nm
Peak to valley roughness R_t	3.864 μm	3.837 μm

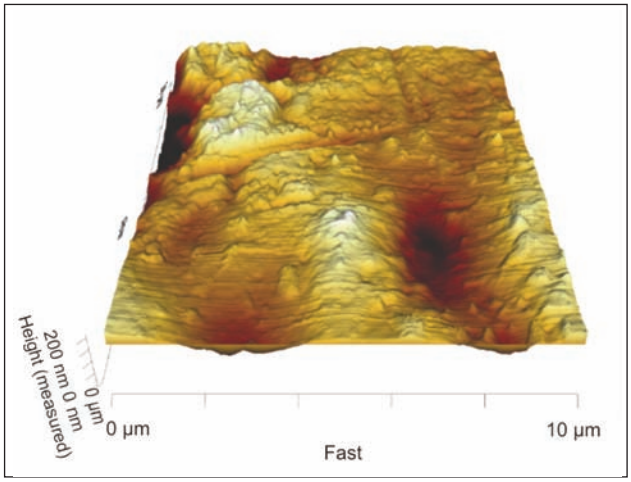

Fig. 5. Surface image normal needle (10*10 μm)

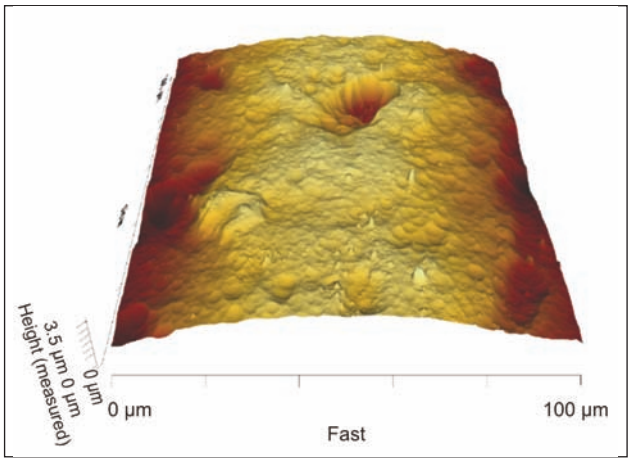

Fig. 6. Surface image normal needle (100*100 μm)

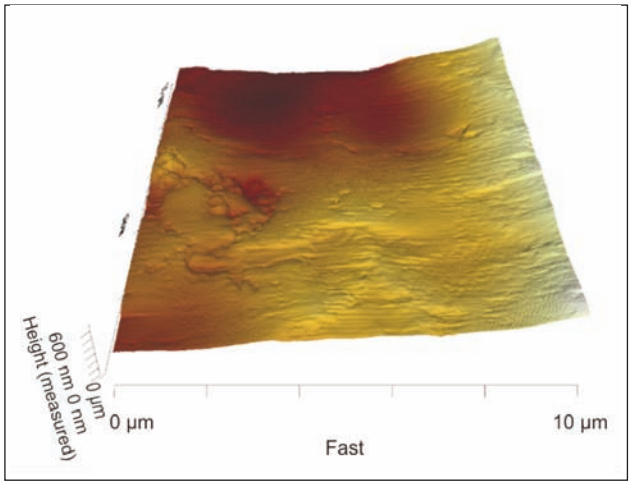

Fig. 7. Surface image of DLC-coated needle (10*10 µm)

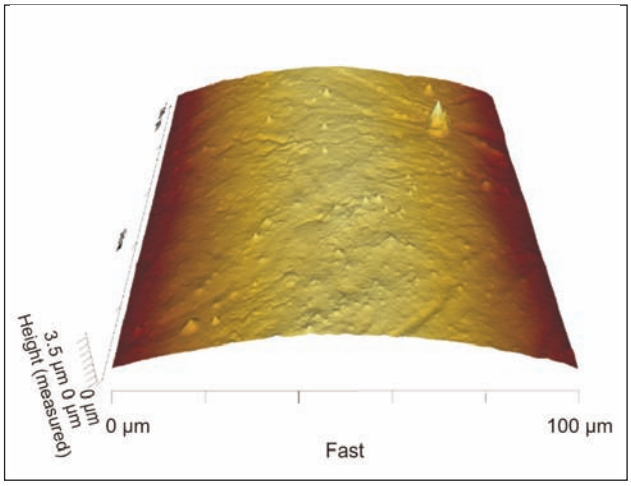

Fig. 8. Surface image DLC-coated needle (100*100 µm)

of fabric to needle surface and secondly by the rubbing of sewing thread to the needle eye. The better roughness properties of needle cause decrease in the needle temperature.

CONCLUSIONS

DLC-coating is getting popular rapidly while its use in the textile industry is still unknown. From our research we conclude that, it's possible to cover the needle with DLC coating but the needle eye complex shape make it impossible to determine if the coating is evenly applied at the inside part of the needle's eye. DLC-coated needles along length shows better roughness property as compared to normal needles by AFM measurement. Diamond polish is also important step in bringing better surface properties of martial but the needle eye due to complex shape was not possible to be diamond polished. There was a small improvement noted in terms of tensile properties and needle temperature for DLC coated needles.

ACKNOWLEDGEMENT

The results of this project (LO1201) were obtained through the financial support of the Ministry of Education, Youth and Sports in the framework of the targeted support of the "National Program for Sustainability I", the OPR&DI project Centre for Nanomaterials, Advanced Technologies and Innovation CZ.1.05/2.1.00/01.0005 and the Project Development of Research Teams of R&D Projects at the Technical University of Liberec CZ.1.07/2.3.00/30.0024.

BIBLIOGRAPHY

[1] Qinwen, Li., and Liasi, E. *A study on the needle heating in heavy industrial sewing part-1.* In: International Journal of Clothing Science and Technology, 2001, vol.13, issue 5, pp. 351-367.

[2] Hersh, S., Grady, P. *Needle heating during high speed sewing.* In: Textile Research Journal, 1969, vol. 39, pp. 101-120.

[3] Midha, V., Mukhopadhyay, A., Chatopadhyay, R., Kothari, V. *Studies on the changes in tensile properties of sewing thread at different sewing stages.* In: Textile Research Journal, 2009, vol. 79, pp. 1 155-1167.

[4] Qinwen, Li., Liasi, E. *A study on the needle heating in heavy industrial sewing, part II.* In: International Journal of Clothing Science and Technology 2001, vol. 13, issue 2, pp. 87-105.

[5] Trung, N., Kus, Z. *Computer Simulation of Sewing Needle Heating.* In: CSCC'99 Proceedings, 1999, vol.1, pp. 1991-1994.

[6] Mazari, A., Havelka, A. *Tensile properties of sewing thread and sewing needle temperature at different speed of sewing machine*. In: Advanced Materials Research, 2013, vol. 627, pp. 456-460.

[7] Li, Q., Liasi, E., Simon, D., and Du, R. Heating of industrial sewing machine needles, FEA model and verification using IR radiometry. In: Thermosense XXI, 1999, vol. 3700, pp. 347-357.

[8] Gurada, A., et al. *The effects of various lubricants on the friction properties of sewing threads*. In: Textile Research Journal, 2013, vol. 83, issue 12, pp. 1273-1282.

[9] Batory, D., et al. *The effects of deposition parameters on the properties of gradient a-C:H/Ti layers*. In: Journal of Achievement in Materials and Manufacturing Engineering, 2009, vol.37, issue 2, pp. 381-386

[10] Mazari, A., Havelka, A., Hes, L. *Experimental techniques for measuring sewing needle temperature.* In: Tekstil ve konfeksiyon, 2014, vol. 24, issue 1, pp. 111-118.

[11] Gurada, A., Kaplangiray, B. and Kanik, M. *The effects of lubrication on properties and seam performance of sewing threads*. In: Tekstil ve Muhendis, 2011, vol. 18, pp. 19-25.

[12] Mazari, A., Havelka, A. *Influence of needle heat during sewing process on the tensile properties of sewing thread*. In: Tekstilec, 2013, vol. 56, Issue 4, pp. 345-352.

[13] Yukseloglu, M., Citoglu, F. Cetinkaya, B. *A study on the needle heating in polyester blend upholstery fabrics*. In: Industria Textila, 2013, vol. 64, issue 5, pp. 246-253.

[14] Mazari, A. and Havelka, A. *Impact of stitch length on sewing needle temperature*. In: World Journal of Engineering, 2014, vol. 11, issue 2, pp. 187-192.

[15] Eryuruk, S., Kalaoglu, F. *The effects of different amounts of lubricant application on sewing thread performance properties*. In: Textile Research Journal, 2010, vol. 80, issue 12, pp. 1232-1242.

[16] Mazari, A., Havelka, A., Zhu, G. *Sewing needle temperature of an Industrial lockstitch machine*. In: Industria Textila, 2014, vol. 65, issue 6, pp. 335-339.

Authors:

ADNAN AHMED MAZARI
ANTONIN HAVELKA
Technical University of Liberec,
Faculty of Textile Engineering,
Department of Textile Clothing, Studentska 2, Liberec,
461 17, Czech Republic

JAKUB WIENER
Technical University of Liberec,
Faculty of Textile Engineering,
Department of Material Engineering, Studentska 2, Liberec,
461 17, Czech Republic

ZBIGNIEW ROŻEK
Technical University of Liberec,
Department of Preparation and Analysis of Nanostructures,
Studentska 2, Liberec,
461 17, Czech Republic

Corresponding author:

ADNAN AHMED MAZARI
e-mail: adnanmazari86@gmail.com

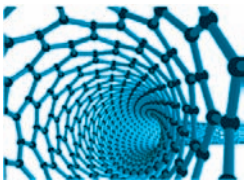

Modelling and simulation of heat transfer through Turcana wool insulated walls

IOAN N. HOSSU
MARIAN-CĂTALIN GROSU
GHEORGHE HORGA
ANDREI IOSUB

IULIANA GABRIELA LUPU
DORIN AVRAM
FLORIN BREABĂN

REZUMAT – ABSTRACT

Modelarea şi simularea transferului termic prin pereţi izolaţi cu lână Ţurcană

Acest articol tratează, prin modelare și simulare, aspecte privind efectele aplicării unei izolații termice din fibre de lână Ţurcană la diminuarea transferului termic în construcțiile civile. Realizată prin cardare și suprapunere succesivă de straturi, pe un tambur rotitor, mostra reală a fost selecționată dintre mai multe structuri, optimizate tehnologic cu un program central compus rotabil cu două variabile. Caracteristicile termice au fost testate pe o instalaţie experimentală din LGCgE, Universitatea Artois, Franţa. Modelarea și atribuirea valorilor materialelor, a fost făcută pentru trei variante de pereți exteriori din componența curentă a locuințelor.
Simularea transferului termic convectiv evidențiază beneficiul net al izolației din fibre de lână Țurcană, atât la exteriorul zidului din cărămidă, cît și la interiorul zidului cu structură din lemn (OSB), prin îmbunătățirea parametrilor de transfer termic prezentați detaliat in lucrare; zidul din cărămidă în varianta neizolată are performanțe termice reduse.

Cuvinte-cheie: straturi din lână de oaie, izolaţie termică, optimizare, modelare, simulare, elemente finite

Modelling and simulation of heat transfer through Turcana wool insulated walls

This paper presents aspects related to the effects of applying Turcana wool fiber insulation on lowering heat transfer in buildings through modelling and simulation. The real sample was obtained by carding and successive overlapping of layers on a rotating drum. The sample was chosen from a variety of technologically optimized structures, by means of a rotatable compound central programme with two variables. The thermal characteristics were tested on an experimental installation from LGCgE, Artois University, IUT, Bethune, France. The modelling and assigning value to materials was has been performed for 3 types of exterior walls commonly found in the structure of buildings.
The simulation of convective heat transfer highlights a net benefit of thermal insulation both on the exterior of brick wall and also inside of wood structure (OSB), by improvement of the heat transfer parameters that are thoroughly presented in this paper. Structures b) and c) were also submitted to a comparative analysis. The uninsulated brick wall has low thermal performance.

Key-words: sheep wool layers, thermal insulation, optimization, modelling, simulation, finite elements

The predictions referring to the consequences of an economic development that would exceed the supportability threshold of the global environment [1–2] have come true.
Climate change, environmental, water and air deterioration are evident. The depletion of resources initiated by the industrial revolution was maintained and even amplified in recently industrialized regions of East Asia. The effects for mankind are presently obvious.
Residential consumptions amount to 40% of the total energy production in the European Union and impact the planet's health. In terms of sustainable development, human activity relies on environment and resources [3–4].
Health, social safety and economic stability are essential for life quality in society. The unified global efforts to reduce energy consumption and polluting emissions in the atmosphere involve: research, development and application of sustainable technological solutions [5–6].
Added to these are the calls of the European community for harmonious sustainable development, social inclusion and technology transfers by opening secure markets and creating new jobs [7].
Natural, renewable and sustainable materials such as fibrous materials of plant origin (bast and wood fibres) or of animal origin (wool, feathers) can provide functional characteristics (humidity and thermal comfort as well as phonic comfort in the residents' proximity) [8–10].
Wool fibres have a complex structure that has improved over thousands of years in order to protect sheep against low and high temperatures and humidity. They were also used since ancient times by men, either in raw form or after specialized processing (spinning, weaving, braiding, felting) for thermal protection (Mongolian nomads' yurts) and in hometech articles and it is being reconsidered in buildtech [11].
The tests of sheep wool blended with synthetic fibres glued with acrylic resin, under the form of Wool Blocks started in New Zealand by the end of '90s and

the blend was validated in 2001 by the Central Laboratory, after several trials [12].
Wool thermal insulations were initially exported by Australians and they were subsequently produced in Europe, according to various procedures. Starting with December 2003, Alchimea lana®, manufactured in Germany, has been officially approved as building material in all European countries It is manufactured by several companies and commercialized in the context of sustainable development [13–18]. Starting with 2012 it is also manufactured in USA [19].
Romania, as the fourth country in the European top of sheep farmers is able to exploit the surplus of wool for thermal protection of buildings.
This study presents the effects of Turcana wool insulation on thermal performances of buildings. Three exterior corners are modelled and analyzed by simulation, using the finite element method, the effects of heat transfer and the influence of Turcana wool insulation.

MATERIALS AND METHOD

Materials

The carded Turcana wool fibrous layers were subjected to research by experimental procedures, by laboratory studies on physical models. The technological characteristics have been optimized by mathematical methods, analytical made by the method of least squares. The thermal characteristics have been determined according to NF EN 12667, NF EN 12664, on an experimental installation that belongs to the Civil Engineering and Geo-Environment Laboratory (LGCgE) of Artois University, in the Technology Institute (IUT) of Bethune, France. [20].
The thermal parameters are calculated according to the methodology detailed in [21]. The technological characteristics were optimized through mathematical, analytical procedures, by means of a compound rotatable central programme with two variables.
We selected for this article a thermal insulation (IzL) from wool fibres, with characteristics as presented in table 1. (IzL) can be obtained in two variants (V): V1) domain staggered overlapping of two layers with a mass of 1.3 kg/m^2, or V2) in situ, by predimensioned deposition of 2.6 kg wool with a thickness of 15 cm/m^2.
Layer V1) was designed to be produced by carding on a wool card with 4 carding groups, by web doffing and successive overlapping of layers on a rotating drum [22]. Layer V2) can be mounted after opening and weighing.

Method

Research methods by mathematical, numerical processes allow a virtual approach of complex phenomena of elasticity, structural analysis, problems in civil engineering, etc.
In the construction physics, heat transfer, vapor diffusion, etc., expressed mathematically by higher order differential equations have an analytical solution only in very simple cases.
Modelling and numerical analysis methods (finite difference method (FDM), finite element method (FEM), etc.), using sometimes specialized sophisticated programs, can solve complex problems by transforming these equations or systems of differential equations with limit conditions attached to the linear systems of algebraic equations whose unknowns are temperature, pressure, velocity in the knots or elements of the selected meshing network.
By using these methods, FDM, FEM, the continuous media with an infinite number of degrees of freedom approximate with discrete environments, with a finite number of degrees of freedom. This is the meeting of smaller subdomains called finite elements (which is the name of the method) and the results obtained are very close to the experimental results [25], [26].

Table 1

CHARACTERISTICS OF THE FIBROUS LAYER

Characteristics of the fibrous layer	Symbol	M.U.	Value
Average fibre length	l_{med}	mm	102.8
Average fibre fineness	Nm	m/g	427
Textile fabric density	r	Kg/m^3	17
Final thermal insulation thickness (IzL)	h	cm	15
Thermal conductivity	λ	W/(mK)	0.05245*
Thermal resistance	R	m^{2}K/W	2.30676
Effusivity	E	JK^{-1}m^{-2}s$^{-1/2}$	48.37
Diffusivity	D	m^2/s	1.18E-06
Mass specific heat capacity (at constant pressure)	cp	J/(kgK)	2698.44
Volumetric specific heat capacity	cv	J/(m^{3}K)	44602.38

** thermal conductivity was determined after conditioning the samples in LGCgE test conditions. The temperature of 20°C and air relative humidity of 65% is in conformity with SR EN ISO 139: 2005/A1:2011;*
*** the values obtained are in accordance with the previous studies [23], [24].*

Modelling

It consists of the formation of a computational model to simplify the physical problem considered but to maintain at the same time the results in reasonable margin of error. This simplification can be applied to the geometry of domain (W) (domain W represents the area enclosed by the outline of the model – by W heat transfer simulation is performed), or the modelled assembly, types of materials and their characteristics, boundary conditions, tested temperature limits, etc. This article presents the virtual models of three flat structures of composite walls.
This paper analyses three samples of corner walls with a height of 1 m and the inner sides with a length of 1.5 m.

Table 2

COMPOSITION OF THE STRUCTURES W1, W2 and W3, MODELLING AND SIMULATION PARAMETERS							
Composition of analysed structures			**Modelling*** **		**Simulation****		
					Density	**Thermal conductivity**	**Volumetric heat capacity**
Crt. no.	**Name**	**Material**	**UM**	**Size**	kg/m^3	W/(mK)	MJ/(m^{3}K)
1	Interior plaster	Sand-lime	cm	2	1600	0.7	1.34
2	Masonry	Solid brick	cm	24	1800	0,8	1.57
3	Exterior plaster	Sand-cement	cm	3	1700	0.87	1.43
4	Insulation support and spacer	Resinous substances*	cm	15	550	0.35	1.38
5	Thermal insulation	Sheep wool	cm	15	17	0.05	0.06
6	Insulation support wall	OSB3	mm	10	600	0.13	1.02
7	Spacer and support	XPS	mm	30	30	0.04	0.04
8	Exterior finish	Alucobond2	mm	3	1500	0.44	0.82
9	Exterior and interior walls	OSB3	mm	18	650	0.13	1.11
10	Thermal insulation walls	OSB3	mm	12	600	0.13	1.02
11	Spacer and support	XPS	mm	50	30	0.04	0.04

* assembling is made perpendicular on the fibre length;
** parameters of convective heat transfer simulation (T_{ext} = –18°C, a_e = 24 Wm^{-2}K^{-1}, T_{int} = 20°C, a_i = 8 Wm^{-2}K^{-1}) [28];
*** internal dimensions of the models analysed are 1.5 m.

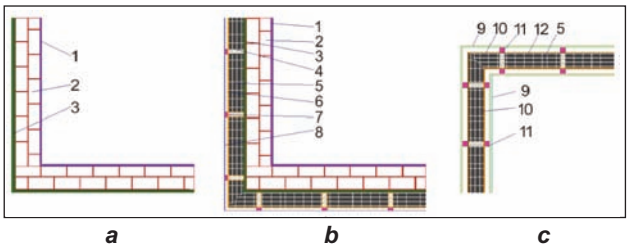

Fig. 1. Modelling and composition of the structures a), b), c), assigning the domains W1, W2, W3: a – corner full brick wall, plastered inside and outside; with simulation domain – W1; b – a) with IzL on the outside, with simulation domain – W2; c – wall made by assembling OSB panels with wooden coniferous elements and IzL core; with the simulation domain – W3

Models and correspondence with simulated and analyzed domains in this paper are shown in figure 1, have the characteristics in table 2 and represent:
a) – the structure of a corner full brick wall, plastered inside and outside with the geometry of the domain (W1) (figure 1a);
b) – the structure of a corner full brick wall, plastered inside and outside with thermal insulation wool (IzL) mounted: on the outside with the geometry (W2) (figure 1b);
c) – Corner wall structure of a wooden structure (OSB) plastered in the central area with Turcana wool and lateral space for installation, with the geometry of the domain (W3) (figure 1c).
Characteristics of materials presented in table 2 have been taken from the database with values found in the Norm C107/2005, the composition of the modelled structure being performed.

Heat transfer simulation through W1, W2 and W3 domains

Thermal domain analysis was performed with the finite element method (FEM), on flat models, with RDM 6.17 program Finite elements, thermal analysis module, [27], with the following steps:
Preprocessing – requires numerical description that can be interpreted by the computer by means of a specialized FEM program, the domain to be simulated, meshing, assigning values to materials and specification of the thermal analysis conditions.
Domain modeling can be done in its own program from RDM 6 or other programs that support saving the file as *.igs sau *.dxf (e.g. AUTOCAD) where the model can be imported.
The operation of choosing the number and type of finite elements with 3 or 4 sides, 6 or 9 knots, combined with the domain division into a number of finite elements is called meshing. The variable mesh network of the domain with finite elements has been performed so that areas of interest in the corners, to be meshed smoother because the final accuracy depends on the dimensions of finite elements (figure 2). Material values were assigned according to table 2, the simulation part and thermal analysis conditions were imposed for convective heat transfer simulation T_{ext} = –18°C, a_e = 24 Wm^{-2}K^{-1}, T_{int} = 20°C, a_i = 8 Wm^{-2}K^{-1}) [28].
Processing – is the automatic processing of the necessary sizes of the model using specialized programs, namely RDM 6.17 Finite elements, thermal analysis module.

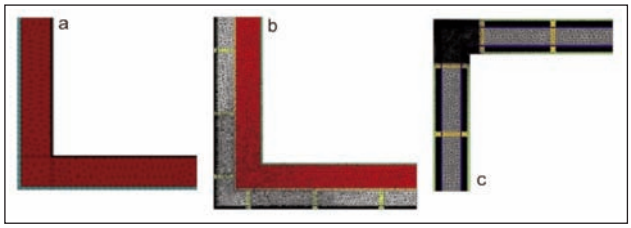

Fig. 2. Meshing of the domains: a – W1, b – W2, c – W3

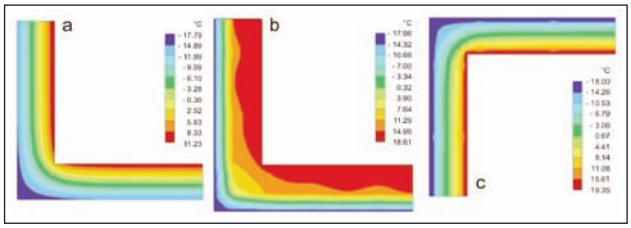

Fig. 3. Temperature maps: a – W1, b – W2, c – W3

Post-processing – is the stage in which the computer processing and presentation of results are performed.

Interpretation of results – is the stage connected especially to the user who must validate the model obtained from simulations and to make decisions on the use of results, if they are expected or a new simulation is required. For more complicated situations that require a larger number of simulations, the user must decide if the technological improvements of the model are required, or if the simulation parameters must be changed according to the results of previous simulations. The stages of pre-processing, meshing and post-processing have been performed in accordance with the thermal parameters required and models b) and c) were successively improved by technology redesigning.

RESULTS AND DISCUSSIONS

Temperature maps shown in figure 3 show a much lower temperature in the uninsulated corner W1, favorable to condensation due to the analyzed temperature difference shown in figure 3a. The contribution of thermal insulation is significant, W2 (figure 3b), due to the removal of the condensation area in the corner and the higher temperatures accumulated in masonry. Domain W3 (figure 3c) has the highest temperature of the inner walls. A comparative analysis of the temperatures is shown in table 3.

Heat flow density maps shown in figure 4 show the overall thermal performance that each of the structures analyzed has in this paper and we can identify the thermal bridges and their effect on energy losses, and we quantify the performances which were partially presented in table 3.

We see that after performing heat transfer simulation in the three domains (figure 5) heat flow vectors that characterize the heat flow temperatures and the densities have the following features:

- The domain structure W1: generally homogeneous structure and a high heat transfer in the corner area;
- The domain structure W2: more heterogeneous structure than the structure domain W1, characterized by lower loss of heat flow in the corner area and the occurrence of thermal bridges in the fixing area of Alucobond2 exterior finish;
- The domain structure W3: generally, a homogeneous structure of the thermal field which has transversal thermal bridges by its fixing and consolidation elements.

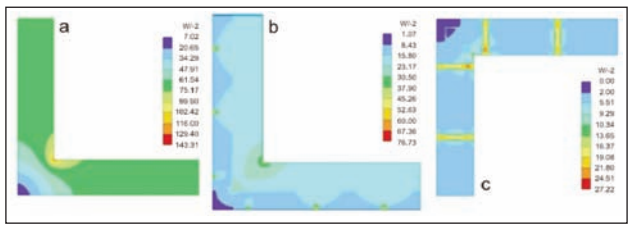

Fig. 4. Heat flow density maps: a – W1, b – W2, c – W3

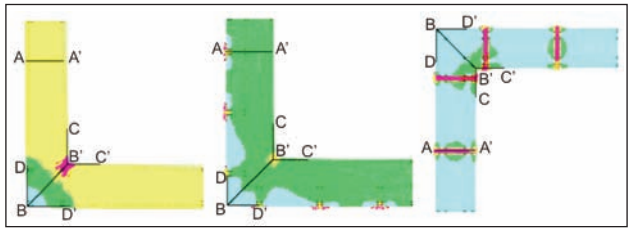

Fig. 5. Unitary heat flow vector representation: a – W1, b – W2, c – W3

Figure 5 shows a different concentration of heat flow vectors in the domain W1, in the corner area. In the case of the domain structures W2 and W3, the heat flow vectors are more uniform in the corners, and thermal effects of the wooden rods are marked.

Analysis by areas of interest

The simulation program allows to display the variation graphs of temperatures and heat flows on a selected cross-section or on an (interior or exterior) surface of the domain:

Comprehensive and comparative analysis shown is structured as follows:

AA' – any wall cross-section; BB' – cross-section through the two corners; CC' – surface of inner corners; DD' – surface of outer corners (figure 5).

Comparative thermal analysis through AA', BB' cross-sections and CC' and DD' surfaces of the analysed domains

Thermal effects through AA' cross-section

In the domain *structure* W1 the temperature descreases linearly between 11.03°C and –15.01°C, on width of the wall.

The domain W2 contains 3 areas of temperature decrease:

- slow decrease through the brick wall between 17.9°C and ~ 10°C;
- the second area between 10°C and –3°C, corresponding to the thermal insulation;
- the last area between –3°C and –17°C. The freeze-thaw phenomenon takes place in the outer half of the brick masonry.

The domain W3 shows a heat transfer with the same tendency of linearity as in the domain structure W1.

Thermal effects through BB ' cross-section and CC' and DD' surfaces (corner domains)

The domain structure W1 shows that in the inner corner area the current temperature of the walls decreases from 11.03°C to 5.88°C. Diagonally between the two corners temperature decreases after a curve.

In the domains W2 and W3 the temperature of the inner corners exceeds 15°C, thus the risk of condensation in the area is eliminated. In the domain W2 the risk of degradation of the wall and its outer corner through freeze thaw phenomenon is also eliminated. The domain W3 shows a higher decrease of temperature in the corner as compared with the domain structure W2.

CC' shows the temperatures in the inner corners with the curvilinear structure of the domain W3 due to the influence of thermal microbridges of the cross-section (figure 4c).

DD' shows a linear variation of the domain structure W1, and the effects of thermal microbridges in the domain structures W2 and W3 identified in figures 5b, c.

Comparative heat flow through AA' and BB' cross-sections, CC' and DD' surfaces of the analysed domains

In domain structure W1 heat flow is uniform in the walls and has distinctive characteristics only in the corner area.

In the domain structures W2 and W3 heat flow density shows areas with distinctive characteristics created by thermal microbridges of fixing elements and stiffeners of the structures.

The major areas found in the heat flow density map are:

- for the domain W1 – in the range 61.54 W/m^2 – 75.17 W/m^2;
- for the domain W2 – in the range 15.80 W/m^2 – 23.17 W/m^2;
- for the domain W3 – in the range 2.8 W/m^2 – 5.5 W/m^2.

Flow density through the analysed cross-sections and surfaces

Flow densities presented in the flow density area in figure 4 are characterized as follows:

Cross-section AA':

- the domain structure W1 present linear variation, gentle slope on the entire wall thickness;
- the domain structure W2 present linear variation, steep slope in the heat insulation area, connected to an area prone to linearization, corresponding to the inner wall;
- the domain structure W3 present curvilinear variation in central area, bordered by linear areas at the edges.

Cross-section BB':

- in the domain structure W1, the wall thickness decreases the slope until the vicinity of inner corner. The freezing area is much closer to the inner corner and favours the occurrence of condensation and degradation, molding and inner degradation of the wall.
- the domain structure W2 is characterized by non-linearities in the contact areas of materials and linearization tendency on the inside. By comparing the structure W2 with structure W1, we see that the flow density remains constant in the range 24–25 W/m^2 on a depth of about 20 cm from the wall, while on the uninsulated cross-section the heat flow decreases linearly between 75 W/m^2 and 30 W/m^2.
- the domain structure W3 has the same tendency as structure W2, but has lower values and in the inner corner a flow interference occurs due to thermal microbridges. This interference is highlighted also in the inner corner surface CC' by the presence of microbridges generated by assembling elements, heat flow density of 15.74 W/m^2 being close to the value found in the corner (18.34 W/m^2). Microbridges thermally affect the structure at a distance of about 5–6 cm.

The following can be noticed in the inner corner area CC':

- in the domain structure W1, in areas adjacent to the corner the heat flow is 73.75 W/m^2, and in the corner area is 176.31% higher.
- in the structure W2 the heat flow at the corner surface reaches 20.73 W/m^2 and in the corner area it increases by 220%.
- in the structure W3 the heat flow in the corner is even higher, of 5.38 W/m^2 and in the vicinity of the corner the density increases by 340.89%.

Heat transfer through the outer corner DD' reveals the reduction of the heat flow out of the wall (W1, W2 and W3), and W2 and W3 show the thermal microbridges from the outside.

The performance of the structures W2 and W3, which are wool insulated, as presented in table 3 are superior to those of the domain of the structure W1.

CONCLUSIONS

This study analyses the thermal effects created by the use of a thermal insulation with a density of 17 kg/m^3 and a thickness of 15 cm made of Turcana wool fibres through minimal processing. Thermal insulation is applied: on the exterior of solid brick masonry and on the interior of a wood structure

Table 3

THERMAL PERFORMANCE OF THE STRUCTURES W1, W2, W3				
Parameter for comparison	**MU**	**Structure W1**	**Structure W2**	**Structure W3**
Indoor temperature	°C	11.03	17.9	19.34
Temperature in the corner	°C	5.23	14.89	17.86
Freezing point diagonally to the corner from outside to inside / diagonally	cm/cm	35/41	24/68	34/42
Freezing point on the width of the wall from outside to inside / diagonally	cm/cm	15/29	5/48	15/31
Heat flow through the walls	W/m^2	71.74	17	5.25
Heat flow through the corners	W/m^2	130.03	41.68	18.50

(OSB). The structures are analyzed from the following points of view:

- Domain b is efficient in terms of energy; masonry walls are protected from the freeze-thaw phenomena, accumulate a large amount of heat at a high temperature and are able to attenuate temperature differences and to ensure a good thermal comfort with discontinuous heat sources.
- We notice that Alucobond has a very strong effect in terms of heat transfer and the slightly ventilated layer in front of wool insulation. The freeze-thaw phenomena occur in the ornamental insulation layer, which in turn gives a very good protection to brick masonry, making heat loss on the outside of the brick wall to be close in value to the internal temperature of the uninsulated wall. Slow temperature decrease of insulated brick wall is due to its massiveness-thermal insertion, which makes it adequate for continuous use.
- In this structure, no condensation or mold appears in the corners.
- Structure c is more efficient in terms of heat transfer than structure b: freeze-thaw phenomena are produced in the most adverse simulated conditions in the middle of the thermal insulation; although thermal protection is very good and heating is rapid, the heat accumulation is reduced: in order to maintain an adequate thermal comfort a continuous heat source is necessary.
- Although the structure c is more efficient than the structure b, from the point of view of heat transfer, in order to maintain an adequate thermal comfort in the room the use of a continuous heat source is needed.
- In this structure no condensation or mold appears in the corners.
- The better the insulation, the higher is the tendency of heat flow to cross through minimum resistance areas.

ACKNOWLEDGEMENTS

This paper was partially written with the support of EURODOC "Doctoral Scholarships for Research Performance at European Level" project, ID 59410, financed by the European Social Found and Romanian Government and POSDRU CUANTUMDOC "DOCTORAL STUDIES FOR EUROPEAN PERFORMANCES IN RESEARCH AND INNOVATION" ID79407 project funded by the European Social Fund and Romanian Government and partially with the support of Université Lille Nord de France, Laboratoire Génie Civil et géo-Environnement.

BIBLIOGRAPHY

[1] Peccei, A., *The Chasm Ahead,* New York, USA, 1969, Macmillan

[2] Donella, H., Meadows, D. L. M., Randers, J., and Behrens III, W. W., *The Limits to Growth.* USA, 1972, Universe Books

[3] Bribián, Z., Capilla, I. A. V., and Usón, A. A., *Life cycle assessment of building materials: comparative analysis of energy and environmental impacts and evaluation of the eco-efficiency improvement potential*. In: Building and Environment, 2011, vol. 46, issue 5, pp. 1133-1140

[4] Sachs, J.D., *Obiectivele de dezvoltare sustenabilă de la Rio+ 20*. In: Mesagerul Energetic, 2012, vol.12, p. 60

[5] Gobin, C., *Éco-conception – Marqueur d'un reengineering de la construction*. Techniques de l'Ingénieur L'expertise technique et scientifique de reference. 2011, C-3020, p. 14

[6] Domus Matériaux Ecologiques, Fiche conseil Daemwool – *Pure laine vierge* (PLVG). In: DOMUS Matériaux Ecologiques, 2006, vol. 3, p. 4

[7] Polat, E. S., *An alternative use of sheep wool: Building insulation*. In: Journal of Biotechnology, Supplement 2012, vol. 161, pp. 14-15

[8] Hossu, I., Grosu, M. C., Horga, Gh., Avram, D. *Thermal Conductivity of the Thick Wool Layers*, In: CORTEP 2012, Sinaia, Sept. 2012, Performantica-Institutul Naţional de Inventică

[9] Wool, K. P., *Sheep's Wool Insulation a Natural & Sustainable Thermal Insulation for Roofs, Walls & Floors – factsheet*.
[10] Asdrubali, F., *Survey on the acoustical properties of new sustainable materials for noise control*. Proceedings of Euronoise, Tampere, Finland, 2006
[11] Drăgănescu, C. *On the pastoral life in Balkans and South-Eastern Europe Past, present-future*. in 3rd Joint Meeting of the Network of Universities and Research Institutions of Animal Science of the South Eastern European Countries, Thessaloniki, 2007
[12] Latitudee Co Wool, Latitude – *Natural Wool Insulation*: Appraisal Certificate No. 1999/21 Wool Bloc Insulation, C. Laboratories, Editor 2001: Lower Hutt, New Zeeland. p. 4
[13] Alchimea lana ®, Wool Thermal insulations – *factsheet*, 2003. p. 2
[14] Black Mountain Insulation Ltd., Sheeps Wool Insulation. p. 3
[15] Sheep Wall Insulation Ltd., *The natural way to save energy*. Technical Specification.
[16] Domus materiaux / Daemwool-France, Dossier Daemwool, 2010: Cornebarrieu – Toulouse, p. 12
[17] Bosia, D., R. Giordano, and L. Savio, *A sustainable building product: advanced insulation panels obtained by recycling regional sheep's wool*. TECHNE, In: Journal of Technology for Architecture & Environment, 2011
[18] Bosia, D., Giordano, R., Savio, L., *Slow Tech: Un Nuovo Modello Per L'architettura Ecocompatibile Lana Di Pecora*, Centro Interuniversitario di Valutazione della Qualità Ambientale del Costruito, In: Titolo volume non avvalorato, Bioedilizia Italia, Torino, 2009, p. 6
[19] Magruder, M., *12 Reasons to Choose Natural Wool Insulation*, Oregon, Sheperd, Rainer, USA, 2012.
[20] Hossu, I., Horga, G. H., Grosu, M. C., Avram, D., Breaban, F., Defer. D., Antczak. E., *Thermal Transfer through Wool Layers*, In: Proceedings of CORTEP 2012, Sept, Sinaia, România
[21] Wu, T., *These – Formalisme des impedances thermiques generalisees application a la caracterisation thermique de parois de batiments*, in Génie Civil, 2011, Université d'Artois: Béthune; FR.
[22] Avram, D., Buhu, L., *Proiectarea tehnologică în filaturile de lână*. 2001, Iasi, Casa de editura Venus
[23] Zach, J., Korjenic, A., Petranek, V., Srudova, J., Bednar, T., *Performance evaluation and research of alternative thermal insulations based on sheep wool*, In: Energy and Buildings, 2012. 49(0): pp. 246-253
[24] Ye, Z., Wells, C. M., Carrington, C. G., Hewitt, N. J., *Thermal conductivity of wool and wool-hemp insulation*. In: Int. J. Energy Res., 2006, pp. 37-49
[25] Preda-Ștefanescu, D., Dolca, A., *Modelarea numericã a comportării higrotermice a clădirilor*, In: Revista Construcțiilor, 2006, vol. 10, pp. 78-84
[26] Preda-Ştefănescu, D., *Higrotermica constructiilor*. 2009, Iaşi: Editura Societăţii Academice "Matei-Teiu Botez"
[27] Yves Debard, Y., RDM 6.17, Élements finis, 2011, Institut Universitaire de Technologie, Departement Genie Mecanique et Productique: Le Mans.
[28] MLPAT, C 107/1/2/3/4/5-2005 *Normativ privind calculul coeficienţilor globali de izolare termică la clădirile de locuit*, 2005: C107/1. p.126.

Authors:

Drd. eng. IOAN N. HOSSU
"Gh. Asachi" Technical University of Iaşi
Faculty of Textile-Leather Engineering and Industrial Management, 29, Dimitrie Mangeron Street, 700050 Iaşi
e-mail: hossu_ioan@yahoo.com

Dr. eng. MARIAN-CĂTĂLIN GROSU
The National Research & Development Institute for Textiles and Leather
16 Lucretiu Pătrăşcanu Street, 3 District,
030508 Bucharest
e-mail: catalin.grosu@certex.ro

Dr. eng. GHEORGHE HORGA
3 Anastasie Panu Street, District 3, 031163, Bucharest
e-mail: horga_gheorghe@yahoo.com

Drd. eng. ANDREI IOSUB
"Gh. Asachi" Technical University of Iaşi
Faculty of Textile-Leather Engineering and Industrial Management, 29, Dimitrie Mangeron Street, 700050 Iaşi
e-mail: iosubandrei84@yahoo.com

**Chief of work. dr. eng.* IULIANA GABRIELA LUPU
"Gh. Asachi" Technical University of Iaşi
Faculty of Textile-Leather Engineering and Industrial Management, 29, Dimitrie Mangeron Street, 700050 Iaşi
e-mail: iuliana68lupu@yahoo.com

Prof. dr. eng. DORIN AVRAM
"Gh. Asachi" Technical University of Iaşi
Faculty of Textile-Leather Engineering and Industrial Management, 29, Dimitrie Mangeron Street, 700050 Iaşi
e-mail: davram@tex.tuiasi.ro

Prof. habil. dr. eng. FLORIN BREABĂN
Artois University, LGCgE. IUT Bethune, S2T 1230,
Université Street, 62408 Bethune
e-mail: florin.breaban@univ-artois.fr

În data de 20.01.2015, Institutul Național de Cercetare Dezvoltare pentru Textile și Pielărie (I.N.C.D.T.P.) a participat la *Simpozionul „**TINERII CERCETĂTORI – CREATIVITATE ŞI PROGRES ÎN SOCIETATEA CUNOAŞTERII**“*, organizat de Universitatea POLITEHNICĂ din Bucureşti, în parteneriat cu Universitatea din București, în cadrul proiectului *„Extinderea oportunităților de dezvoltare a competențelor studenților în activități de informare și documentare – EduFor Competence!“*, cofinanțat din Fondul Social European prin Programul Operațional Sectorial Dezvoltarea Resurselor Umane 2007–2013.

Simpozionul, care a avut loc în sala E 3.29, etajul 3, al clădirii Bibliotecii Centrale – Universitatea POLITEHNICĂ din Bucureşti, Splaiului Independenţei, nr. 313, sector 6, Bucureşti, s-a bucurat de o largă participare a mai multor reprezentanţi ai instituţiilor centrale şi locale, cu responsabilităţi în domeniul educaţiei şi formării, ai universităţilor, ai unităţilor de învăţământ, institute de cercetare, precum şi reprezentanţi ai asociaţiilor de studenţi, ai mediului economic etc.

Participarea I.N.C.D.T.P. s-a încadrat în scopul evenimentului de a promova domeniul cercetării-dezvoltării-inovării în rândul studenților, în vederea stimulării și dezvoltării unei cariere științifice în sectorul de textile-confecții-pielărie-încălțăminte.

Astfel, studenților le-au fost prezentate rezultatele ştiinţifice recente şi proiectele în care sunt implicaţi tineri cercetători, precum şi perspectivele în dezvoltarea vieţii ştiinţifice şi de cercetare.

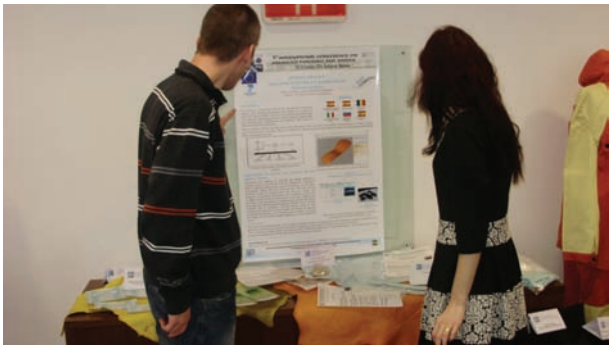

Acțiunea se încadrează în viziunea strategică a I.N.C.D.T.P., care are convingerea că resursa umană este cel mai important activ deținut, strategia managerială urmărind crearea unei masei critice de cercetători cu specializări multidisciplinare, precum și atragerea tinerilor în activitatea de cercetare. Tot în cadrul aceloraşi acțiuni se încadrează și organizarea evenimentelor **„Ziua porţilor deschise“,** în anul 2014 fiind organizate 2 astfel de evenimente, la care au participat elevi de la liceele de profil – liceul Gheorghe Asachi din București, liceul Petru Poni din București, precum și participarea la alte evenimente, cum ar fi **Noaptea Cercetătorilor** (26 septembrie 2014), la care Institutul a participat cu stand propriu.

De asemenea, în data de 6 februarie 2015, a avut loc o vizită a elevilor și a cadrelor didactice de la colegiul tehnic Ghe. Asachi din București, în scopul dezvoltării de competenţe antreprenoriale şi formare în domeniul tehnic textil pentru viitorii absolvenţi de profil Industrie Uşoară şi Design vestimentar.

Marius Iordănescu – Redactor Șef

INFORMATION FOR AUTHORS

Industria Textila magazine is an international peer-reviewed journal published by the National Research & Development Institute for Textiles and Leather – Bucharest, in print editions.

Aims and Scope: *Industria Textila* magazine welcomes papers concerning research and innovation, reflecting the professional interests of the Textile Institute in science, engineering, economics, management and design related to the textile industry and use of fibres in consumer and engineering applications. Papers may encompass anything in the range of textile activities, from fibre production through textile processes and machines, to the design, marketing and use of products. Papers may also report fundamental theoretical or experimental investigations, practical or commercial industrial studies and may relate to technical, economic, aesthetic, social or historical aspects of textiles and the textile industry.

Submission of Manuscripts

The paper submitted for publication shall concern problems associated with production and application of fibers and textiles.

Please include full postal address as well as telephone/ fax/e-mail details for the corresponding author, and ensure that all correspondence addresses are included. Also include the scientific title of the authors.

Industria Textila magazine considers all manuscripts on the strict condition that they have been submitted only to the *Industria Textila* journal, on this occasion, and that they have not been published already, nor are they under consideration for publication or in press elsewhere. Authors who fail to adhere to this condition will be charged with all costs which *Industria Textila* magazine incurs and their papers will not be published.

Manuscripts

Manuscripts of the following types are accepted:
Research Papers – An original research document which reports results of major value to the Textile Community
Notes – see below
Book Reviews – A brief critical and unbiased evaluation of the current book, normally invited by the Editor
Correspondence – Communications based on previously published manuscripts

Manuscripts shall be submitted in English in double-spaced typing, A4 paper, size font 10, Arial, margins 2 cm on all sides, under electronic version in Word for Windows format.

The volume of the submitted papers shall not exceed 10 pages (including the bibliography, abstract and key words), typescript pages including tables, figures and photographs.

All articles received are reviewed by a reviewer, renowned scientist and considered expert in the subject the article concerns, which is appointed by the editorial board. After the article has been accepted, with the completions and the modifications required by the reviewer or by the editorial staff, it will be published.

The submission of the above-mentioned papers is by all means the proof that the manuscript has not been published previously and is not currently under consideration for publication elsewhere in the country or abroad.

There may also be published papers that have been presented at national or international scientific events, which have not been published in volume, including the specification related to the respective event.

The articles assessed as inappropriate by the reviewer or by the editorial staff, concerning the subject matter or level, shall not be published.

The manuscript shall be headed by a concise title, which should represent in an exact, definite and complete way the paper content. Authors should also supply a shortened version of the title, suitable for the running head, not exceeding 50 character spaces.

The manuscript shall also be headed by complete information about the author(s): titles, name and forename(s), the full name of their affiliation (university, institute, company), department, city and state, as well as the complete mailing address (street, number, postal code, city, country, e-mail, fax, telephone).

Tables and figures (diagrams, schemes, and photographs) shall be clear and color, where possible.

The photographs shall be sent in original format (their soft), or in JPEG or TIF format, having a resolution of at least **300 dpi**.

All tables and figures shall have a title and shall be numbered with Arabic numerals, consecutively and separately throughout the paper, and referred to by the number in the text.

Generally, symbols and abbreviations shall be used according to ISO 31: specifications for quantities, units and symbols. SI units must be used, or at least given comprehensive explanations or their equivalent.

Cited references shall be listed at the end of the paper in order of quotation and contain: **for a paper in a periodical** – the initials and surname of the author(s), title of journal and of the article, year and number of issue, number of volume and page numbers; **for a book** – the initial and surname of the author(s), full name of the book, publisher, issue, place and year of publishing, and the pages cited; **for patents** – the initial and surname of the author(s), the title, the country, patent number and year.

[1] Popescu, D., Popa, I., Cicea, C., Iordănescu, M. *The expansion potential of using sales promotion techniques in the Romanian garments industry*. In: Industria Textilă, 2013, vol. 64, issue 5, pp. 293-300

Authors are requested to send an abstract of the paper, preferably no longer than 100 words and a list of 5-6 key words (preferably simple, not compound words, in alphabetical order). Avoid abbreviations, diagrams and direct reference to the text.

All manuscripts with the material proposed for publication, shall be sent to:

marius.iordanescu@certex.ro

Complimentary issue – The corresponding author will receive a complimentary print copy of the issue in which his/her article appears. It will be up to the corresponding author if he/she decides to share or route his/her copy to his/her co-author(s).